
4 Carding Theory

In [Chapter 3](#), it was explained that one of the main functions of a card is to disentangle tufts of fibers into a web of individual fibers. In this respect, important considerations are the process of fiber individualization, the formation of the doffer web, the fiber extent and configuration, and the degree of fiber damage during carding. This is because, in processes subsequent to carding, fiber breakage and poor fiber configuration may lead to unacceptable yarn irregularity and imperfections. As described in [Chapter 5](#), fiber individualization and fiber hooks have a major influence in combing and drafting processes and therefore, ultimately, on the yarn quality and spinning performance.

In this chapter, we consider in greater detail the way fibers are disentangled in the revolving-flat and roller-top cards, along with the carding actions that lead to fiber hook formation, the blending of fibers, the leveling of variations in fiber mass, and fiber breakage.

4.1 OPENING OF FIBER MASS

4.1.1 TAKER-IN ACTION

We learned in [Chapters 2](#) and [3](#) that the fiber mass fed to the card (i.e., the batt) is an assembly of tufts and that the principal objective of the taker-in is to open up these tufts. This means beginning the process of disentangling fibers by reducing the tufts into smaller sizes, which we called *tuftlets*. The taker-in opens tufts effectively when one end of a tuft is momentarily held while the teeth of the taker-in pulls individual fibers and groups of fibers from the other end.

4.1.2 FEED-ROLLER, FEED-PLATE SYSTEMS

[Figure 4.1](#) illustrates the way tufts are opened by the taker-in on the short-staple card. The batt is composed of various sizes of tufts. Therefore, when opening a fiber mass of a typical short-staple fiber diagram, the leading ends of tufts (i.e., the batt fringe) must be positioned in such a way that the trailing ends of fibers that are much shorter than the mean fiber length are nipped along with longer fibers during the opening action. The importance of the “feed roller and feed plate” combination is that the surface of the feed plate tends to profile the roller, enabling the nipping

of all fibers to take place close to the taker-in teeth. Figure 4.1 illustrates how the compression forces on the batt, resulting from the feed roller loading, increase as the batt approaches the taker-in. The front of the feed plate facing the taker-in has a narrow horizontal plateau and then bevels steeply toward the taker-in, making a wedge space in which the batt fringe comes into contact with the taker-in teeth. This wedge space enables the taker-in teeth to progressively penetrate the batt thickness. The top layer is first removed, bringing the remaining fibers nearer to the teeth. In this way, most tufts are effectively opened.

Fiber properties such as fineness, length, friction coefficient, and elastic characteristics will play an important role in opening of the fiber mass. However, for a

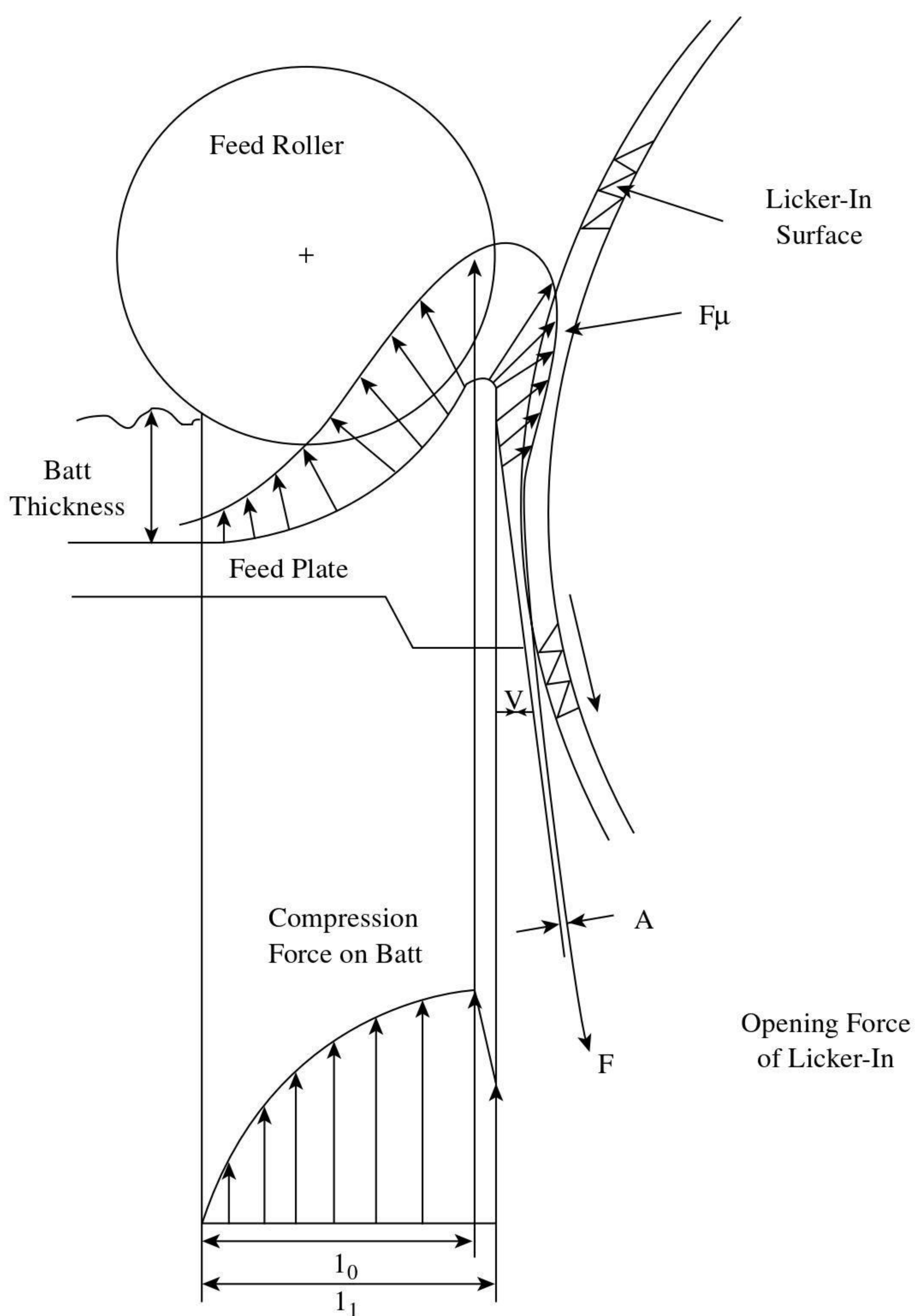


FIGURE 4.1 Opening of tufts by feed-roller, feed-plate taker-in combination. (Courtesy of Artz, P. and Schreiber, O., *Melliand Textilberichte*, 2, 107–115, 1973.)

given fiber type, the process variables that have been studied in relation to tuftlet size produced during opening by the taker-in of a revolving-flat card are

1. Basis weight of the batt (i.e., g/m²)
2. Feed rate
3. Taker-in speed
4. Taker-in clothing (angle of tooth and point density)
5. Setting of feed-plate to taker-in
6. Ratio of cylinder and taker-in surface speeds
7. Presence of rear fixed flats

Photographs taken of the fiber mass on a taker-in^{2,3} during the carding of cotton fibers showed that around 40 to 50% of the mass comprised individual fibers, and the remainder was tuftlets of various sizes. [Figure 4.2](#) shows a typical distribution of weighed tuft sizes before the action of the taker-in and the distribution of weighed tuftlets resulting from the licker-in action on the batt fringe. As can be seen, the tuft sizes are reduced to tuftlets, of which the vast majority are less than 3 mg. The figure also shows examples of the superficial size (i.e., surface area base on two-dimensional photographs) of the tuftlets. It is evident that the constituent fibers of some tuftlets appear less compact than in other tuftlets. The reason for this can be seen in [Figure 4.3](#), which shows a batt fringe from which fibers were removed by a taker-in.

The fibers indicate a combing type action by the taker-in. Individual fibers can be seen projecting from the fringe; the projecting lengths at the bottom of the batt are longer than those at the top.³ Also at the fringe are tufts that lie at various orientations to the direction of feed, i.e., the machine direction. They have dissimilar geometry, size, and density. Tufts that are not in line with the machine direction are likely to be either split into tuftlets of a few milligrams or, if already tuftlet size, to be removed unchanged rather than separated into individual fibers.^{2,3}

Nittsu et. al² studied the effect of the first five of the seven process variables listed above. Five classes of tuftlet size (i.e., areas) were established through measurements taken from photographic images of tuftlets on the taker-in surface. [Figure 4.4](#) depicts the changes in the number per taker-in revolution of each tuftlet class with changes in processing conditions. The total number of tuftlets decreases with closer feed plate settings, lower feed rates, smaller angles of saw-tooth clothing, and higher taker-in speed; the decrease is for all the tuftlet classes. Since the taker-in opens the batt into tuftlets and individual fibers, a decrease in the total number of tuftlets suggests an increase in the mass of individual fibers.

In Chapter 3, we learned that the surface speed of the cylinder is around twice that of the taker-in. When the fiber mass is transferred onto the cylinder by the *front-of-tooth* to *back-of-tooth* action, this speed difference tends to thin the fiber mass. That part of the mass comprising individual fibers is effectively attenuated by a draft of two, and so the number of tuftlets per unit area is reduced. The tuftlets, however, are not reduced in size — they become elongated.² Both the individual fibers and the tuftlets become more aligned to the machine direction.^{2,4} On making contact with the stationary flats at the back of the card, the tuftlets are reduced in size, and

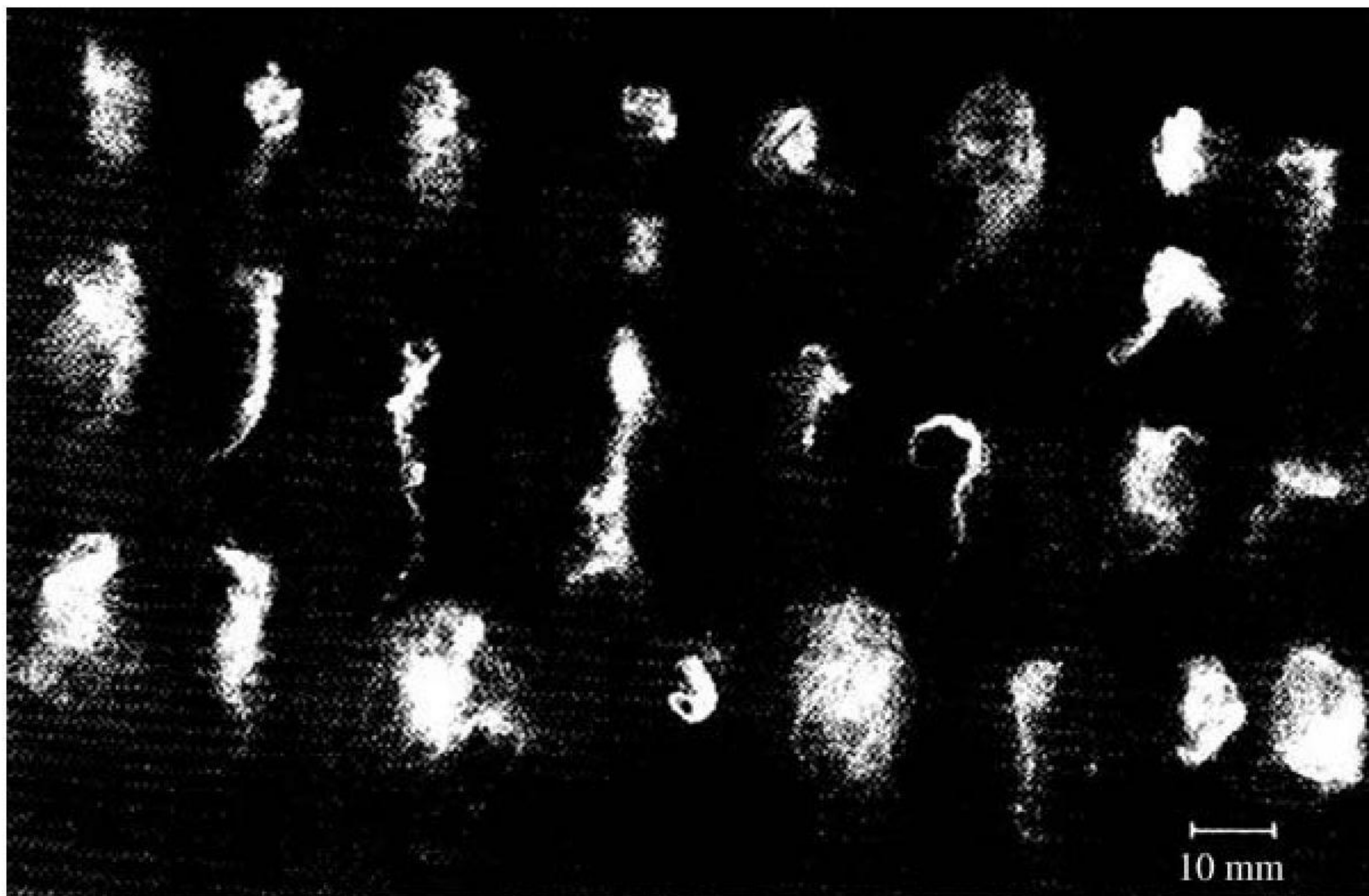
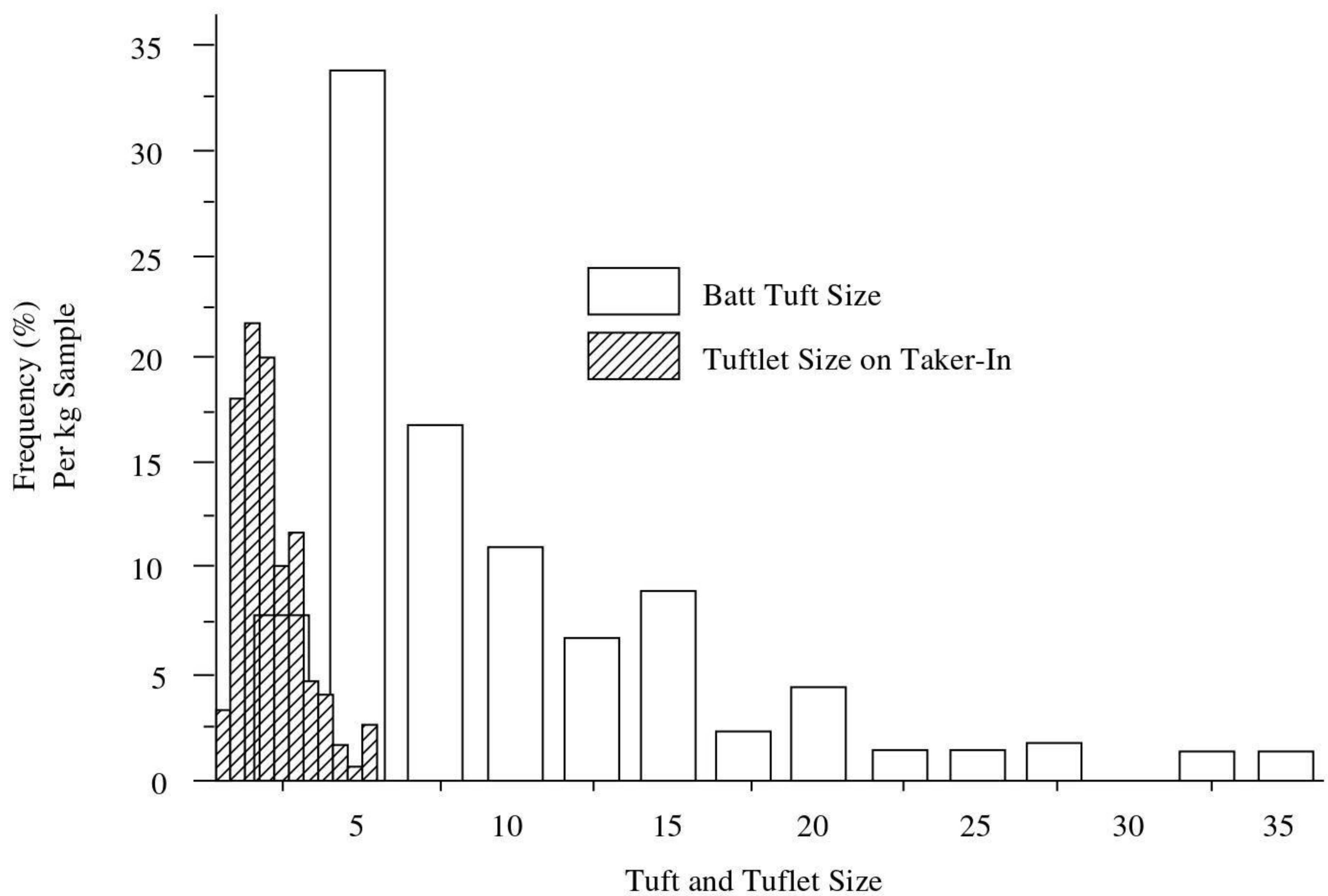


FIGURE 4.2 Distribution of tuft and tuftlet sizes.

this facilitates better fiber disentanglement and separation by the subsequent interaction of the revolving flats and cylinder.

4.1.2.1 Feed-Roller Systems

Figure 4.5 illustrates an example of the saw-tooth clothed, single-pair feed roller and the triple-merelle feed-roller systems used, respectively, on woolen and worsted

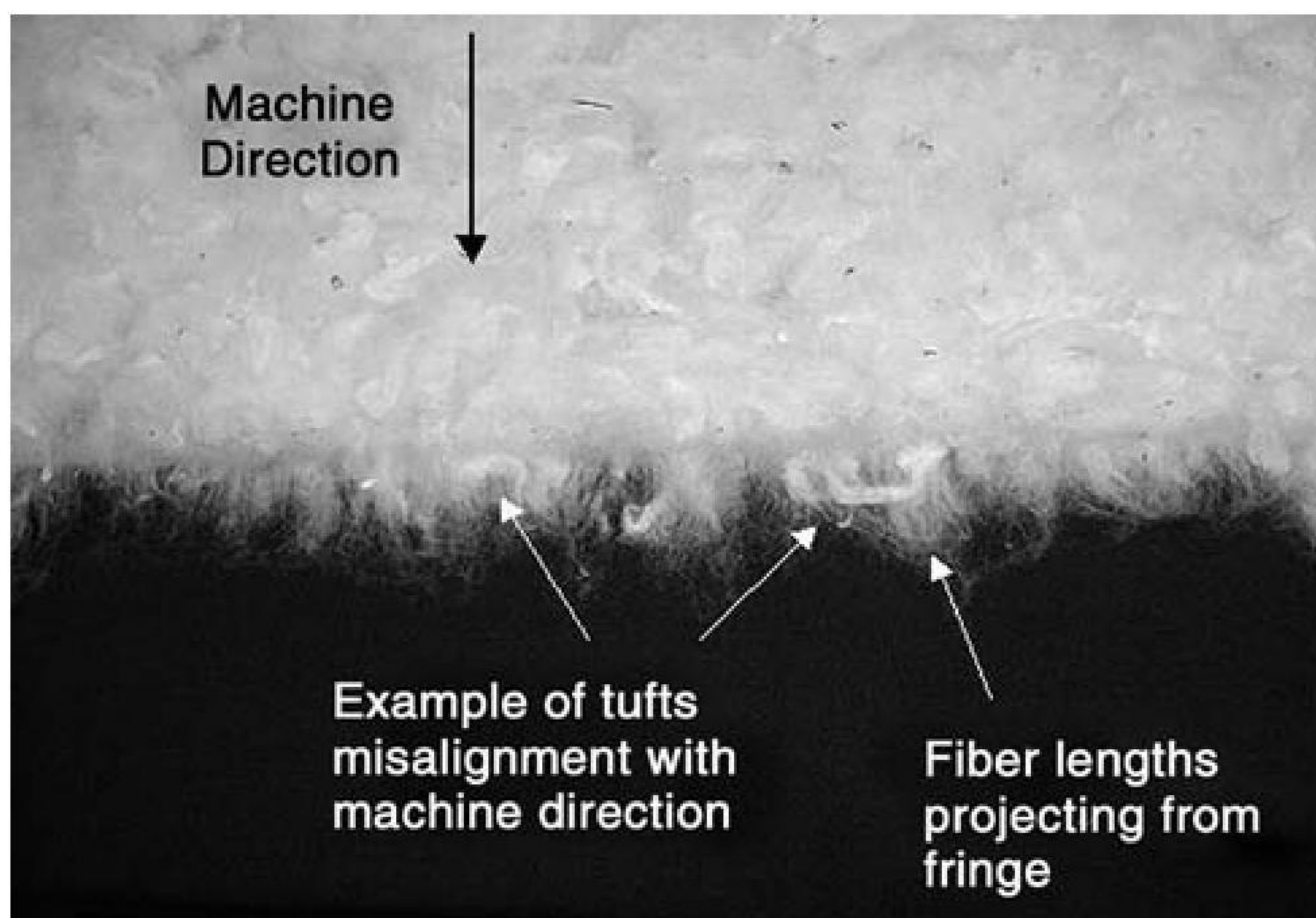


FIGURE 4.3 Cotton batt fringe fed to taker-in.

cards. With the merelle system, the first pair of rollers are clothed with saw-tooth wire, and the second pair are fluted and run at three times the surface speed of the first pair. The third pair are pin-rollers and have a surface speed half that of the second pair. The single-pair arrangement subjects fibers to a sudden step increase in speed as they make contact with the taker-in, similar to the feed-roller, feed-plate arrangement for short staples. However, with longer-staple fiber (in particular wool), the objective is to achieve a gentler, less aggressive opening and thereby lower the potential for fiber breakage resulting from the entanglement of fibers in the tufts. Fiber breakage will be discussed in more detail later. Townend et al.⁵ demonstrated that by having a series of roller trains, each pair running faster than the preceding pair, scoured wool tufts that were oriented at various angles to the mass flow would, through the small draft applied, become less entangled, more elongated, and closely oriented to the machine direction prior to their point of contact with the taker-in. As mentioned above, the more elongated a tuft is in the machine direction, the more easily it is to disentangle the constituent fibers. The increase in speed toward the taker-in provides a gentler progressive opening by the taker-in.

4.2 CARDING ACTIONS

4.2.1 CYLINDER-FLAT ACTION

The setting of the flats to cylinder leaves too small a gap for photographic observations of the way tuftlets are separated into individual fibers. Therefore, the consensus view is based on interpretation over many years of experimental data. Essentially, the very narrow gap between the flats and cylinder clothing enables tuftlets on the cylinder to be easily caught by the flats. Prior to the carding zone, air is dragged along by the rotating cylinder and, at the carding zone, the flow is suddenly restricted by the narrow gap. As a result, the air movement lifts the tuftlets toward the flats, assisting them in being easily caught. As explained in [Chapter 3](#), part of the fibrous waste from the carding process includes flat strips. Bodgan⁶ and Hodgson⁷ found

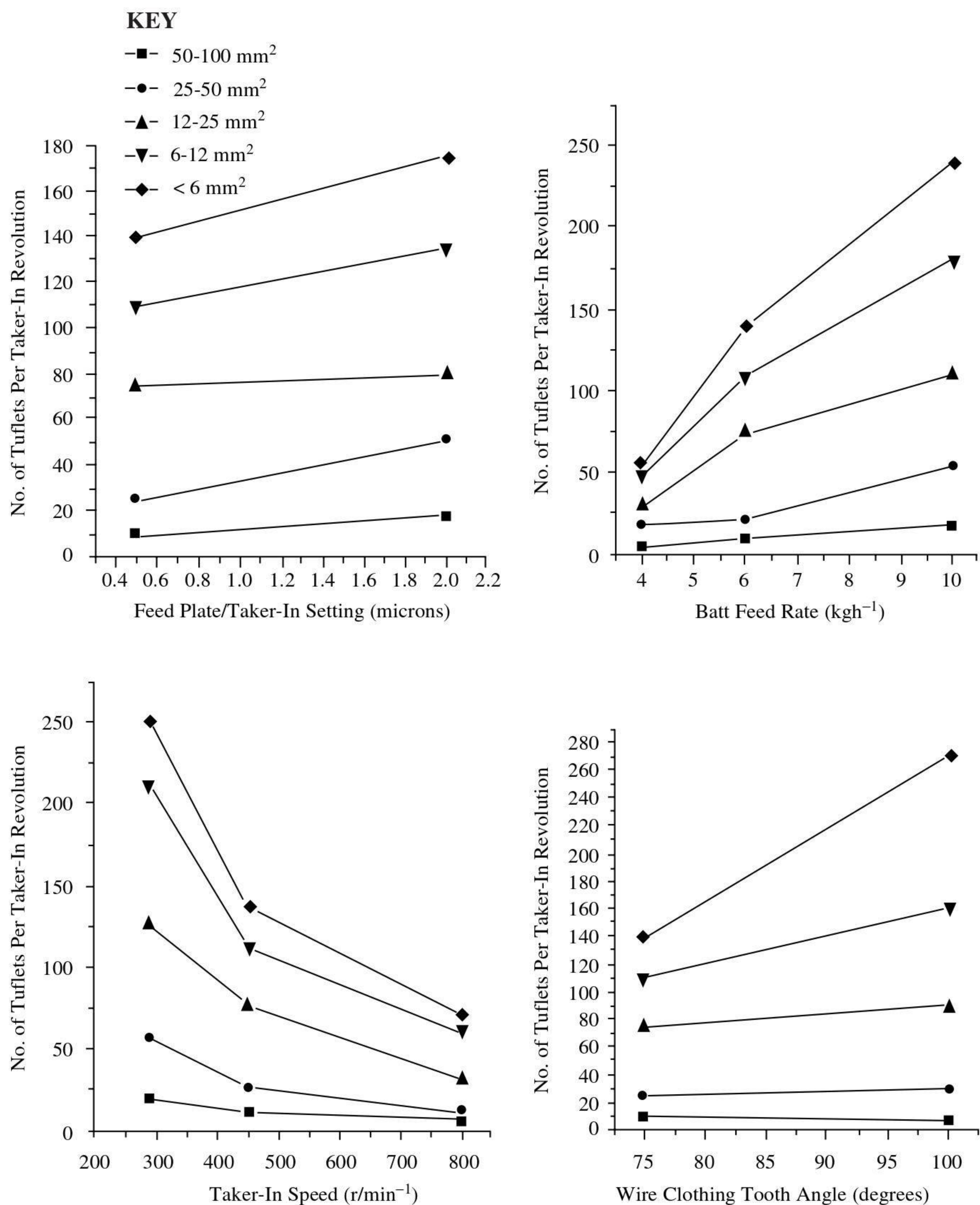


FIGURE 4.4 Effect of process variables on the number of tuftlets per taker-in revolution. (Courtesy of Nittsu, Y., et al., Cleaning action in the licker-in part of a cotton card, part 1: Opening action in the licker-in part., *J. Text. Mach. Soc. Japan*, 10, 218–228, 1964.)

that, as flats move in the direction of the cylinder rotation, they tend to load quickly with tuftlets as they reach the interface with the cylinder, acquiring two-thirds of their final load for each working cycle of the carding action with the cylinder.

Varga⁸ suggests that what is commonly called the carding action, i.e., the *point-of-tooth to point-of-tooth* for disentangling and separating fibers, is actually a combination of two sub-actions, shearing and combing. The shear action occurs first,

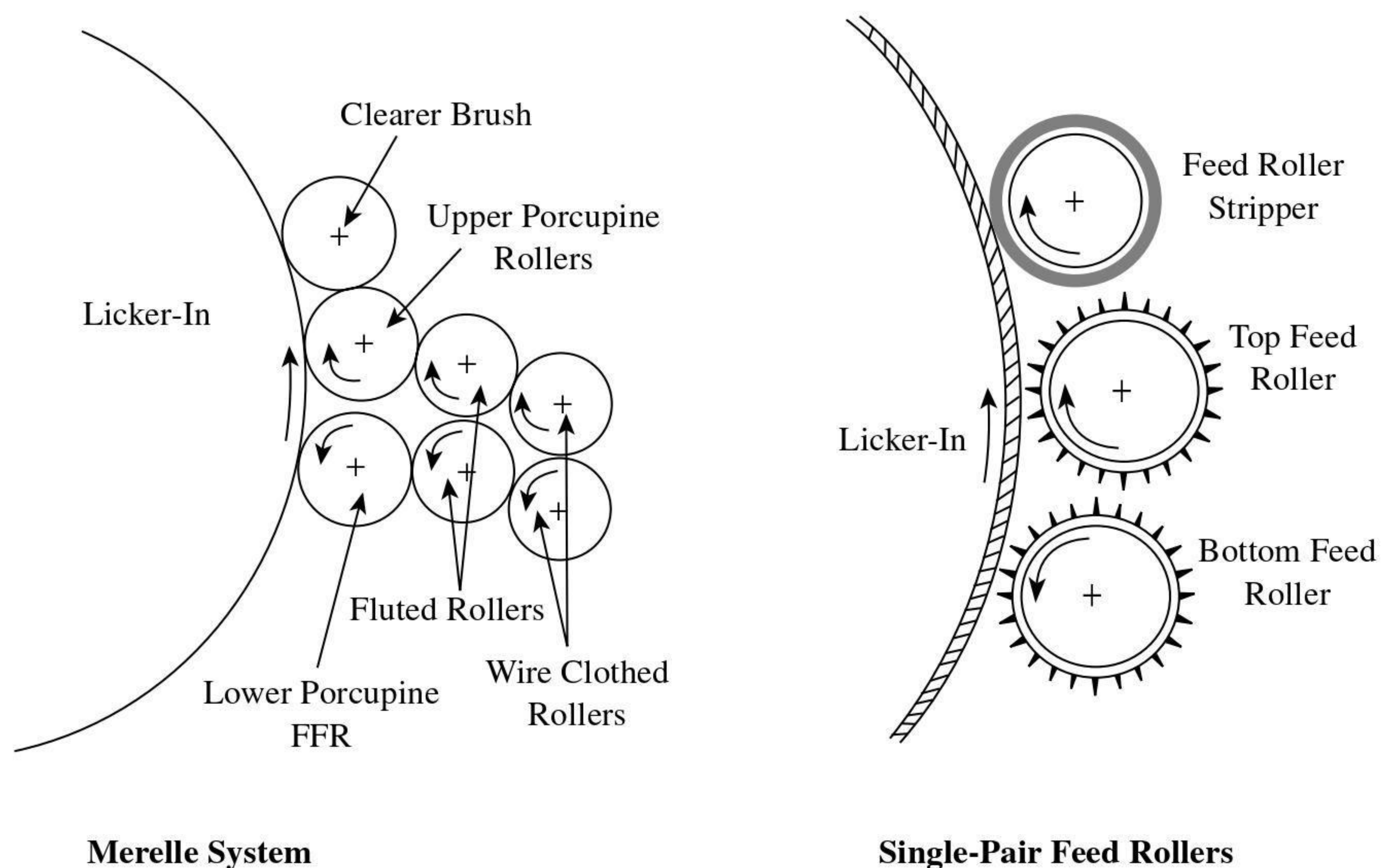


FIGURE 4.5 Feed-roller systems on woolen and worsted card.

whereby the upper layer of a tuftlet or a loosely opened fiber group is caught and held by a flat, while the bottom layer is sheared away by the faster-moving cylinder surface. The bottom layer comprises a much smaller number of fibers than the original tuftlet and can be termed a *minituftlet*. The top layer hangs from the flat and makes contact with subsequent teeth of the cylinder clothing as they pass by. This gives rise to combing, where the teeth hook single fibers or very small groups of fibers (microtuftlets) and comb them from the top layer. Flats downstream of the initially caught tuftlet catch the sheared-away bottom layer on the cylinder and any other mini- or microtuftlet, and the shear and combing actions are repeated on these. In this way tuftlets and mini- and microtuftlets are separated, i.e., carded, into individual fibers.

Oxley⁹ showed that a tuftlet is separated, as described, into individual fibers through the flat-cylinder interchange of fibers taking place over the four flats that precede the one on which the tuftlet was initially caught. It is reasonable to assume that the number of flats over which a tuftlet is reduced to individual fibers will depend on the tuftlet size, the mass flow rate, and the flat setting. For a fixed cylinder speed, the larger the tuftlet, the higher the production rate; and the closer the flat settings, the more flats will be involved in the separation of a tuftlet.

Sengupta and et al.¹⁰ made measurements of the shear and combing forces and found that, in general, the separation of tuftlets was confined to the first ten working flats in the carding zone. Thus, fiber individualization of tuftlets does not occur over the full carding zone. The full carding zone, however, aligns and parallelizes fibers in the machine direction. Generally, as Figure 4.6 shows, fibers are most aligned after leaving the cylinder-flat zone, and their alignment decreases during transfer to the doffer. The figure also shows that the relative alignments are affected by increased taker-in speed, flat speed, doffer speed, and calender draft.⁴

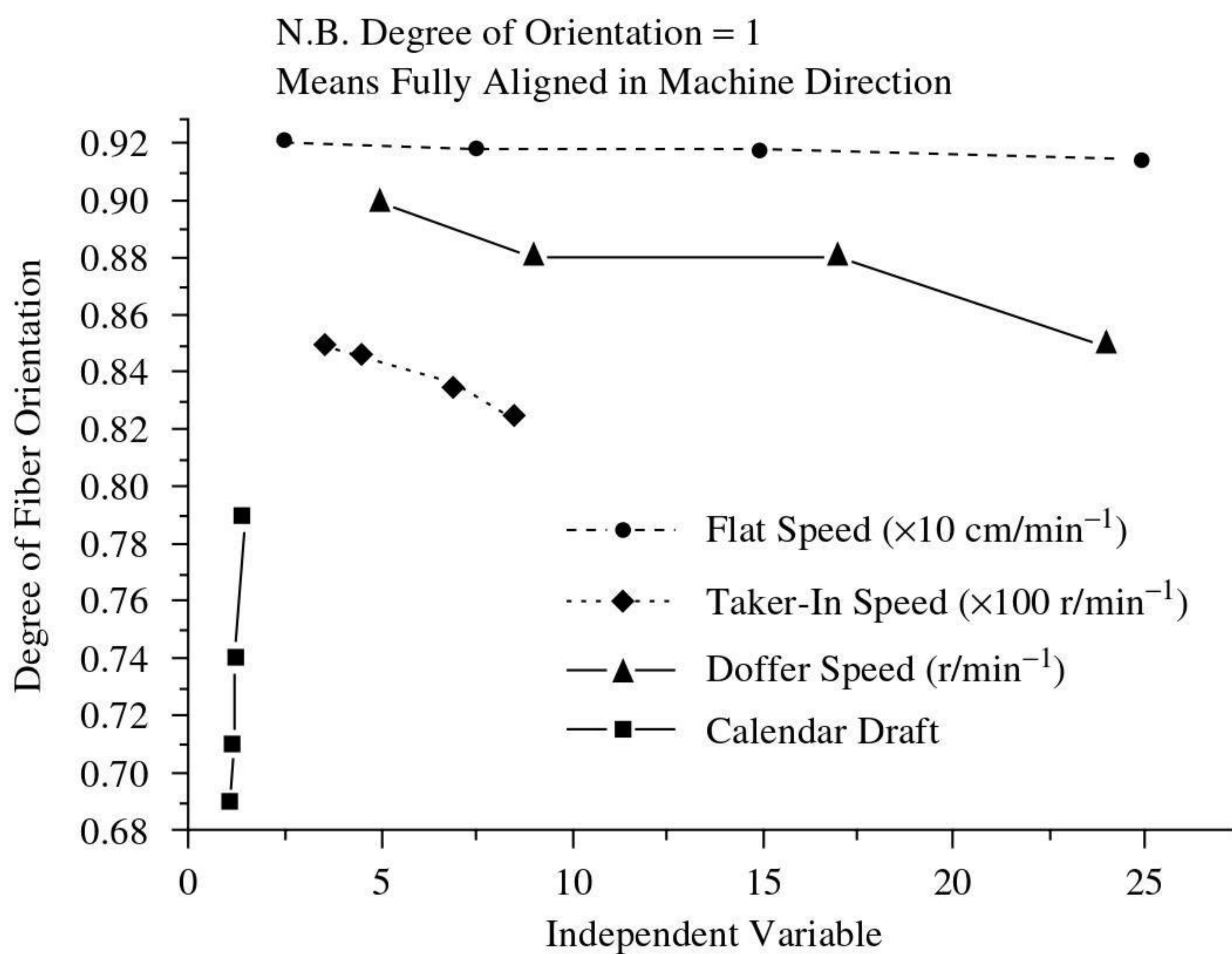


FIGURE 4.6 Fiber orientation during carding.

How well the revolving-flats card disentangles and individualizes fibers is often reflected in the propensity of thick and thin places in a carded-ring spun yarn. It is important that microtuftlets do not get caught at the base of the cylinder teeth, in particular between the teeth of the clothing (i.e., within the spiral pitch), because they then miss contact with the flats clothing and subsequently form thick places in the yarn. Artzt and et al.¹¹ studied the effect of cylinder and flat clothing parameters and cylinder speed on carded ring-spun yarn strength and imperfections. Only changes in the imperfections were statistically significant. Their results showed a complex interaction between fiber fineness, cylinder speed, and cylinder and flat teeth densities. Their findings can be summarized as follows:

1. Thick places in the yarn are generally microtuftlets.
2. Propensity of thick and thin places decreases with increased tooth density.
3. Coarse fibers are easier to individualize and, therefore, lower tooth densities are effective.
4. High tooth densities and the lower cylinder speed are as effective as lower tooth densities and high cylinder speed.

4.2.2 SWIFT-WORKER-STRIPPER ACTION

In [Chapter 3](#), we saw that the swift-worker-stripper combination involves *point-of-tooth to point-of-tooth* action between swift and worker, and *point-of-tooth to back-of-tooth* between swift and stripper. The two actions give almost a similar shearing and combing effect as that proposed by Varga, only here tufts or tuftlets are sheared between the worker and swift and combing between stripper and swift. Shearing is the dominant action and contributes most to fiber disentanglement and individual-

ization. Importantly, a worker can subject the fiber mass it retains to several shear cycles. The combing effect is small, because the surface speed ratio of stripper and swift is much lower than revolving flats and cylinder.

It was stated in Chapter 3 that the swift-worker-stripper action gives a blending of the fiber mass and a leveling of irregularities in the mass on the swift. To understand how effective the swift-worker-stripper combination is at individualizing the fibers of a tuftlet, and at blending and leveling the fiber mass, we must consider the fraction of the material retained by the worker as a result of the shearing action. In the literature, this fraction, p , is called the *collecting power*, as part of the fiber mass on the swift is initially collected by the worker. Alternatively, it is called the *lifting power*, since the worker lifts part of the fiber mass from the swift during the shearing action, or the *retaining power*, because part of the fiber mass is retained on the worker after the shearing action. The latter term seems more appropriate and is used throughout the following text.

It is important to know how the retaining power is affected by carding conditions, in particular the speed and setting of workers, and by fiber type. Martindale¹² published a simple formula for the retaining power of a worker. Referring to Figure 4.7, and assuming steady state running conditions, let

Q (g/min) = the uniform rate of the fiber mass on the swift passing point A and leaving point C

m (g) = the fiber mass on the worker (i.e., worker load)

n (rpm) = the speed of the worker

r = the radius of the worker

f = the fraction of the worker surface retaining the fiber mass

θ = the angle subtended at the center of the worker by f

Then, $f = \theta/360$, and the fiber mass on the worker is retained for $\theta/360n$ minutes, i.e., the time the worker takes to rotate through the angle θ . During this time, the

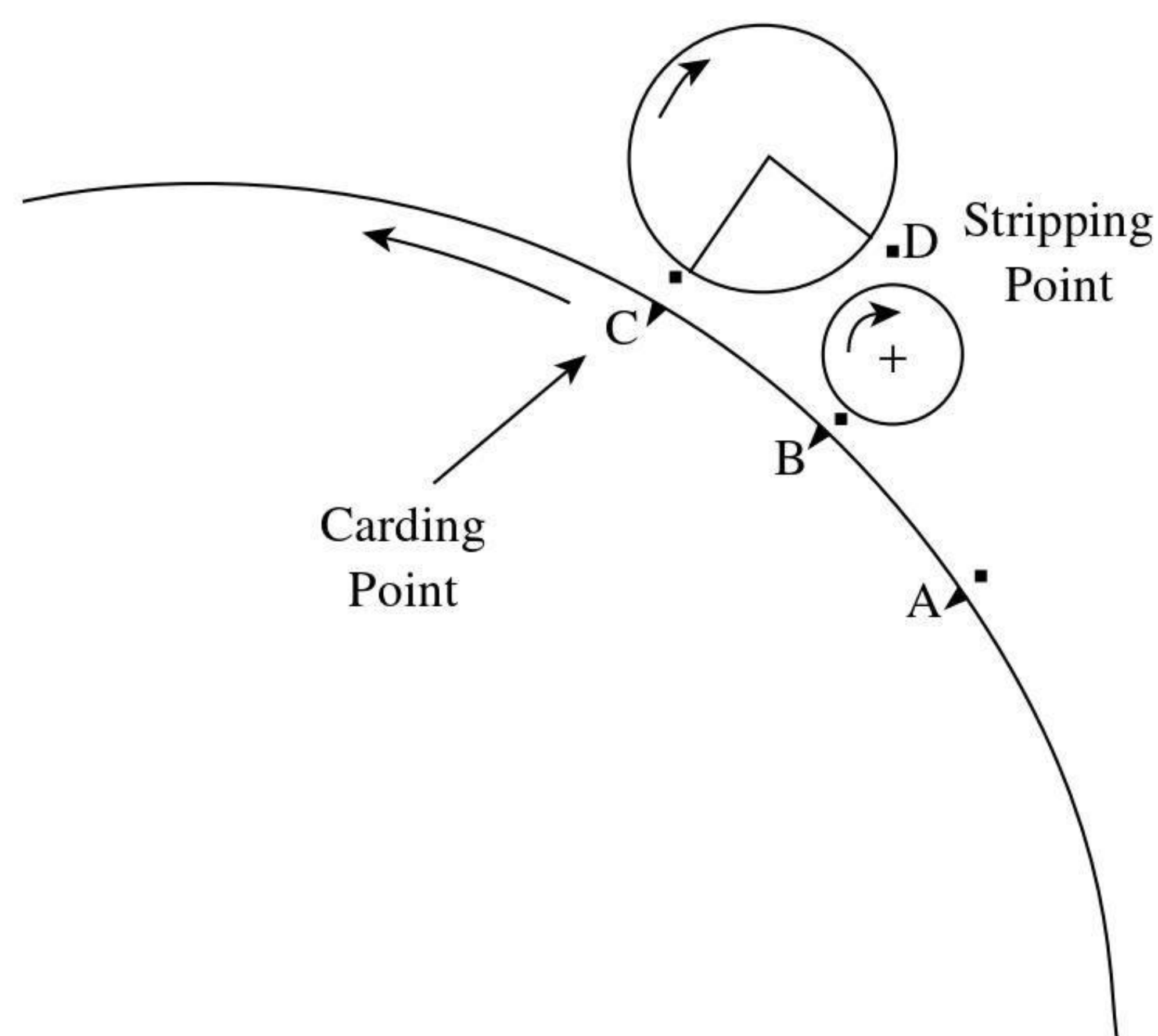


FIGURE 4.7 Swift-worker interaction.

amount of fiber reaching B from A is $Q\theta/360n$, and the amount laid down at B by the stripper is m . Therefore, the fiber mass reaching C is $[m + (Q\theta/360n)]$. However, the amount of fiber collected by the worker at C is m . Hence, the retaining power is given by

$$P = \frac{m}{\left(m + \frac{Q\theta f}{n}\right)} \quad (4.1)$$

Thus, P is the ratio of the mass per unit time being removed by the worker from the swift and the mass per unit time being taken into the carding zone by the swift. Practically, by stripping the worker, m can be determined; f and n are measured through observation, and Q can be obtained by either the Krylov¹³ or the Kaufman¹⁴ method. With a given fiber type and fixed carding conditions, experimental measurements have shown that P remains reasonably consistent for each worker-stripper pair around a swift.

Consider now the case for a blend of two fiber types. As an example, take a 50/50 blend of fibers A and B. If initially considered separately and then as the blend, we can see from the above equation that

$$m_A = \frac{P_A Q f}{[1 - P_A] n}; \quad m_B = \frac{P_B Q f}{[1 - P_B] n}; \quad m_C = \frac{P_C Q f}{[1 - P_C] n} \quad (4.2)$$

where P_A , P_B , and P_C are the corresponding retaining powers, and $m_C = m\#_A + m\#_B$.

A worker will retain $m\#_A$ from the 50% of fiber A contributing to Q and, similarly, $m\#_B$ from the 50% of fiber B. Thus, $m\#_A = 1/2 m_A$, and $m\#_B = 1/2 m_B$; hence,

$$m_C = \frac{P_A 1/2 Q f}{[1 - P_A] n} + \frac{P_B 1/2 Q f}{[1 - P_B] n} = \frac{Q f}{2n} \left(\frac{P_A}{1 - P_A} + \frac{P_B}{1 - P_B} \right)$$

$$\frac{P_C}{1 - P_C} = \frac{1}{2} \left(\frac{P_A}{1 - P_A} + \frac{P_B}{1 - P_B} \right) \quad (4.3)$$

This shows that a blend of different fibers does not affect the way the workers deal with each fiber individually. [Table 4.1](#) gives experimental and calculated p-values that confirm this.

[Figure 4.8](#) shows p-values for a four worker-stripper pair combination over the top of the swift on a scribbler and on an intermediate. The effect of worker speed and setting is also illustrated. It is evident that the retaining powers of the workers differ from each other. On both swifts, P decreases as the fiber mass moves forward toward the doffer, but the decrease is less rapid for the intermediate and would be even less if a carder were included in the system. Noticeably, the p-value is greater for the first intermediate worker than it is for the fourth scribbler worker, and this would be similar for the carder. This trend of decreasing P is assumed to be common

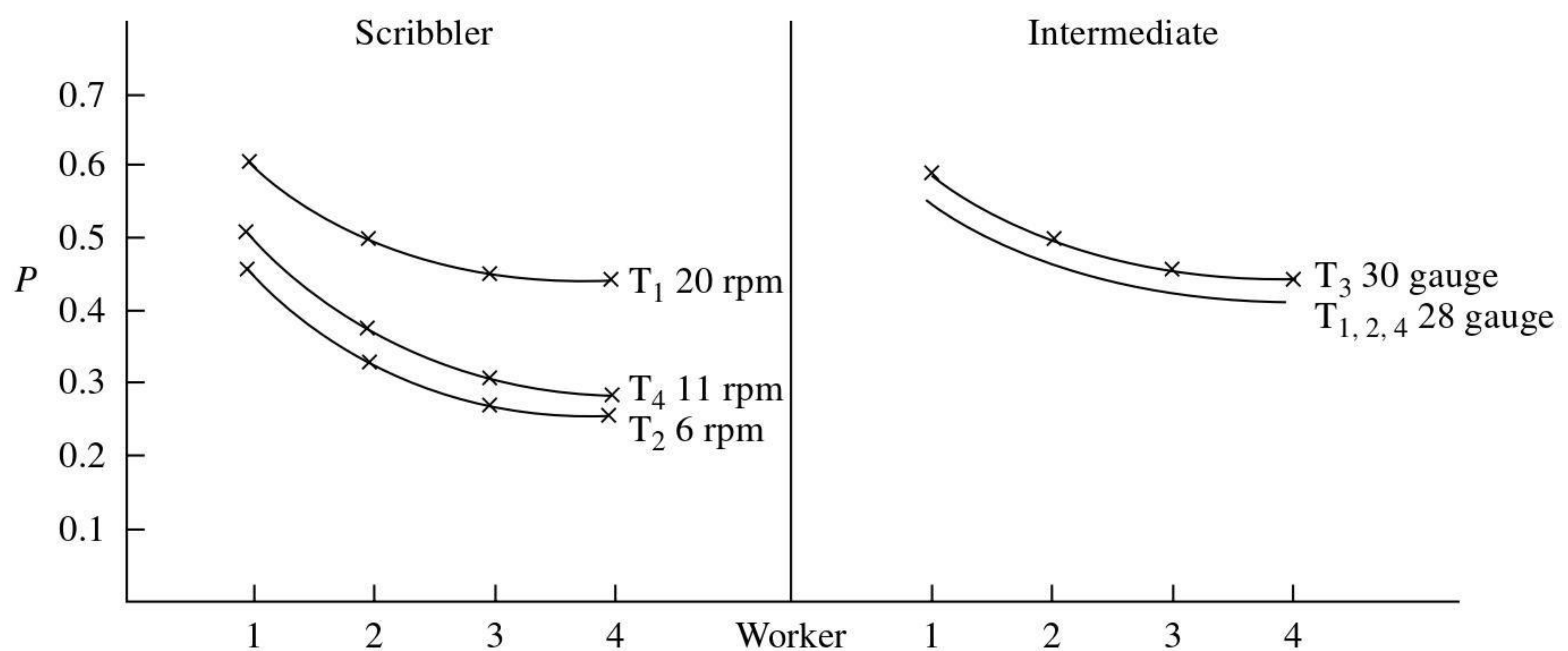


FIGURE 4.8 Mean p-values for workers on scribbler and intermediate. T_1 , T_2 , T_3 , T_4 , refer to sequence of workers.

TABLE 4.1
Effect of Collecting Power of Workers for a 50/50 Wool Blend*

Scribbler	P_A	$P_A/(1 - P_A)$	P_B	$P_B/(1 - P_B)$	$P_C/(1 - P_C)$	P_C (calculated)	P_C (experimental)
1st worker	0.430	0.754	0.606	1.538	1.146	0.534	0.533
2nd worker	0.346	0.529	0.473	0.897	0.713	0.416	0.418
3rd worker	0.304	0.437	0.414	0.706	0.572	0.364	0.368
4th worker	0.253	0.339	0.375	0.600	0.470	0.320	0.318

*Schlumberger noils = 10% oil/Australian pieces = 10% oil.

to both worsted and woolen carding where one or a combination of cards in a set is used. It is attributed to the idea that the first worker on the card does most of the work. The tufts or loose fiber groups are larger prior to the first worker and are therefore more easily caught by the first worker.

As the fiber mass on the swift moves toward the front of a card or a card set, it will have a greater percentage of individual fibers aligned in the machine direction and progressively smaller and fewer minituftlets or microtuftlets. Therefore, the fiber mass on the swift will be less easily caught by downstream workers operating with the same machine conditions. It is also the case that, as fibers on the swift pass by successive strippers, and the fibers from the worker are returned to the swift, the pressure between the swift-stripper roller surfaces causes fibers to be pushed deeper into the swift clothing. This makes it more difficult for the downstream workers to catch fibers. The action of the fancy before the doffer is to lift the fiber mass to the tip of the clothing to enable easier fiber transfer to the doffer. The use of a small fancy between worker-stripper pair has also been used to increase p-values.

The significance of a high p-value is illustrated in Figure 4.9. Here, PM is the quantity of fiber removed by a worker, which is initially set to run with a p-value of 0.4 and is then changed to operate at 0.8. M is the input fiber mass on the swift

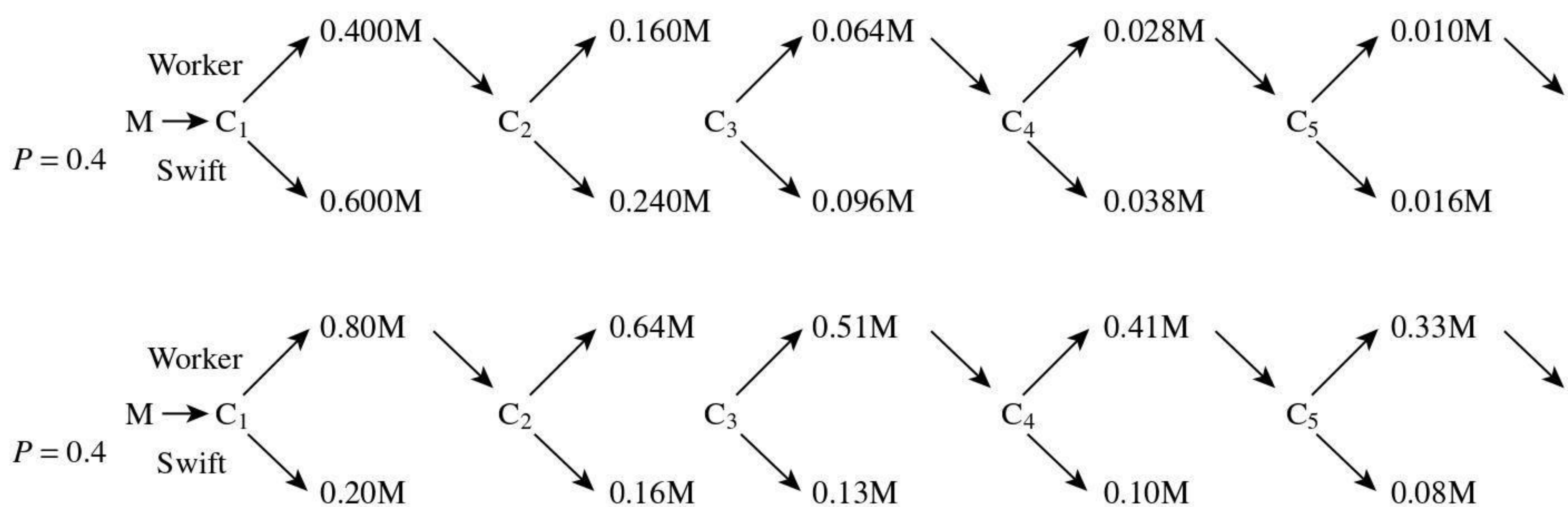


FIGURE 4.9 Effect of p-value on carding.

entering zone C (see Figure 4.7) Although with each revolution of the worker an equal mass will be retained, the figure shows what happens to the first mass of fiber, $0.4M$, removed from the swift and then fed back to the swift within a short time by the stripper, and a portion removed again by the worker. This cycle is shown for five revolutions of the worker. Thus, for $P = 0.4$ in the first cycle, C_1 , 0.4 of M is removed from the swift by the worker. This leaves $0.6M$ to move forward with the swift. The $0.4M$ is subsequently stripped from the worker and returned to the swift, and it becomes mixed with new tuftlets coming into this particular part of the carding zone. In the second cycle, C_2 , the worker will again remove 0.4 of the mass entering the carding zone. This means $0.4 \times 0.4M = 0.16M$ is now retained by the worker — that is to say, 0.16 of the first mass fed into the zone. At C_3 , $0.4 \times 0.16M = 0.064M$ is retained, and at C_4 and C_5 , $0.026M$ and $0.010M$, respectively. For $P = 0.8$, the retained mass per cycle is greater than for $P = 0.4$.

It can be seen that, with each revolution of the worker, the fraction of fiber mass M , taken forward by the swift, decreases. The higher p-value results in much smaller fractions taken forward. This means that, with an increase in the p-value of a worker, the fiber mass will undergo a higher number of shear cycles and therefore better carding.

The closeness of swift-worker settings, the density and condition of the worker clothing, the card production rate, and the relative surface speeds of worker to swift are the four principal factors controlling the p-value of a worker.¹⁵

Figure 4.10 shows that worker load varies almost exponentially with the closeness of setting; the closer the setting, the higher the p-value. This is because fiber capture by the worker depends on the height fibers project above the teeth of the swift clothing, and most fibers project only a shorter distance from the clothing. Thus, the closer the worker is to the swift, the greater the worker load and the higher the p-value.

In Chapter 3, it was explained that the worker, swift, and doffer clothing should be sharp (i.e., of a small land) for effective carding and low nep levels. Having sharp points to the worker clothing allows better penetration and retention of tuftlets and therefore a higher p-value. However, with regard to tooth density, the fraction of the unit area occupied by the wire points is as important as the number of points per unit area. Table 4.2 shows the effect on worker load of these two factors for fillet wires of different count, crown, and gauge. It can be seen that increasing the density of points is effective only if the area occupied by the points does not decrease.

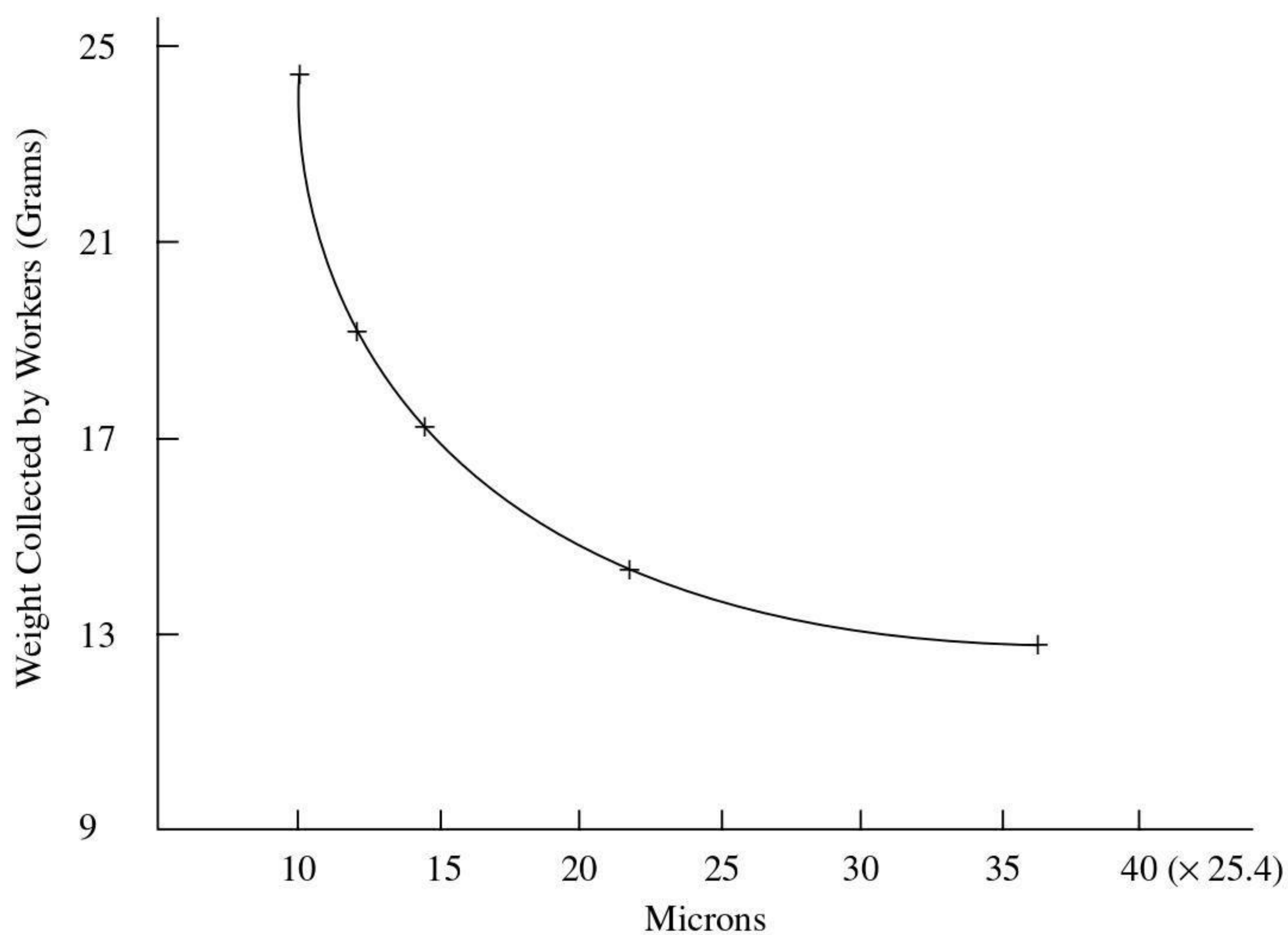


FIGURE 4.10 Effect of worker setting on p-values.

As would be expected, worker load increases proportionally with production rate; however, at wide settings, this does not hold true because of the effect of fiber protrusion height. Generally, increased worker speed gives the greatest increase in p-values. The reason is simply because, in a given interval of time, a larger surface area of worker clothing points will interact with the swift and retain more fibers. Thus, the higher the production rate of the card, the more important the choice of worker speed, as well as the worker setting, is for effective carding.

TABLE 4.2
Effect of Points Per Unit Area and Fraction of Area Occupied by Wire Points

Details of card clothing	Wire dia. (mm)	Points/25.4 mm ²	Area of wire in 25.4 mm ²	Mass collected by worker (g)
55/6/23	0.5842	132	0.055	2947
80/8/28	0.3910	256	0.045	2963
100/10/32	0.3048	400	0.045	5971
120/12/33	0.3048	576	0.065	4058
140/14/34	0.2794	784	0.075	3179

Although the carding action is the most important function of the swift-worker-stripper combination, the way in which this action occurs gives rise to two other important functions, namely blending and leveling. For the moment, only a basic description will be given of the blending-leveling effect. A more detailed treatment is provided in the next section, where the influence of the swift-doffer interaction is included.

The worker-stripper action (i.e., removing fibers from the swift and laying them down again after a short time delay) blends the material being carded and levels out variations in the feed from the hopper. The blending-leveling effect occurs in two ways: along the length of mass flow (i.e., lengthways) and by the superposition of fibers as the material passes through the card. Consider Figure 4.11. This shows that for $P = 0.5$, it would take about nine revolutions of a worker for the swift to remove all the fibers in a mass M fed to point C in Figure 4.7. To identify the mass, imagine that it was dyed red and fed among a mass of white fibers. Then, as Figure 4.11 shows, successively smaller amounts of it, each separated by an interval d_1 , would appear mixed with the other fibers taken forward by the swift. It can be seen that increasing P reduces the size but increases the number of small amounts removed and, thereby, the lengthways blending-leveling effect. The interval d_1 is the distance the swift surface rotates in the time it takes for the fraction of the fiber mass on the worker to return to the swift-worker interface and undergo the shearing action. The interval d_1 is therefore related to the time delay between each successive small amount, and this delay depends on the ratio of the worker and swift surface speeds. Thus, in the figure, the ratio for (c) is greater than that of (a) and (b), and consequently $d_1 > d_1'$.

To consider the second means of blending-leveling, i.e., by superposition, we need to imagine now that the material on the swift entering the swift-worker-stripper

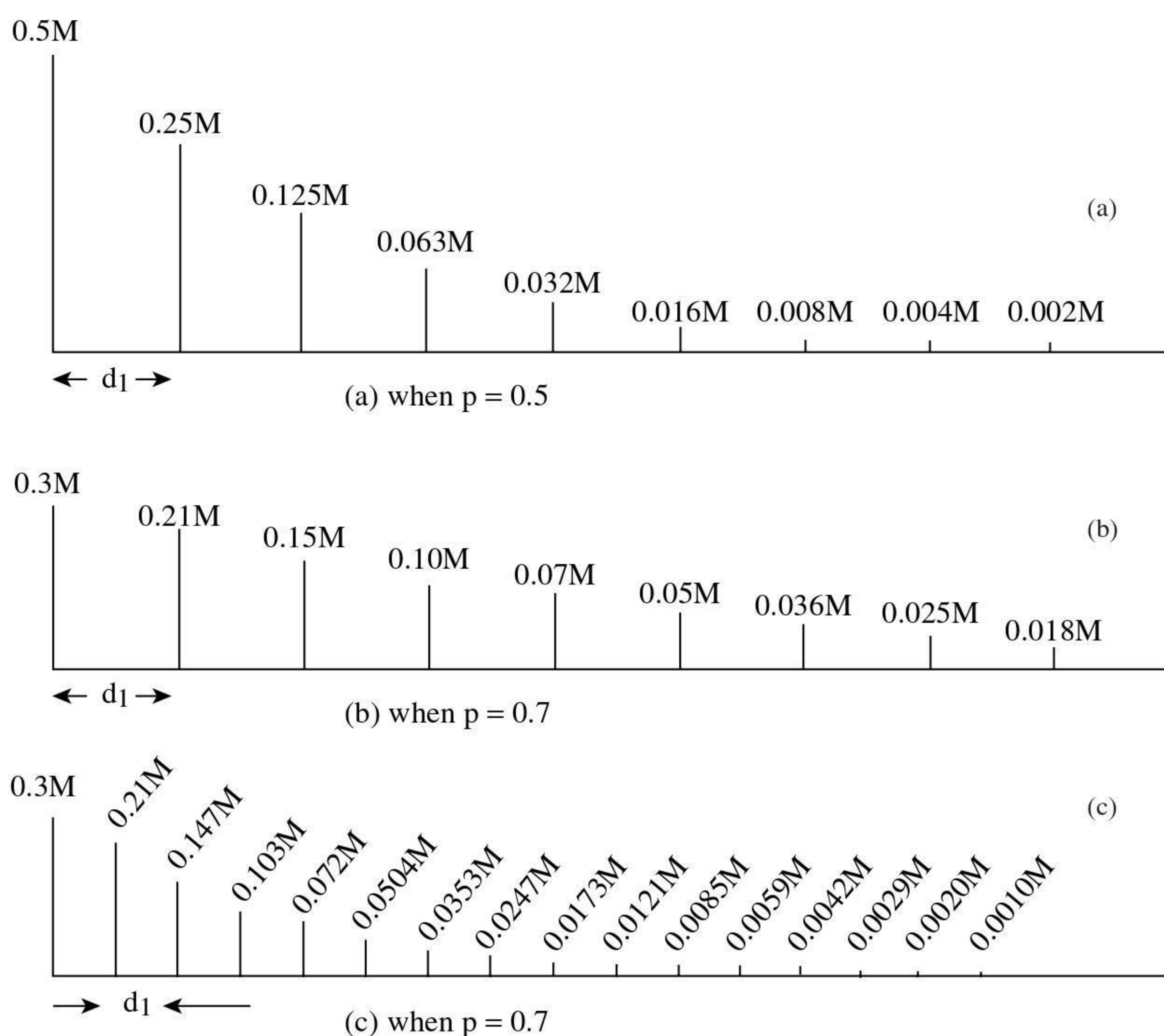


FIGURE 4.11 Blending effect of retaining power of worker. Data show decreasing amounts of red fiber mass removed by the swift per worker revolution.

carding zone is marked as successive blocks of fibers, A, B, C, ..., G, as shown in Figure 4.12. Each block is of a different color and of length d_1 . If A is our red block, then, when the worker-swift action first separates this fiber mass, the portion removed by the worker will be deposited on B (say, blue fiber mass) as the swift moves B to the point of the swift-stripper interface. If we follow this reasoning through to G (say, green fibers) and think of what the cross section of the fiber mass being taken away by the swift from the worker would look like, the appearance should be a layered structure as illustrated in Figure 4.12. This superposition of fibers is equivalent to a doubling action at the drawframe or gillbox (see Chapter 5). As depicted, the higher p-value, resulting in smaller amounts of fiber mass being removed by the swift, gives a better superposition blending-leveling effect.

Although increased p-values give better blending and leveling, increased worker speeds can militate against this in two ways. For example, if the worker speed is doubled, the time taken to redeposit the fiber retained by the worker will be halved. This reduces the blending-leveling effect, since the amounts of the red tuftlet carried forward by the swift, even though smaller, will now be half the distance apart.

Figure 4.13 illustrates the situation in which two worker/striper pairs are run at the same speed. A and B are the respective fractions carried forward by the swift and retained by the first worker and, similarly, D and C at the second worker/swift interface. If the distance between the two worker/striper pairs is such that, by the time B arrives at the second stripper, C is deposited on it, it can be seen that, when

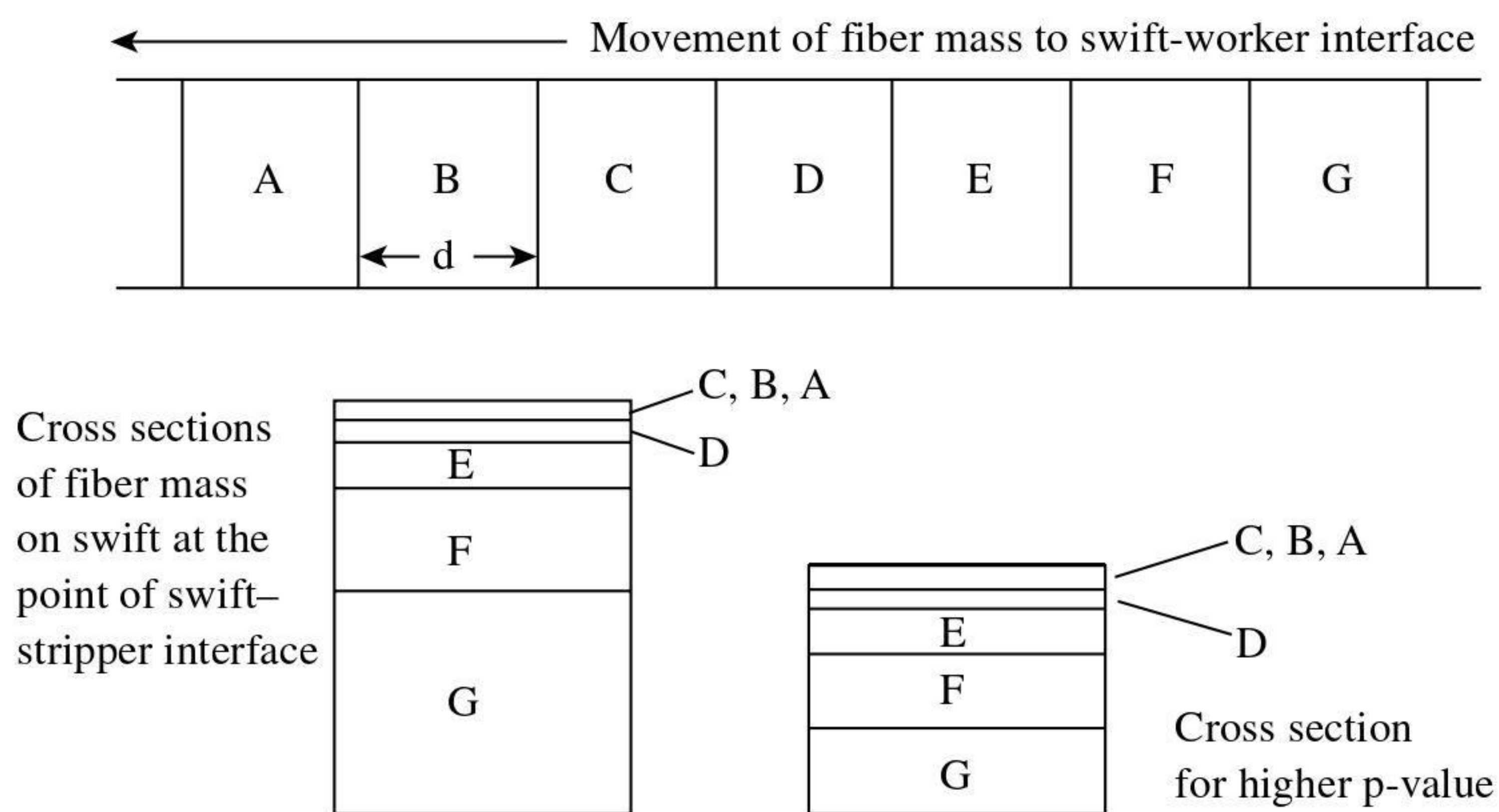


FIGURE 4.12 Effect of worker retaining power on blending by superposition.

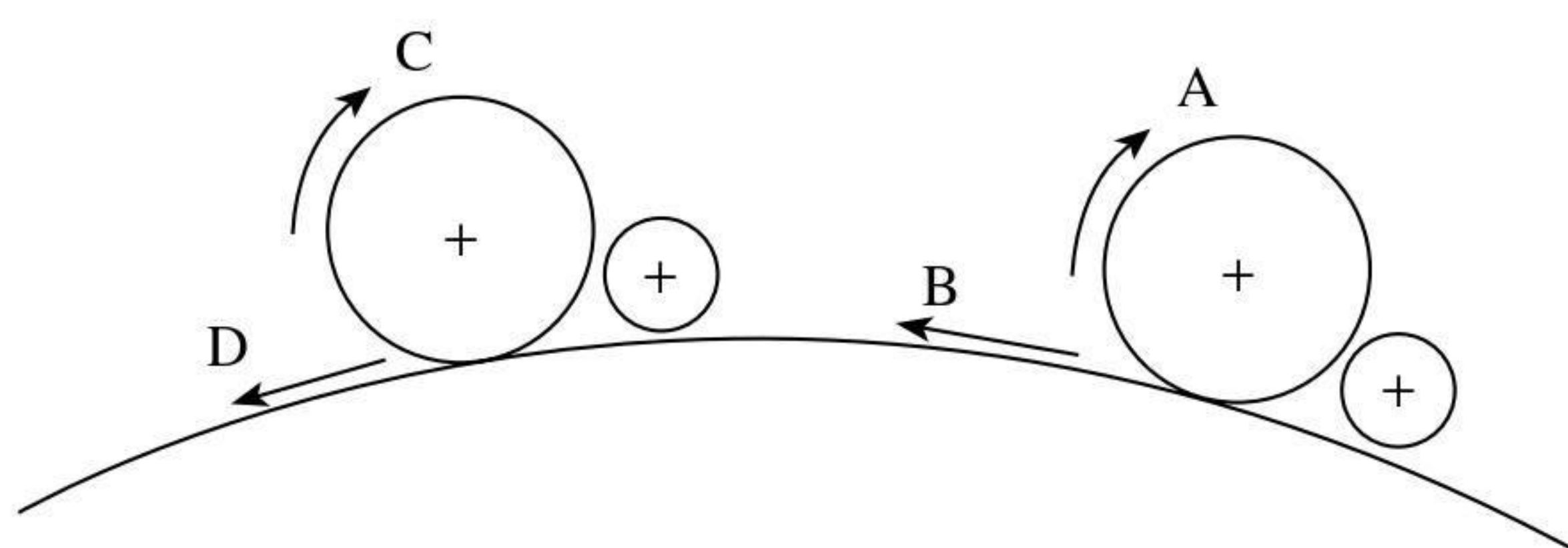


FIGURE 4.13 Effect of multiple worker-stripper pairs.

the workers have the same surface speed, as A arrives at the stripper of the second worker, B will be deposited on it. Since A and B are portions of the same retained material, the superposition of B on A militates against the blending and leveling actions. Worker/stripper pairs are usually mounted fairly close to each other so as to fit multiple positions over the top of a swift. It is therefore important that workers on the same swift run at different speeds.

4.3 WEB FORMATION AND FIBER CONFIGURATION

4.3.1 CYLINDER-DOFFER ACTION

In [Chapter 3](#), it was stated that fibers on the cylinder or swift were transferred onto the doffer and accumulated to form the doffer web as a result of the opposing directions of the saw-tooth-wire clothing of each roller set in close proximity, i.e., point-of-tooth to point-of-tooth action. In this section, we consider in greater detail the mechanism of fiber transfer with reference to the many studies undertaken to elucidate the possible effect of process variables. For ease of explanation, only the term *cylinder* will be used, since the swift is essentially the cylinder of the roller-clearer card.

Like the carding zone, the close cylinder-doffer setting has made it difficult to use photography to directly observe fiber transfer. However, several studies have made useful attempts at doing so, including the use of laser-doppler anemometry.^{2-4,16-18} These, along with other research, have helped to establish an understanding of the transfer mechanism. The referenced studies include work on the roller-clearer card, since the way fibers behave in the cylinder-doffer zone is comparable in both card types.

4.3.1.1 Fiber Configuration and Mechanism of Fiber Transfer

First, it is important to remember from [Chapter 3](#) that, ideally, there should be only individual fibers on the cylinder clothing as the cylinder surface leaves the carding zone and approaches the doffer transfer zone. Although, when viewed on the cylinder, these individual fibers appear to form a thin, filmy web (i.e., the cylinder web), they are transferred from the cylinder to the doffer not in the form of a web of fibers but as individual fibers. This gives rise to the shapes fibers have in the doffer web, i.e., the fiber configurations. The work by Sengupta and Chattopadhyay¹⁹ demonstrates this point.

While carding viscose fibers, they placed specially prepared viscose fiber tufts into the batt feed to a revolving-flats card. The fibers in these tufts were parallelized and had their ends dyed different colors so that they could be easily identified among the bulk of the fibers when observed on the cylinder surface prior to transfer, and then in the doffer web immediately after transfer. The idea was that these tracer fibers would be representative of the shapes fibers adopt before and after transfer. The fiber shapes observed were grouped into the five classes of configuration, illustrated in [Figure 4.14](#), and the relative frequencies of occurrence were determined.

[Table 4.3](#) shows that, both before and after transfer, most fibers had a hooked configuration. Prior to transfer, the vast majority of tracer fibers observed had a

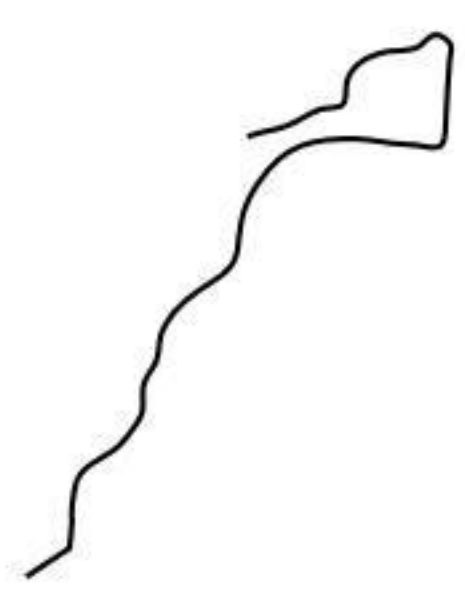
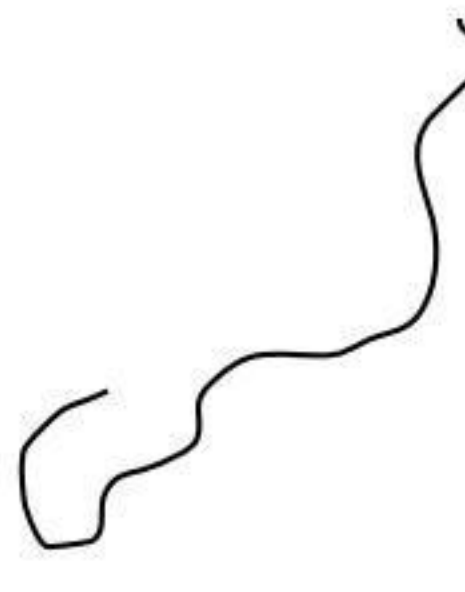

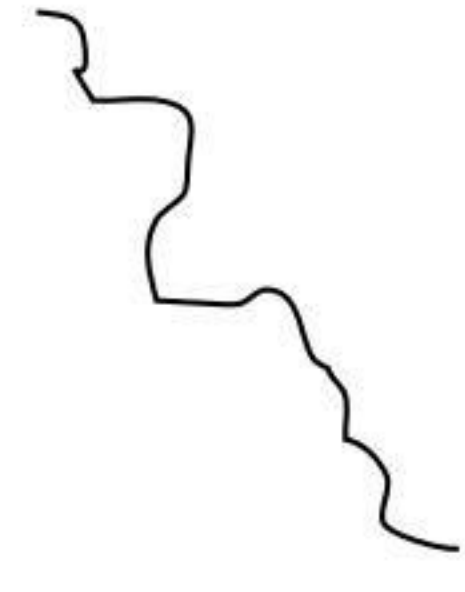

Group I	Group II	Group III	Group IV	Group V
				Other
Direction of Sliver Delivery from the Card 				

FIGURE 4.14 Classification of observed fiber configurations in doffer web.

leading hook configuration, i.e., hooked around the saw-teeth of the cylinder clothing. Their trailing ends showing no hooked configuration. In the doffer web, the greater proportion of the tracer fibers had trailing hooks. However, leading hooked and double-hooked fibers constituted a sizeable percentage of the observed tracer fibers, and there was a substantial drop in the number of straight fibers. A much earlier study by Morton and Summer²⁰ considered only the fiber configurations in the sliver but, although the relative values for the five classes were different from Sengupta and Chattopadhyay's data, the general trend was the same.

An important observation by Sengupta and Chattopadhyay was the mode of transfer of fibers from the cylinder to the doffer. Table 4.4 shows that around 50% of fibers underwent reversal during transfer so that their trailing ends became leading ends. The majority did so with a change of configuration. Of the 50% that did not undergo reversal, the majority also changed configuration. In total, 73% of fibers changed configuration. This particular observation of reversal, nonreversal, and change and no-change of configuration indicates that fibers transfer from the cylinder to the doffer as individuals and not in the form of a web of fibers.

TABLE 4.3
Fiber Configuration Before and after Cylinder-to-Doffer Transfer

Location	Trailing hooks*	Leading hooks†	Double hooks‡	No hooks (straight)	Other§	Total
Cylinder surface	61%	4.3%	4.3%	26.1%	4.3%	100%
Doffer web	43.5%	19.6%	21.7%	10.9%	4.3%	100%

*Trailing ends hooked, leading ends not hooked.

† Leading ends hooked, trailing ends not hooked.

‡Both ends hooked.

§Other configurations.

Figure 4.15²¹ shows that the cylinder-doffer region can be divided into two by an imaginary line passing through the point of closest approach of the two rollers,

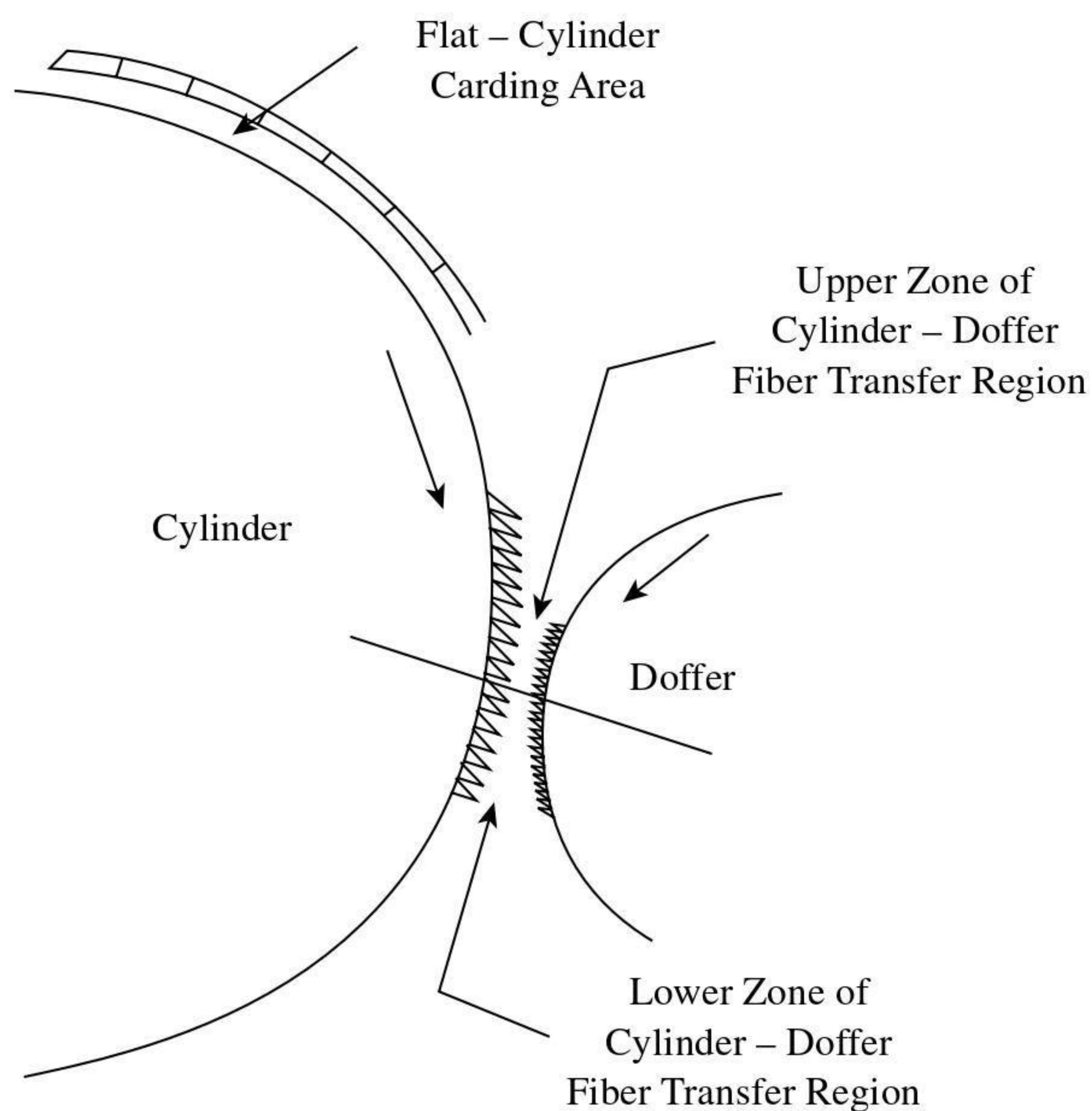


FIGURE 4.15 Upper and lower fiber transfer zones.

TABLE 4.4
Mode of Fiber Transfer from Cylinder to Doffer

Configuration in doffer web	Configurations and relative frequency cylinder surface			
	Leading (L) (65%)	Trailing (T) (4%)	Double hooks (D) (4%)	No hooks (N-H) (27%)
L (%)	5 (R-C) 5 (NR-NC)	2 (R-NC)	2 (NR-C)	3 (R-C) 4 (NR-C)
T (%)	16 (R-NC) 16 (NR-C)		2 (R-C)	7 (RC) 5 (NR-C)
D (%)	4 (R-C) 12 (NR-C)	2 (R-C)		2 (R-C) 2 (NR-C)
N-H (%)	5 (R-C) 2 (NR-C)			2 (R-NC) 2 (NR-NC)

Change of configuration during transfer from cylinder to doffer and mode of change: R-C = reverse + change, R-NC = Reverse + no change, NR-C = no reverse + change; NR-NC = no reverse + no change.

i.e., the cylinder-doffer setting line. The two regions may be referred to as the top and bottom cooperation arcs¹⁷ or, more simply, the top and bottom transfer zones.²¹ Most published studies support the idea that fiber transfer from the cylinder to the doffer largely occurs in the top zone, leading to the formation of the five classes of fiber configurations.

Based on their work with woolen cards, WIRA (formerly, the Wool Industry Research Association, now the British Textile Technology Group, BTTG)²³ reports that the transfer of fibers from cylinder (i.e., swift) to doffer is mainly a mechanical action involving the clothing of the two rollers, and that aerodynamic effects are small. A simple experiment was used to demonstrate this idea.

While carding an undyed fiber, a small square web of colored fibers was pressed into the doffer clothing to fully occupy the length of each tooth within the area of the square. Following fiber transfer, only a few undyed fibers were found on the web of colored fibers, even though the undyed fibers had formed a web surrounding that of the colored fibers. The web of colored fibers had therefore shielded the doffer clothing and prevented the mechanical action of fiber transfer within the area of the square. In the top zone, the circumferences of the two rollers converge toward the setting line and then diverge away from it in the bottom zone. It was assumed that the mechanical action of transfer would take place mainly in the top zone.

A second experiment established that, in the top zone, as fibers on the cylinder approached the setting line, their trailing lengths were lifted from the cylinder surface by the action of circular motion and centrifugal forces. This lifting of the trailing lengths makes it easier for fibers to be caught by the doffer clothing.

The experimental method used was to direct a narrow, rectangular beam of light onto the cylinder surface and take sideways photographs of the rotating surface along a line parallel to the axis of rotation. From the photographs, measurements were made of the distances that the fiber trailing ends lifted from the cylinder surface, i.e., the distance of projection, and Figure 4.16a shows a distribution of the measured distances. Because the cylinder-doffer setting is smaller than the average distance of projection, fibers will make contact with the doffer clothing over a certain length of the doffer circumference. Figure 4.16b and c show that this length of arc depends

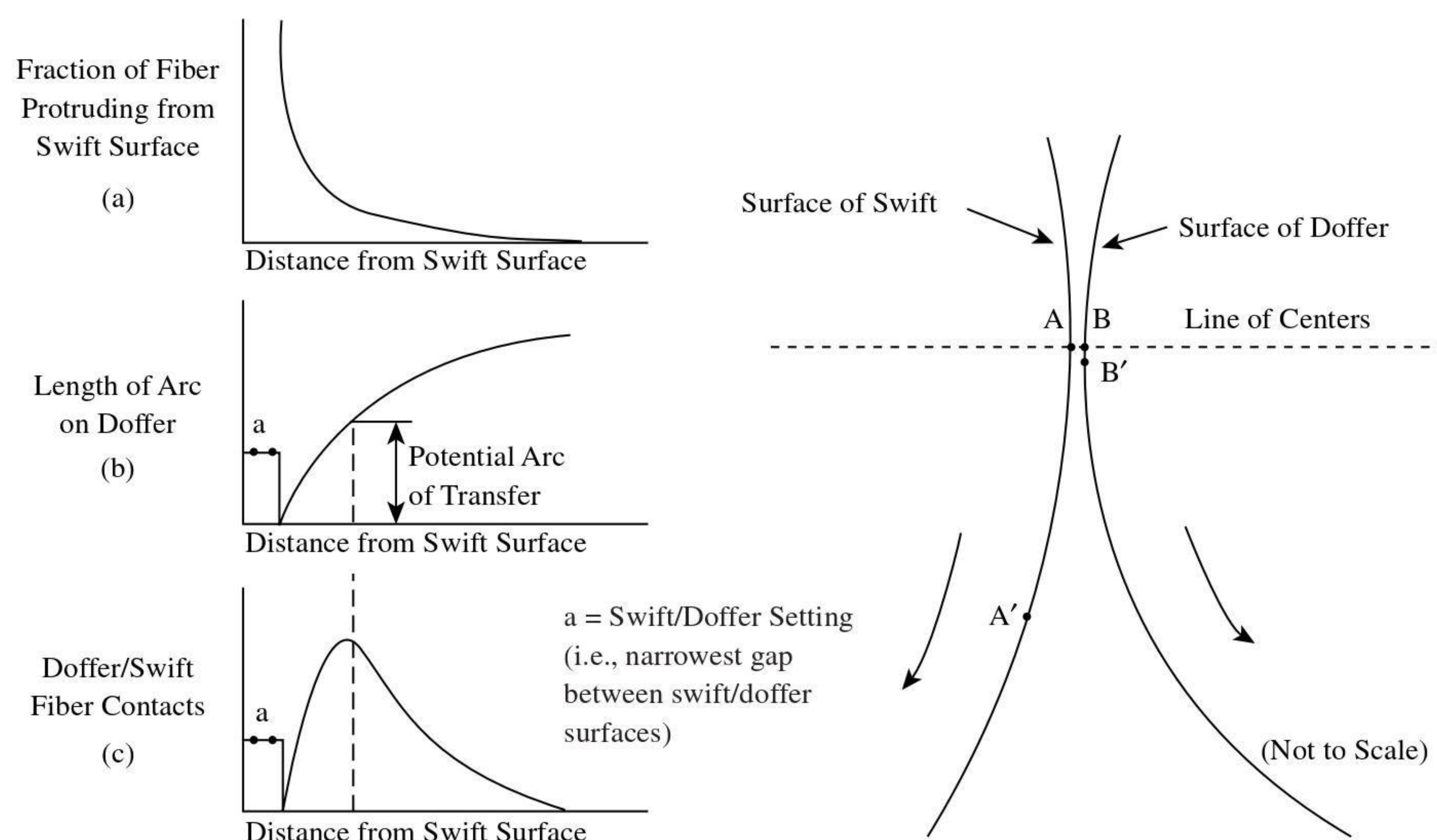


FIGURE 4.16 Cylinder-doffer transfer of fibers. (Courtesy of WIRA.)

on the fiber's distance of projection, and superimposing the two curves gives an indication where most fibers will be in contact with the doffer clothing, i.e., the potential arc of transfer.

Morton and Summers²⁰ suggest that, as the trailing ends of fibers lift from the cylinder surface, some become hooked around the teeth of the doffer clothing. The saw-tooth geometry of the doffer clothing has a steeper working angle and a longer length than the cylinder clothing; therefore, the frictional drag of the doffer clothing eventually removes these fibers from the cylinder clothing. This mechanism of fiber transfer explains Sengupta and Chattopadhyay's observations of fibers in the doffer web having trailing hooks without undergoing the reversal of their leading and trailing ends. A second mechanism for the formation of trailing hooks, attributed to Modi and Joshi,²² is simply that leading-hook fibers on the cylinder undergo reversal during transfer but without a change of configuration.

Sengupta and Chattopadhyay proposed two mechanisms for the formation of leading hooks in the doffer web. The first is that some leading hooked fibers, particularly those near the tip of a sawtooth, slide off the cylinder clothing and land on the doffer without reversal or change of configuration. The second is that other fibers slip from the cylinder with a reversal of trailing and leading ends. What was the trailing end gets buckled during landing on the slower-moving doffer surface. If, during reversal, the end sliding off the cylinder clothing becomes straightened, then a leading hook configuration will be formed. However, if the end retains its shape, a double hook configuration occurs.

No suggestion is reported in the literature of how the *nonhooked* and *others* configurations may be formed. However, we can use the above ideas to conjecture on how these shapes could occur. It is likely that, as the trailing ends of some fibers lift, they make contact with the cylinder housing just prior to the doffer. The frictional drag of the housing would be sufficient to pull such fibers from around the sawteeth of the cylinder clothing and, in doing so, straightening the leading hooked end. These fibers would be entrained in the boundary air-layer moving with the cylinder rotation and would eventually land onto the doffer in a *nonhooked* configuration.

Although most researchers consider that fiber transfer occurs in the top zone, Simpson²¹ suggests that transfer can take place in both zones and that the particular zone in which transfer actually occurs influences the fiber configuration and is

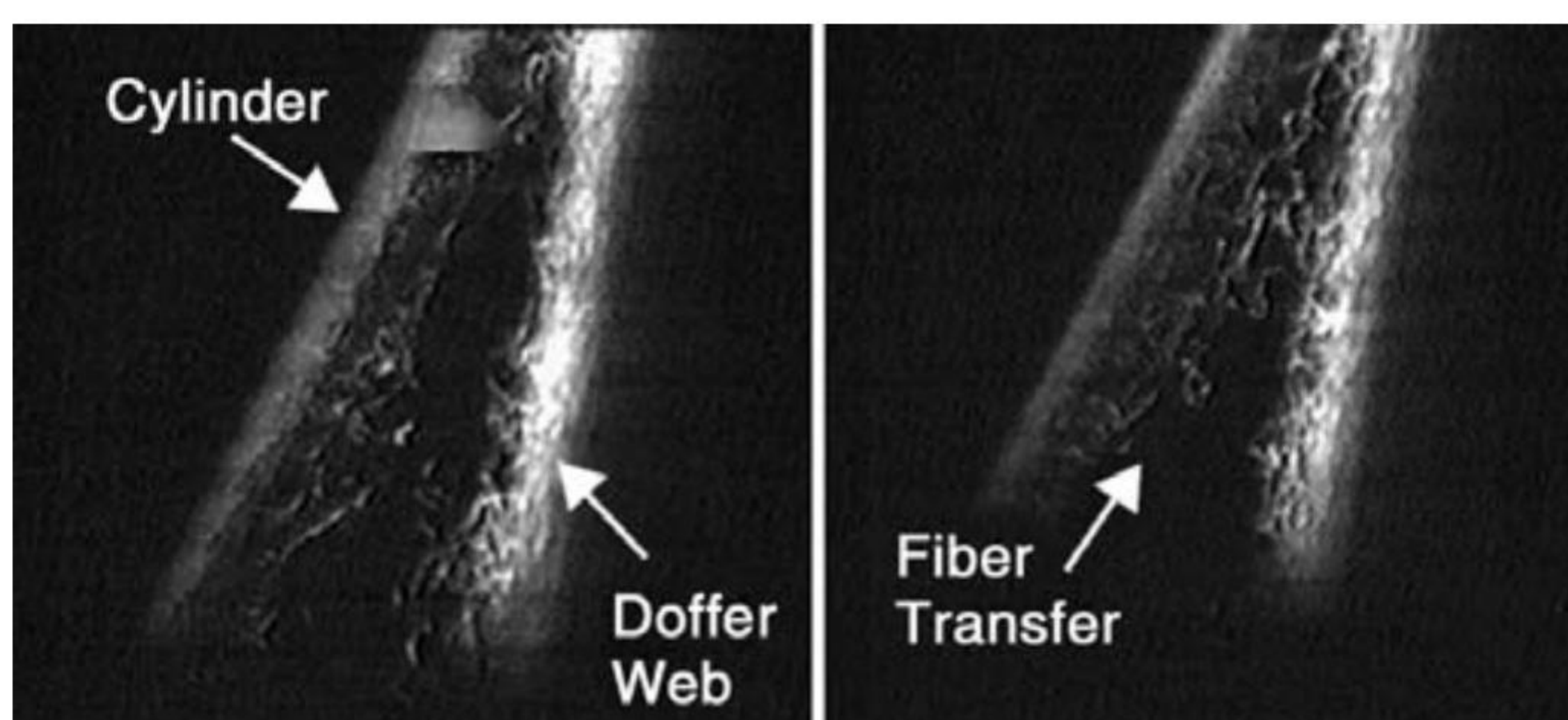


FIGURE 4.17 Fiber transfer from cylinder to doffer in revolving flats card.

dependent on the cylinder-doffer surface speed ratio. The majority of fibers transfer in the top zone, and increasing the ratio results in an increase in the number of such fibers and a larger number of trailing than leading hook fibers. Decreasing the ratio causes more fibers to be transferred in the bottom zone, and the percentage of trailing hooks increases, whereas leading hooks decrease. Let us look, therefore, at the possibility of fiber transfer in the bottom zone.

Consider the two points, A and B, shown in [Figure 4.16](#) on the cylinder and doffer surfaces, respectively.²³ For a revolving-flats card, A will be moving at, say, a speed of 26 m/s and B at 1.5 m/s. After, say, 0.01 s, A will have moved 26 mm to A' and B 1.5 mm to B'. The vertical distance between A' and B' will be within the range of a typical fiber length distribution of a Middling grade of cotton. It is possible that the transfer of those fibers that make contact with the doffer clothing and become hooked by the clothing close to the setting line will take place in the bottom zone, having started in the top zone. It can be also reasoned that the higher the doffer speed, the greater the chance that bottom-zone transfer will occur.

Lauber and Wulforth¹⁷ and Dehghani and et al.,²⁴ using laser-doppler anemometry and high-speed photography, studied the fiber dynamics in the bottom zone. Their analysis showed that, in this zone, air turbulence occurs between the two roller surfaces and may disturb fibers that are not securely held by the doffer. [Figure 4.17](#) shows a typical photograph from Dehghani's work. It can be seen that a thin layer of fibers has remained on the cylinder clothing. The outer edge of the doffer web is irregular in appearance, and fibers are caught in the air turbulence. There was also evidence that some fibers were initially held between the two surfaces and subsequently pulled onto the doffer surface. These observations would seem to support Simpson's view that fiber transfer can occur in the bottom zone.

4.3.1.2 Effect of Machine Variables on Fiber Configuration

Ghosh and Bhaduri²⁵ studied the effect of various machine parameters on the fiber configuration in the doffer web. The taker-in speed was found to have no significant effect on the relative proportions of the five classes of configuration. Because of the relative proportion of trailing to leading hooks in the web, it has become the convention to call the former configuration *major hooks* and the latter *minor hooks*. [Table 4.5](#) shows that, with a constant cylinder speed and production rate, increasing the doffer speed reduces the percentage of major hooks but increases the proportion of minor and double hooks. However, increasing the cylinder speed for a fixed doffer speed decreased minor and double hooks without significantly affecting the proportion of major hooks.

It can also be seen from the table that varying the sliver count by increasing doffer speed, while keeping a fixed cylinder to doffer speed ratio and production rate, gave similar results. For a fixed sliver count, an increased production rate means an increase in the doffer speed and a decrease in the cylinder-doffer speed ratio. The associated results show an increased number of minor hooks and a decreased number of major hooks. [Table 4.5](#) indicates that, irrespective of whether the cylinder or doffer surface speed is changed, yarn imperfections increase with increasing cylinder-to-doffer surface speed ratio. However, varying the ratio did not affect yarn strength or yarn irregularity.

TABLE 4.5
Effect of Cylinder and Doffer Speeds, and Sliver Count of Fiber Configuration

Sliver count (ktex)	Doffer speed (rpm)	Cylinder-doffer surface speed ratio	Hook %			Uster imperfections
			MAJ	MIN	B	
I						
4.9	5.0	86.0	75	19	12	114
4.4	5.6	77.1	73	19	12	102
3.5	7.0	61.4	68	28	16	92
2.8	8.0	48.5	64	30	17	82
II	Cylinder speed (rpm)					
3.5	65	18.6	64	43	25	276
3.5	180	51.4	75	29	18	120
3.5	215	61.4	68	28	16	92
3.5	270	77.1	68	24	14	–
3.5	315	90.0	69	21	14	87
III	Cylinder speed (rpm)	Doffer speed (rpm)				
4.4	5.9	158	74	19	11	133
3.2	8.3	220	79	27	18	118
2.2	11.8	315	65	39	22	88

I = cylinder (rpm), 215; carding rate, 3.2 kg/h. II = doffer (rpm), 7; carding rate, 3.2 kg/h. III = cylinder–doffer surface speed ratio, 53.3; carding rate, 3.6 kg/h; MAJ = major hooks; MIN = minor hooks; B = double hooks.

Simpson^{26–29} used an indirect method called the *cutting ratio*³⁰ for determining major and minor hooks and reported similar results to Ghosh and Bhadwi. However, the effect of increasing the cylinder-doffer speed ratio on major hooks became smaller as the card production rate increased but was larger for minor hooks.

Using either a three-roller doffing device or a doffer comb to remove the card web from the doffer was found to have no effect on fiber configuration.²⁵ However, the draft applied to the web as it is stripped from the doffer and condensed into a sliver, i.e., calender draft, can alter the relative proportions of the fiber classes of configuration. The tendency is to straighten fibers.^{20,25} Increasing the calender draft decreases the percentages of hooked fibers and increases that of nonhooked fibers. The average fiber extent for the various configurations increased with calendar draft. The fiber extent for major hooks was found to be smaller than for minor hooks, which suggests that the former has a longer length of hook, making it more difficult to straighten by the calendar draft.

4.3.1.3 Recycling Layer and Transfer Coefficient

The presence of a fiber layer on the cylinder clothing in the bottom transfer zone, observed by Lauber and Dehghani, indicates that not all the fiber mass on the cylinder leaving the carding zone becomes part of the doffer web on first contact with the

doffer clothing. Using the tracer fiber technique of different-colored fiber ends, Ghosh and Bhaduri²² found that fibers generally went around with the cylinder for several revolutions before being incorporated in the doffer web. Earlier work was carried out by Debar and Watson³¹ in which radioactive tracer fibers were employed to determine the motion of fibers during carding. They found that, on first contact with the doffer clothing, only 20% of tracer fibers became part of the doffer web; most fibers passed the doffer up to a maximum of 20 times before being incorporated into the doffer web. Some tracer fibers, as they made several cylinder revolutions, were caught more than once by the flats. Other researchers^{13,25,32} have reported figures within the range of 10 to 25 cylinder revolutions before fibers are transferred. Whatever the actual figure, it is clear that only a fraction of the fiber mass on the cylinder clothing leaving the carding zone is transferred to the doffer, and that a recycling layer is present on the cylinder after the transfer zone.

Krylov¹³ showed that the relative distribution of the fiber mass in a revolving-flats card operating under steady conditions may be depicted by Figure 4.18. A similar approach can be taken to illustrate the mass distribution for the roller-clearer card.

Important to an understanding of fiber transfer are the following fiber mass values per revolution of the cylinder:

- Q_o , the operational layer, i.e., the fiber mass leaving the carding zone
- Q_1 , the mass transferred from cylinder to doffer
- Q_2 , the mass of the recycling layer

The ratio of Q_1 to Q_o is termed the transfer coefficient, K , and can be measured as described below.

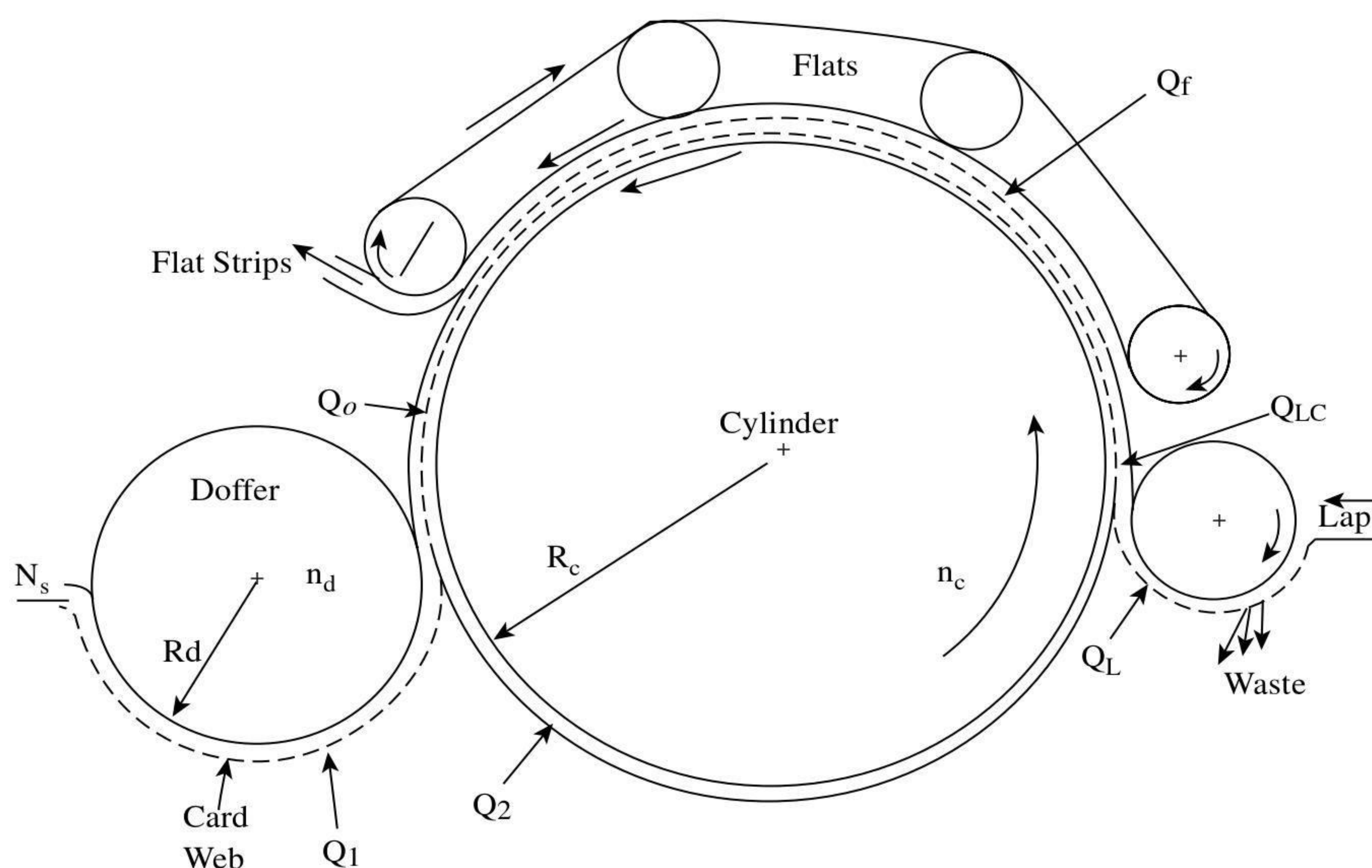


FIGURE 4.18 Representation of the fiber mass distribution within a revolving-flats card.

After the card has reached a steady running state, the feed, doffer, and flats (or workers and strippers) are stopped while the cylinder continues running. The doffer is then restarted with the feed and flats (workers and strippers) out of action. Initially, the doffer will present the part of the web that was on it when it was stopped. This is easily detached along a visible dividing line formed when the feed roller was stopped. The mass of the remaining part of the web will be Q_o .

Within a single revolution of the cylinder, a point on the doffer would travel a distance of

$$L_d = \frac{2\pi R_c V_d}{V_c} \quad (4.4)$$

where R_c = the cylinder radius (m)

V_c = cylinder surface speed (m/min)

V_d = doffer surface speed (m/min)

If T is the sliver count in ktex, and P is the card production rate in kg/h, then

$$P = 3.6V_d T$$

$$Q_1 = TL_d = \frac{2\pi R_c T V_d}{V_c} = \frac{200\pi R_c P}{3.6V_c}$$

and

$$Q_o = \frac{200\pi R_c P}{3.6KV_c} \quad (\text{in grams}) \quad (4.5)$$

Hence, from the measurement of Q_o , K can be calculated for known production parameters. Reported values for K are within the range of 0.02–0.18,^{13,22,61} This means that, with each cylinder rotation, 82 to 98% of the fiber mass (Q_o) remains on the cylinder as the recycling layer, Q_2 .

From [Figure 4.18](#), if Q_L is the fiber mass on the taker-in, then this will be drafted to give the mass Q_{LC} fed to the cylinder with each cylinder revolution,

$$Q_{LC} = \frac{Q_L V_t}{V_c} \quad (4.6)$$

where V_t and V_c = the taker-in and cylinder surface speeds, respectively

The mass going into the carding zone with each revolution of the cylinder is $Q_{LC} + Q_2$ and is called the *cylinder load*; that leaving the zone is

$$Q_o = Q_{LC} + Q_2 - Q_f \quad (4.7)$$

where Q_f = the fiber mass per cylinder revolution contributing to the flat waste

An equation for the roller-clearer card would not include Q_f .

Although an important parameter, Q_f is much smaller than $Q_{LC} + Q_2$. Therefore, Q_o may be taken as a practical estimation of the cylinder load for the card. Hence, from the start of carding, the buildup of cylinder load, Q_o , the doffer web, Q_1 , and the recycling layer, Q_2 , will follow the geometric progression given in [Table 4.6](#).

When n is very large, there is continuity of fiber mass and, ignoring the flat-strap waste, the mass from the taker-in onto the cylinder, per revolution of the cylinder, equals the mass transferred to the doffer, i.e., $Q_1 = Q_{LC}$.

4.3.1.4 Factors that Determine the Transfer Coefficient, K

There are two actions that form the recycling layer. The first is termed the *retaining power of the cylinder*.²³ We learned earlier that the leading ends of most fibers on the cylinder are hooked around a tooth of the cylinder clothing. The remaining length of a hooked fiber is, however, longer than the tooth pitch and will make contact with several teeth and with other close-by fibers. The resulting frictional forces will oppose transfer of the fiber. Where such frictional forces are sufficiently large, they will retain fibers on the cylinder. Circular and centripetal forces will try to lift fibers off the cylinder surface to be caught by the doffer. Therefore, the retaining power is inversely proportional to the square of cylinder surface speed and to the working angle of tooth of the cylinder clothing, but directly proportional to the fiber-fiber and fiber-metal friction coefficients.³²

The second action is the cylinder clothing taking back, from the doffer web, previously transferred fibers. It was explained earlier that most fibers are transferred onto the doffer in the top zone to form the doffer web. In forming this web, fibers build up to fill the doffer clothing, and some will project beyond the tooth height of the clothing. Those fibers protruding beyond the total distance of tooth height plus the cylinder-doffer setting will be subsequently caught by the cylinder teeth moving toward the setting line. The effect is a robbing back by the cylinder of previously transferred fibers that are not securely held by the doffer clothing. DeSwann³³ demonstrated that fibers are removed from the doffer by the cylinder clothing. In pulling fibers back onto the cylinder surface, the saw-tooth clothing of the cylinder is said to impart a combing action on the doffer web and may influence fiber configuration by straightening leading hooks.²²

Based on the mechanism for fiber transfer, particularly in the top zone, the transfer coefficient is governed by the tooth angle, tooth density, and the circular motion and diameters of the cylinder and the doffer. These factors influence the effectiveness of the two rollers to hold fibers onto their respective clothing, i.e., their retaining powers and thereby determine the transfer coefficient K . [Figures 4.19](#) and [4.20](#) illustrate forces that control the retaining power. There are two situations to consider. First, there is the case of fiber shedding, where fibers are thrown off the cylinder before contact with the doffer. Second, there is the opposing action of the respective clothing when they are simultaneously in contact with a fiber.

In the case of fiber shedding, for simplicity,³⁴ we can refer to the centrifugal force and the opposing frictional force acting on a fiber. These forces will give rise to the resultant force S . The resolved component J slides the fiber to the tip of the

TABLE 4.6
Buildup of Cylinder Load, Doffer Web, and Recycling

Cylinder revolution	Fiber mass feed to cylinder	Cylinder load, Q_0	Fiber mass transferred to doffer, Q_1	Recycling layer, Q_2
1	Q_{LC}	Q_{LC}	$Q_{LC}K$	$Q_{LC}[1 - K]$
2	Q_{LC}	$Q_{LC} + Q_{LC}[1 - K]$	$K \{Q_{LC} + Q_{LC}[1 - K]\}$	$[1 - K] \{Q_{LC} + Q_{LC}[1 - K]\}$
3	Q_{LC}	$Q_{LC} \{1 + [1 - K] + [1 - K]^2\}$	$Q_{LC} \{1 + [1 - K] + [1 - K]^2\}$	$[1 - K] Q_{LC} \{1 + [1 - K] + [1 - K]^2\}$
n when $n \rightarrow \infty$		$Q_{LC} \frac{\{1 - [1 - K]^n\}}{K}$	$Q_{LC} \{1 - [1 - K]^n\}$	$Q_{LC}[1 - K] \frac{\{1 - [1 - K]^n\}}{K}$
$[1 - K]^n \rightarrow 0$	Q_{LC}	$\frac{Q_{LC}}{K}$ (4.8)	Q_{LC} (4.9)	$Q_{LC} \frac{[1 - K]}{K}$ (4.10)

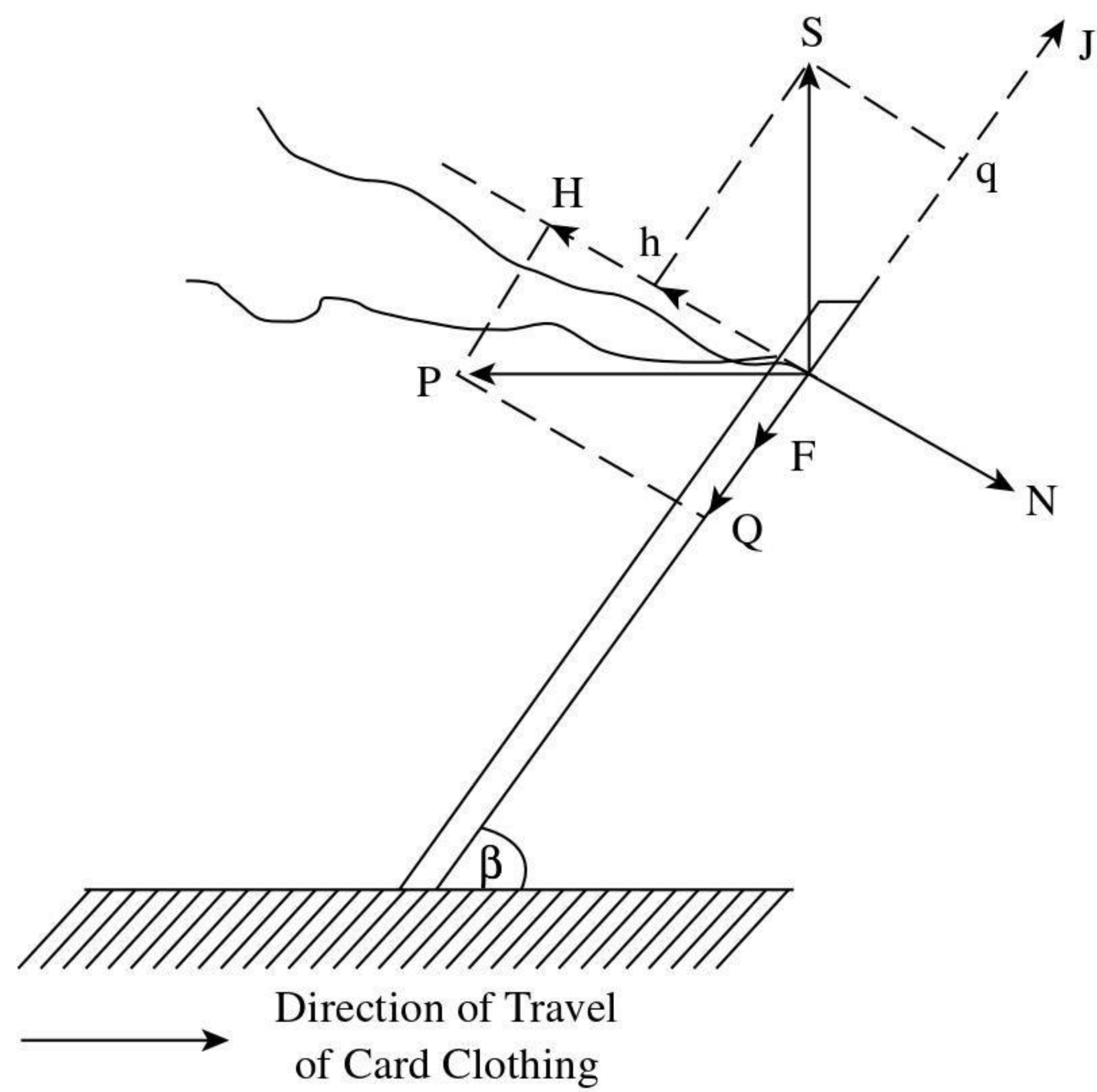


FIGURE 4.19 Fiber shedding forces.

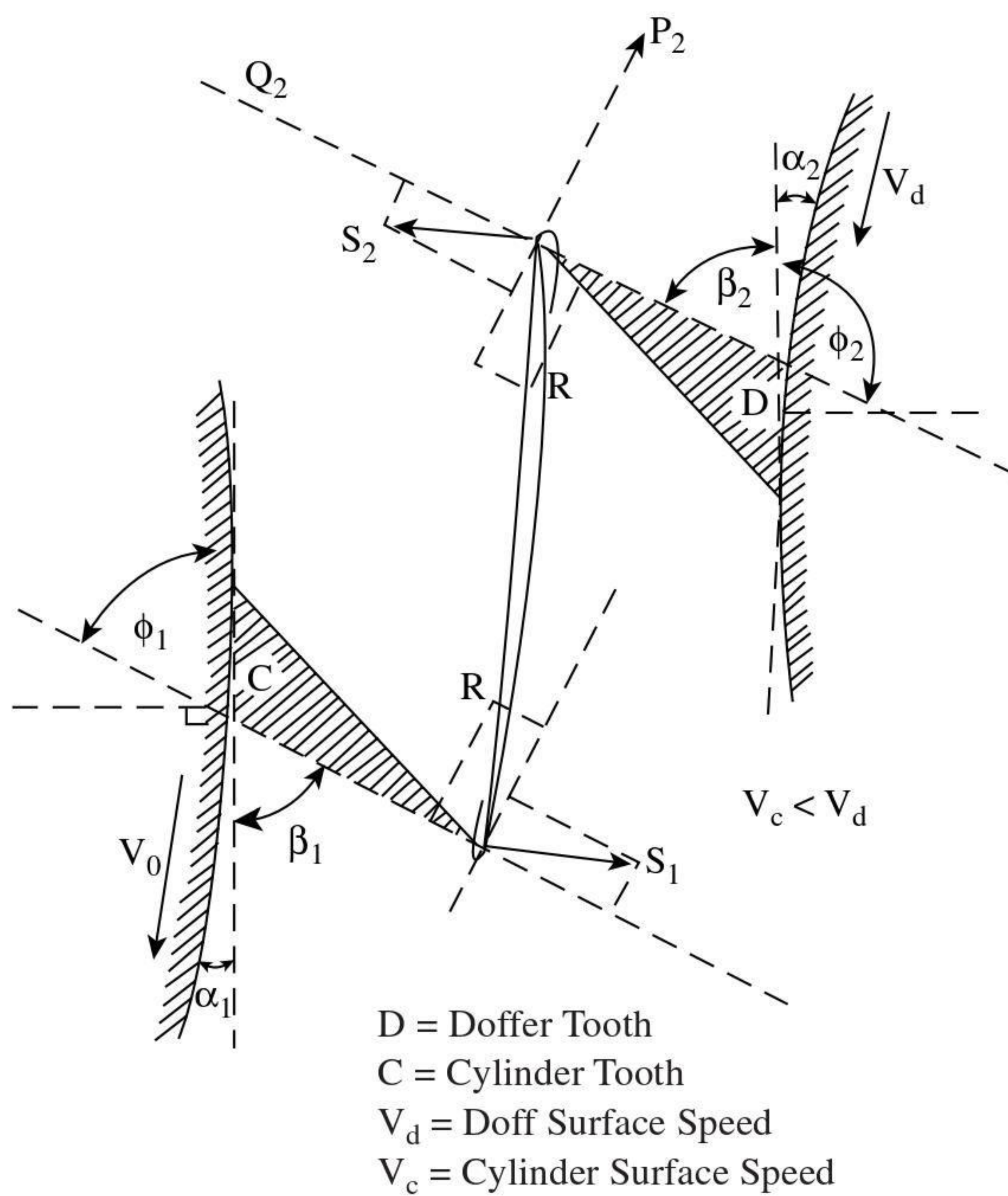


FIGURE 4.20 Interaction of cylinder-doffer fiber transfer.

tooth against the opposing forces Q and F , as shown in Figure 4.19. The fiber motion will be affected by aerodynamic drag giving rise to force P . We may assume that S and P are acting at the point of interaction between the tooth and the fiber. Thus, resolving along the working face of the tooth (direction q) and normal to the face, (direction h) to derive forces H , Q , F , and J , we get the equations of equilibrium,

$$P \sin \beta + S \cos \beta = N \quad (4.11)$$

$$P \cos \beta + \mu N = S \sin \beta \quad (4.12)$$

Hence, the condition for fiber shedding must be $P \cos \beta + \mu N < S \sin \beta$.

Substituting for N ,

$$\frac{S}{P} > \frac{\cos \beta + \mu \sin \beta}{\sin \beta - \mu \cos \beta} \quad (4.13)$$

Table 4.7 gives the required minimum values for S/P ratio for differing β and μ , and we can see that fiber shedding occurs more readily at larger angles and smaller coefficients of friction. S increases with the cylinder speed more significantly than P . Thus, the tendency for fiber shedding will increase with cylinder speed. The opposing frictional force acting on a fiber-trailing length will be higher for longer fibers. Fiber shedding is more likely to occur with short fibers.

TABLE 4.7
S/P Ratios for Differing β and μ

Fiber-Metal Friction Coefficient (μ)	Angle of Inclination (β) (Degrees)	Ratio S/P
0.20	66	71
0.23	60	93
0.23	66	75
0.23	70	66
0.26	66	80

Figure 4.20 shows the interaction of the cylinder and doffer and the principal forces involved in the opposing action of the clothing in the transfer zones. Using this arrangement, Baturin³⁵ derived an equation for the transfer coefficient as a function of the machine parameters. The angles β_1 and β_2 are the working angles of the clothing, and α_1 and α_2 are results of the curvature of the roller surfaces in relation to the tangent at the base of tooth of the roller clothing. The boundary of the bottom transfer zone is a distance H from the setting line. If the fiber length is L_f , then the vertical distance from the setting line to the base of the tooth on the doffer in the bottom transfer zone is approximately $(H - L_f/3)$ and $(H + L_f/3)$ for the cylinder. Hence,

$$\alpha_1 = \arcsin \frac{(H + L_f/3)}{R_c} \quad \text{and} \quad \alpha_2 = \arcsin \frac{(H - L_f/3)}{R_d}$$

where R_c and R_d are cylinder and doffer radii, respectively.

The action of the teeth on the fiber sets up a tension R within the fiber. Thus, $R \cos[\beta + \alpha]$ tends to push the respective fiber ends to the base of the teeth. This is, however, opposed by a component of the force S and the frictional force, $\mu(R \sin[\beta + \alpha] + S \cos[\beta + \alpha])$. Resolving along the working surface of the tooth for the respective clothing, we get the equations for equilibrium,

$$R (\cos \phi_1 + \mu \sin \phi_1) = S_1 (\sin \phi_1 - \mu \cos \phi_1) \quad (4.14)$$

$$R (\cos \phi_2 + \mu \sin \phi_2) = S_2 (\sin \phi_2 - \mu \cos \phi_2) \quad (4.15)$$

where $\phi = \beta + \alpha$

Since S tends to reduce the retaining power of the clothing, we may assume it to be inversely proportional to the retaining power. Thus, the ratio $S_2:S_1$ will be related to the ratio of the fiber masses on the two rollers after transfer, i.e., Q_1 and Q_2 .

Hence,

$$Z_1 = \frac{S_2}{S_1} = \frac{(\cos \phi_2 + \mu \sin \phi_2)(\sin \phi_1 - \mu \cos \phi_1)}{(\sin \phi_2 - \mu \cos \phi_2)(\cos \phi_1 + \mu \sin \phi_1)} \propto \frac{Q_1}{Q_2} \quad (4.16)$$

(The symbol \propto indicates “proportional to.”)

The cylinder and doffer usually have differing tooth densities of clothing. We may assume that, if N_d and N_c are the respective densities, their ratio will be proportional to the ratio of the retained fiber masses on the two rollers.

$$Z_2 = \frac{N_d}{N_c} \propto \frac{Q_1}{Q_2} \quad (4.17)$$

Although Z_1 was determined from S_1 and S_2 , it only gives a measure of the effect of the working angles of the clothing. Experimental studies by Krylov¹³ show that the ratio of the retained fiber masses on the cylinder and doffer is inversely proportional to the cylinder surface speed.

$$Z_3 = \frac{1.6 \times 10^6 R_c}{V_c} \propto \frac{Q_2}{Q_1} \quad (4.18)$$

Thus, the relationship between the fiber mass transferred to the doffer, Q_1 , and that retained by the cylinder, i.e., recycling layer Q_2 , is given by

$$Q_1 = Q_2 \frac{Z_1 Z_2}{Z_3} \quad (4.19)$$

$$Q_1 = Q_2 M \quad (4.20)$$

If q and q^* are the fiber mass per unit length of the recycling layer and of the layer transferred to the doffer per cylinder revolution, then $q^* = qM$; $Q_2 = q 2\pi R_c$; $Q_1 = q^*V_d/n_c$; and $Q_o = Q_2 + Q_{LC}$, where n_c is the revolutions per minute of the cylinder, and Q_{LC} is the new fiber layer passing from the taker-in to the doffer. Under steady-state running of the card, $Q_{LC} = Q_1$. The transfer coefficient K is therefore given by

$$\begin{aligned}
 K &= \frac{Q_1}{Q_o} = \frac{q^*V_d/n_c}{\left[\frac{q^*M2\pi R_c}{M} + q^*V_d/n_c\right]} \\
 &= \frac{V_dM}{[M V_c + MV_d]} \\
 &= Z_3 \frac{V_dZ_1Z_2}{[Z_3V_c + Z_1Z_2V_d]}
 \end{aligned} \tag{4.21}$$

Equation 4.21 gives the machine factors that govern the transfer coefficient. Simpson⁶¹ and Brown⁶² found that K is more dependent on Z_1 and Z_3 than on Z_2 , because tooth angle, roller diameter, and roller speed have a greater effect than tooth density on the recycling layer, Q_2 . The greater the ratios of cylinder to doffer tooth angles, diameters, and surface speeds, the lower Q_2 . However, a change in the roller diameters has less effect than changes in tooth angles.

4.3.1.5 The Importance of the Recycling Layer

Reported values show K to be small, ranging from 0.2 to 18%. This means, from Equations 4.8 and 4.10 in Table 4.6, that the recycling layer constitutes a significant part of the cylinder load. Q_2 is therefore important in two respects.

First, because it forms part of the cylinder load, its constituent fibers will be subjected to several cycles of the carding action before permanently being incorporated in the doffer web. Second, by contributing to the cylinder load, it tends to reduce irregularities in the fiber mass transferred from the taker-in to the cylinder and is said to contribute to the *evening action* of the card. It is therefore useful to know what effect the recycling layer has on the carding action and to see how changes in the process parameters affect the size of the recycling layer and the evening action.

To determine the effect of Q_2 on the carding action, Karasev³⁶ used a suction extractor to remove it while the card was in operation. He found that, without the recycling layer, the fiber mass transferred from the taker-in to the cylinder became embedded into the empty teeth of the cylinder clothing. Only the larger tuftlets and groups of individual fibers were then subjected to an effective carding action. There was a greater chance of microtuftlets and small groups of entangled fibers becoming part of the doffer web. The recycling layer therefore acts as a support to new layers of fiber mass from the taker-in, keeping the new fiber mass at the tips of the teeth of the cylinder clothing and thereby enabling better interaction of fibers with the flats (or workers) and cylinder clothing. It should be noted that Q_2 is much greater

than Q_{LC} . Therefore, as both are spread over the cylinder surface entering the carding zone, the fibers in the recycling layer will also make contact with the flats (workers) and ultimately the doffer clothing. Gupta suggests that the rotating cylinder could be considered as a large centrifuge that causes fibers in Q_2 to migrate to the periphery and make contact with the flats (workers) and doffer clothing.

Although the presence of a recycling layer assists the carding action, research findings show that a large recycling layer causes too high a cylinder load and consequently a poor carding action. A number of researchers³⁷⁻³⁸ have applied stochastic theory to the movement of fibers through the card. The mathematical details of such studies are beyond the scope of this book, but it is nevertheless useful to consider some results concerning the influence of the cylinder load on the effectiveness of the carding action. The reported work was for the revolving flat card; however, the reader should note that the trends are applicable to roller-clear cards.

The probability, P_f , of a fiber being carded between the cylinder and flats during one cylinder revolution is given by the ratio of the fiber mass held between flats and cylinder in the carding state, Q_{FC} , to the cylinder load, Q_o , i.e.,

$$P_f = Q_{FC}/Q_o \quad (4.22)$$

The inaccessibility of fibers in the carding state makes it impossible to obtain an exact measurement for Q_{FC} . However, an estimate can be made by assuming the maximum holding capacity of the flats, Q_{FM} , is the sum of the fiber mass held by the flats in the carding state and mass of the flat strip, Q_f . Hence,

$$Q_{FC} = Q_{FM} - Q_f \quad (4.23)$$

By running the card flats at the lowest possible speed and collecting the flat strip at different production rates, a set of increasing values will be obtained until the saturation point is reached. This maximum is a close approximation of Q_{FM} .

P_f is related to the total carding action, so changes in process parameters that affect carding quality will give corresponding changes in the value of P_f . Any process parameter causing a change in the cylinder load Q_o and/or Q_{FC} will either increase or decrease P_f . Figure 4.21 shows how carded ring-spun yarn strength, irregularity, and nep content varied with P_f , and it is evident that better yarn properties are obtained with higher P_f values. The improvement in yarn strength is attributed to the improvement in irregularity.

From the definition of P_f , we can reason that the higher the P_f value, the greater the percentage of the cylinder load that will be fully carded. This means that there will be a more efficient breaking down of tuftlets into individual fibers, reducing the opportunity for microtuftlets and entangled fibers getting into the doffer web and ultimately degrading the yarn properties. Hence, process parameters that reduce Q_o and increase Q_{FC} are important to efficient carding.

Referring to the Equations 4.8, 4.9, and 4.10 in Table 4.6, we can see that the effect of decreasing Q_{LC} is to decrease Q_1 , Q_2 , and Q_o . In practice, there are several card parameters that can be altered to change the value of Q_{LC} . Equation 4.6 shows that the taker-in and cylinder surface speed ratio can be used to decrease Q_{LC} . Because

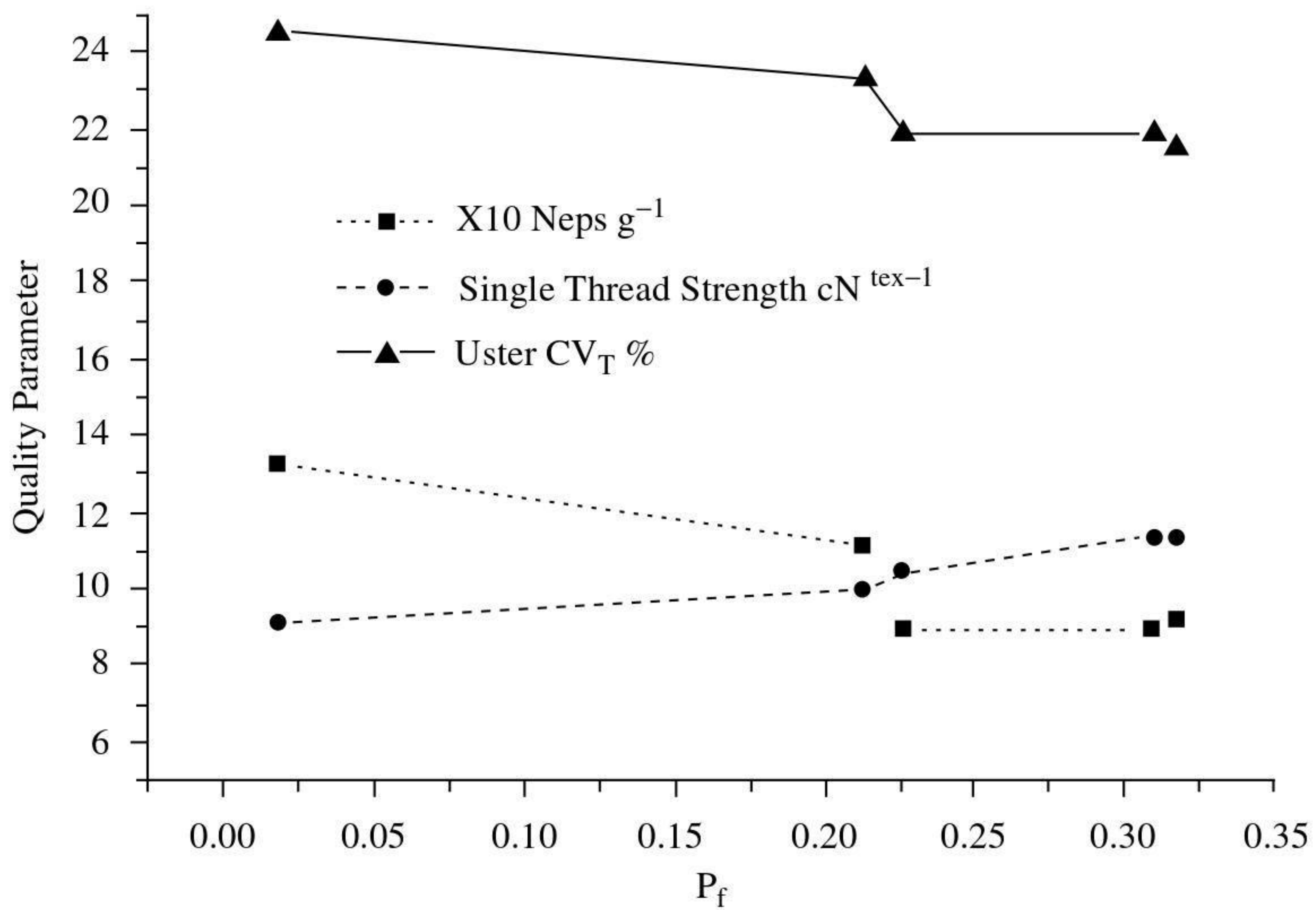


FIGURE 4.21 Effect of P_f on yarn quality.

the taker-in is required to give small tuft sizes, it is more appropriate to reduce Q_{LC} by increasing the cylinder speed. Table 4.8 confirms that increasing only the cylinder speed reduces Q_o , Q_2 (even though K increases), and Q_1 . In Figure 4.22, P_f is seen to increase with cylinder speed, so the carding action improves with cylinder speed.

Table 4.8 shows that, although Q_1 decreases, K increases with increasing cylinder speed. A number of factors contribute to the increase in K . The mechanism for fiber

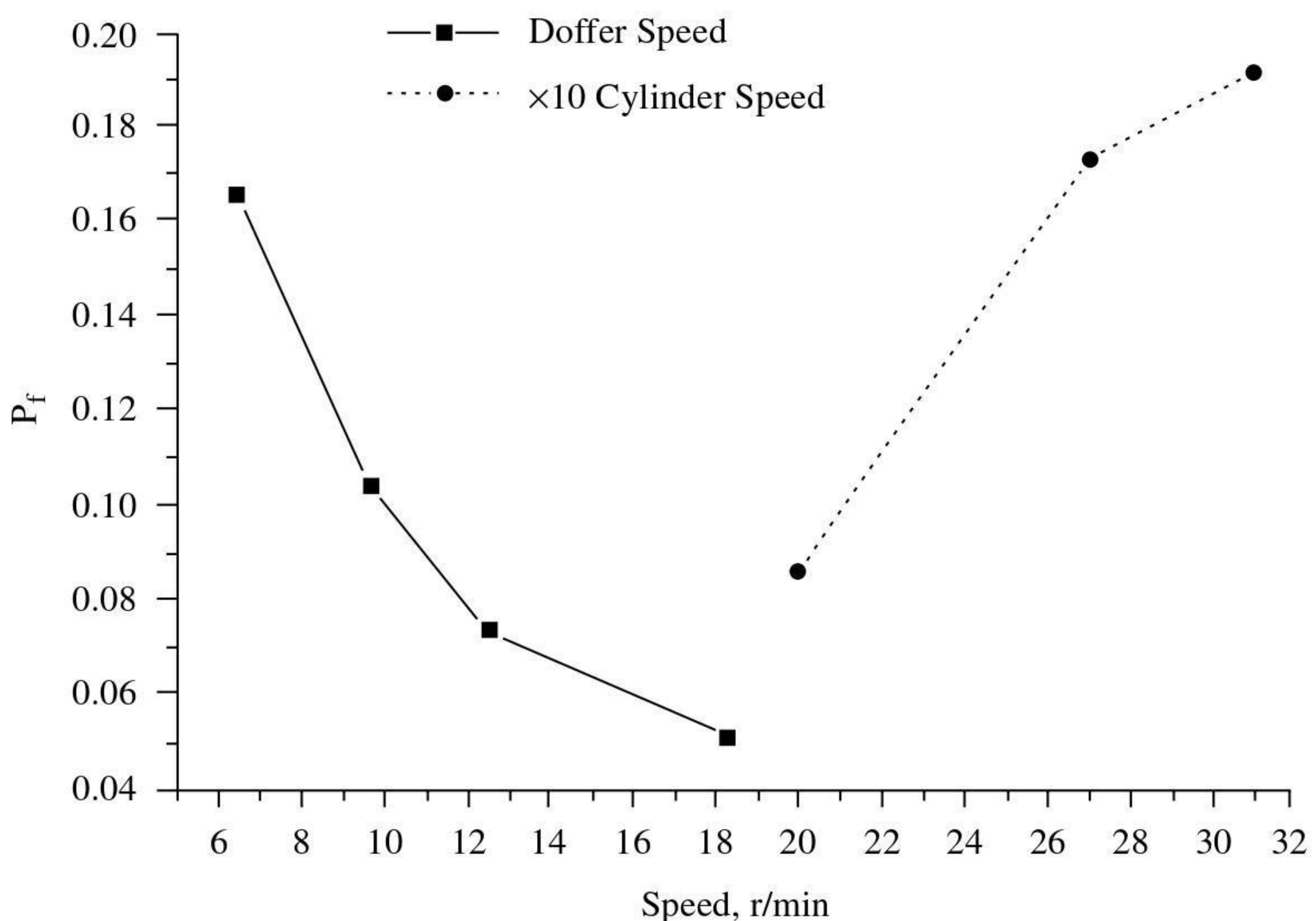


FIGURE 4.22 Effect of cylinder and doffer speeds on P_f .

TABLE 4.8
Effect of Increased Cylinder and Doffer Speed on Fiber Mass Transfer

Cylinder speed (rpm)	Q_o (reduction) (%)	Q_1 (reduction) (%)	Q_2 (reduction) %	K (%)
180	–	–	–	4.90
220	17	20	17	4.92
260	41	40	41	5.76
315	52	40	52	5.82

transfer is dependent on circular motion and centripetal forces; therefore, increasing the cylinder speed will increase K . However, we should remember that the transfer coefficient is the ratio of Q_1 to Q_o and consequently should be considered in relation to the cylinder load.

Given that increased cylinder speed reduces the cylinder load, the increased speed does in effect reduce the *retaining power* of the cylinder. As Q_1 is also reduced, the *robbing back* effect of the cylinder will be less. Thus, K will increase. This shows that the recycling layer is an important contributing factor to the cylinder load. This means that having a higher transfer coefficient does not always give an increase in the mass transferred.

Altering Q_L by changing the sliver count and/or the production rate will change the value Q_{LC} . If the sliver count is kept constant, Q_L will increase with increasing doffer speed, because the production rate increases. Q_o increases and K decreases with increased doffer speed,^{25,29} and Figure 4.22 shows that the carding action is poorer because P_f decreases with doffer speed. As illustrated by Figure 4.23, the web quality deteriorates.

If we keep a constant production rate and increase the doffer speed, the sliver count will decrease. This means Q_{LC} decreases, and therefore also Q_1 , Q_2 , and Q_o . It is evident from the table of results that the percentage decrease in Q_2 corresponds with the decrease in Q_o .

From the above discussion, we can conclude that the sliver count, production speed, and cylinder speed are key factors that control Q_{LC} and Q_2 , and thereby the cylinder load and the efficiency of the carding action. Thus, the lighter the sliver and the higher the cylinder speed, the lower will be the recycling layer and cylinder load, and the higher the transfer coefficient.

From Equation 4.22, Q_{FC} is also an important factor for efficient carding. Figure 4.24 shows that increasing the revolving-flat speed increases P_f without changing Q_o and K . Generally, the percentage of flat strip waste increased with flat speed, but the loading of each flat decreases and, therefore, so does Q_f . This means (see Equation 4.23) that Q_{FC} increases with flat speed and thereby also P_f .

From the above description, we can see the importance of Q_o to the efficiency of the carding action and to the improvement in properties of carded ring-spun yarns. Yarn properties are strongly influenced by the propensity of major and minor hooks in the card sliver. It is therefore useful to see how changes in Q_o relate to changes

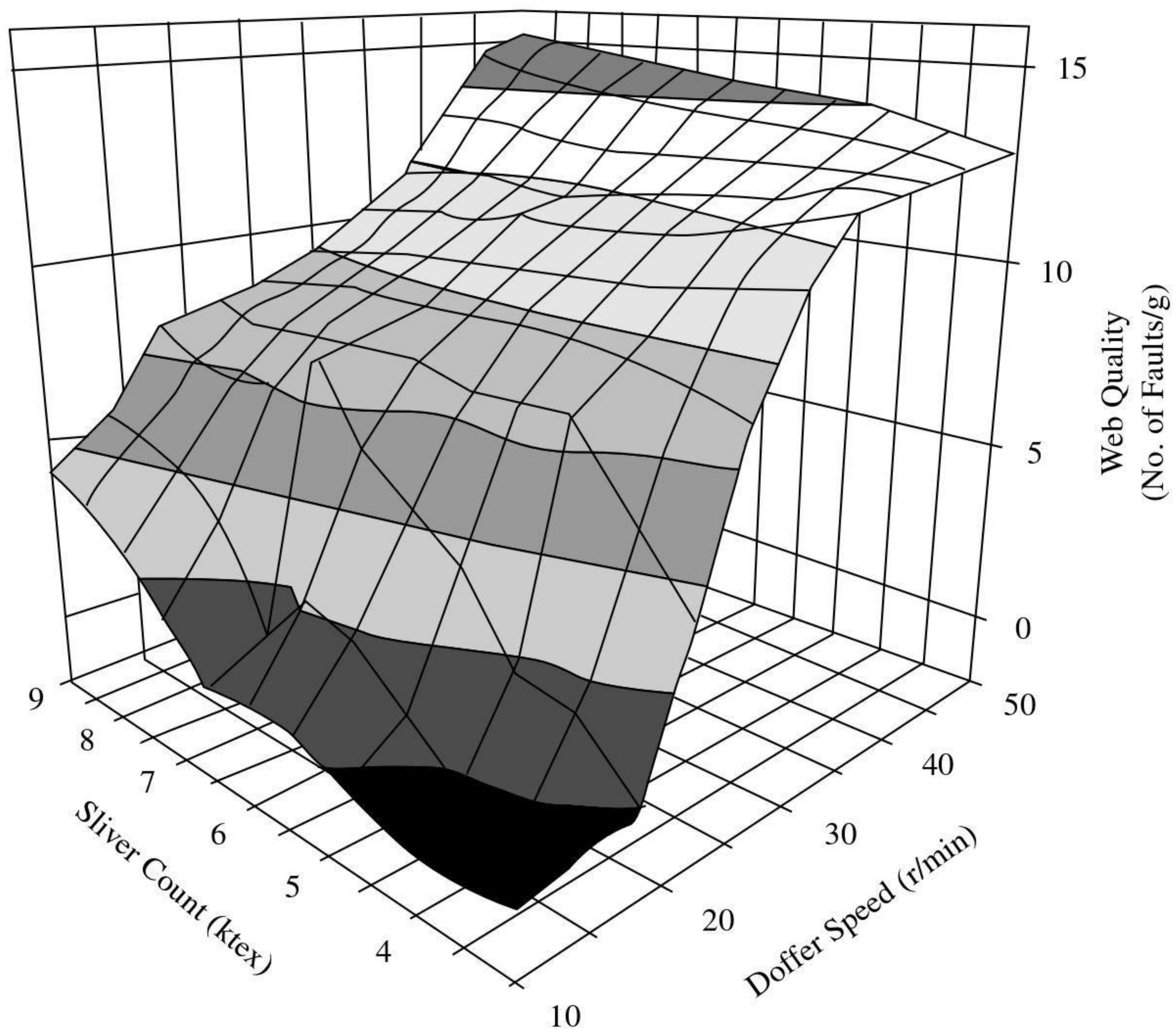


FIGURE 4.23 (See color insert following page 266.) Effect of cylinder and doffer speeds on web quality.

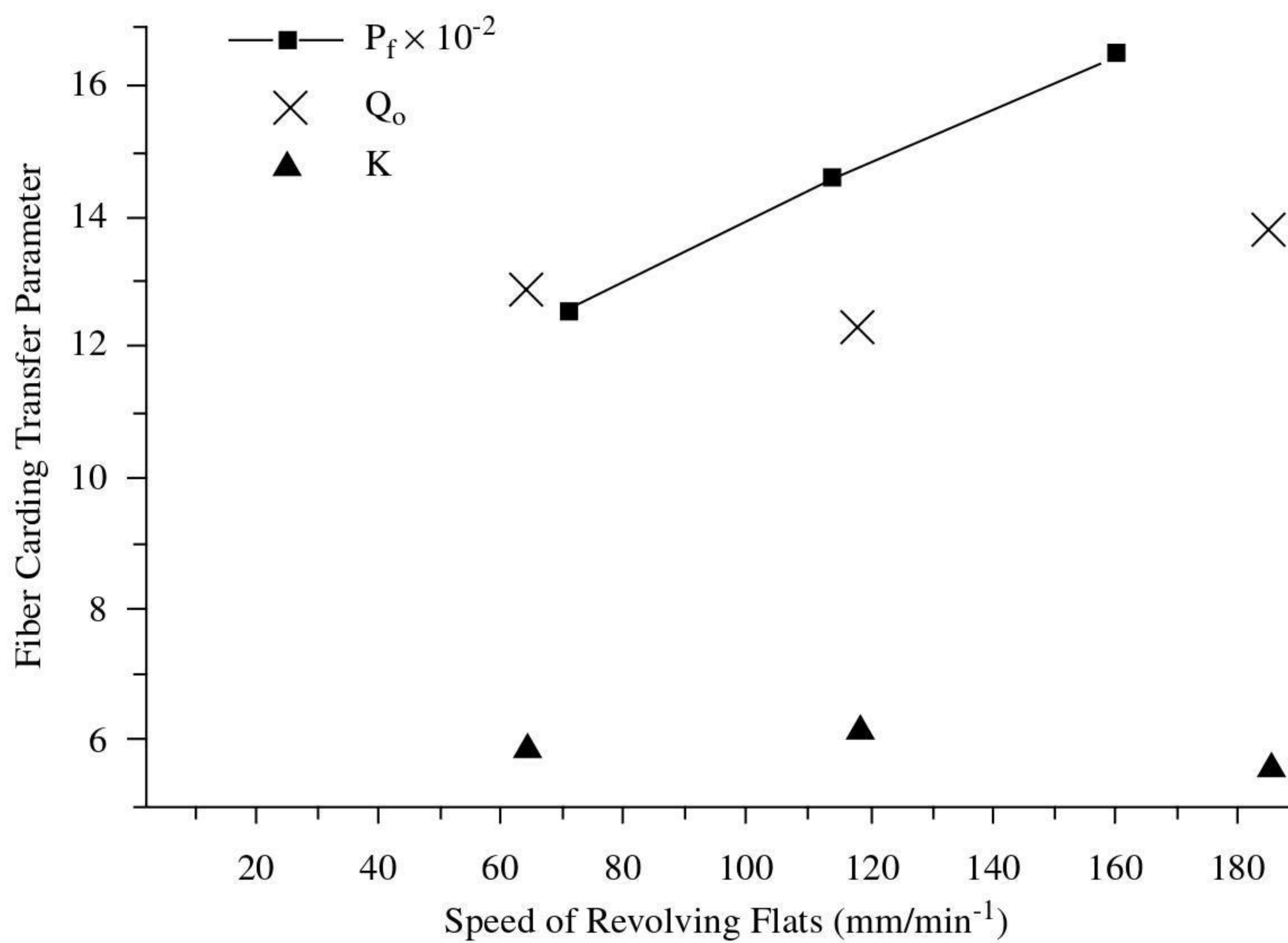


FIGURE 4.24 Effect of revolving-flat speed on fiber transfer parameters.

in the percentage of such fiber configurations. We can determine this by comparing [Tables 4.5](#) and [4.8](#). Although the latter table is for a fixed doffer speed, the above discussion showed that Q_o decreases with both doffer and cylinder speeds. It is therefore evident from the tables that, as the cylinder load decreases, the proportion of major to minor hooks decreases. Studies carried out by Simpson^{26,27} on a range of cotton types show similar results. It is essential that both types of hook configuration be straightened during drafting. As explained in [Chapter 5](#), two passages of drawing (or gilling, in case of worsted card sliver) prior to drafting at the roving and ring frames are necessary for removing hook configurations. Having a nearly equal number of major and minor hooks offers a better chance of straightening such configurations because of the even number of material reversals during the process stages that follow carding.

From the above discussion, it is apparent that, for improved card web quality, increasing K and thereby reducing Q_o and Q_2 without the need for a very high cylinder speed becomes important at very high production rates. Baturin's equation shows that the development of the card wire clothing is a key step in achieving this.

4.3.2 BLENDING-LEVELING ACTION

4.3.2.1 Evening Actions of a Card

We have seen that the carding zone gives a leveling effect, particularly for roller clear cards. A similar effect occurs with the cylinder–taker-in–doffer interactions. To explain this, let us ignore for the moment the leveling effect of the carding zone and consider the distribution of the fiber mass on the cylinder, the deposition onto the cylinder from the taker-in, and the transfer of fiber to the doffer.

Assume that Q_o is always 100 g prior to fiber transfer to the doffer. Let $K = 10\%$. Then, under steady-state conditions and for each revolution of the cylinder, $Q_{LC} = Q_1 = 10$ g and $Q_2 = 90$ g. Let us denote the first 100 g on the cylinder as A and subsequent Q_{LC} layers as B, C, and so on. A is the aggregate of previous Q_{LC} . [Figure 4.25](#) shows that the fiber mass removed from each layer to form part of the doffer web decreases with each cylinder revolution corresponding to $Q_{LC} K[1 - K]^n$ as $n \rightarrow \infty$ (see [Table 4.6](#)), and the amounts would be spaced at intervals of $d_2 = 2\pi R_d n_d / n_c$. If it took N cylinder revolutions for all the fibers in a layer to be transferred, this spacing of the amounts removed per cylinder revolution would be spread over Nd_2 . This shows a lengthways blending and leveling of the fiber layers. With each cylinder revolution, each new Q_{LC} layer will be superimposed on the previous layers constituting the recycling mass Q_2 . Thus, this superimposition and the effect described for the carding zone will combine with the lengthways blending and leveling to reduce irregularities in the feed to the card.

The total blending-leveling effect of a card is a combination of the carding zone effect and the cylinder-doffer–taker-in effect, $d_1 + d_2$. Generally, n_c is much greater than n_d , so d_2 will be very small compared with d_1 for the carding zone involving worker-stripper combinations, but it will be much larger than for revolving flats, say $d\#_1$. In practice, therefore, only roller-top cards give meaningful blending-leveling

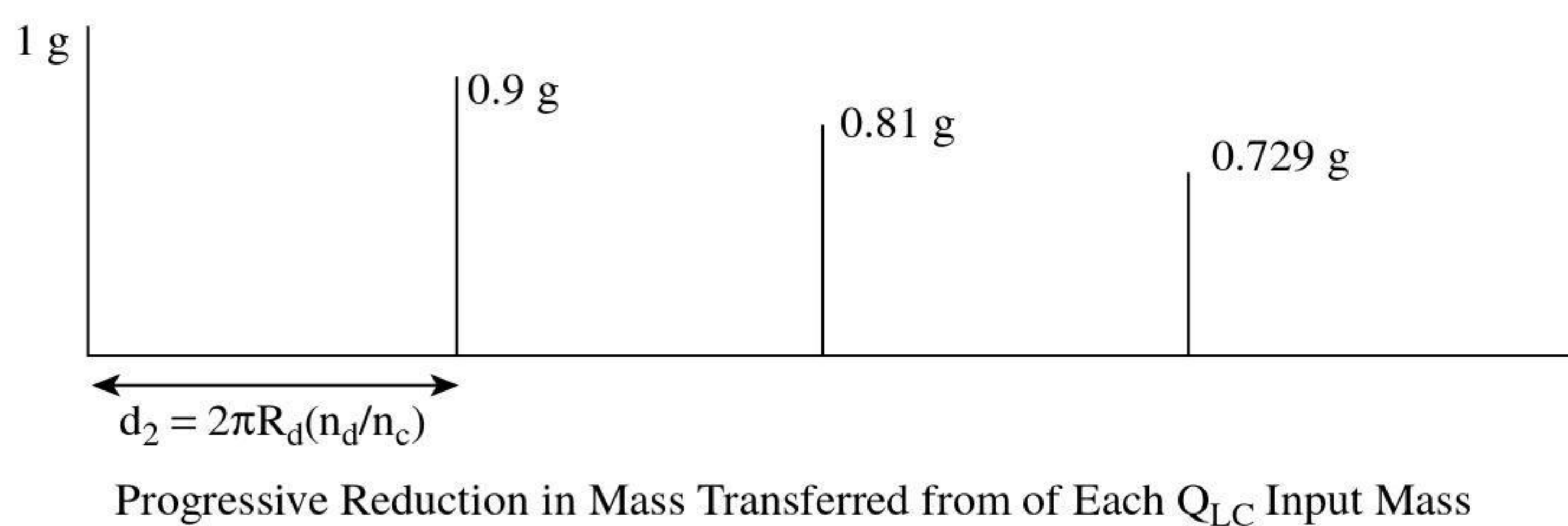
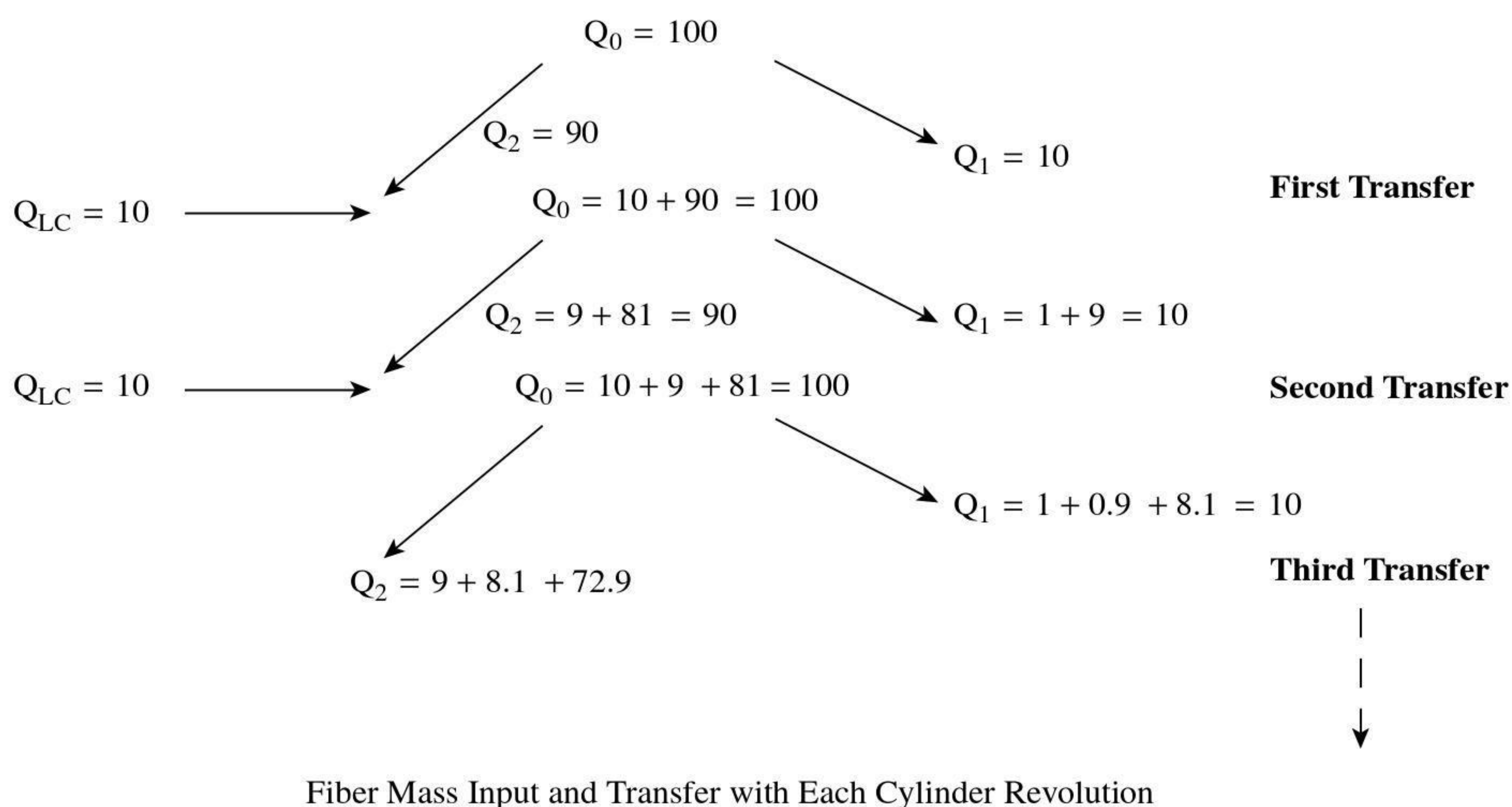


FIGURE 4.25 Lengthways blending and leveling.

actions, and our study of the evening effect of cards will now be limited to these machines.

The fiber batt feed to the card is generally of a fixed width. Therefore, as a reference measure of the feed irregularity, we can take the variation of mass per unit length. Over a range of different unit lengths, we may see differing mass variation. Such irregularities may be classified according to their wavelengths (see [Table 4.9](#)). It is therefore of interest to develop some means of determining the range of wavelengths over which the evening actions of the card would be effective. To do this, a number of researchers³⁹⁻⁴¹ have likened the blending-leveling actions of cards to an automatically self-regulating machine system and have applied control theory to develop computer simulations of the evening effect. However, the following simpler approach may be used to determine the evening effect of a roller-top card.

First, we must note that we have so far assumed that, per revolution of the swift, each worker retains a constant amount of fiber and also that a constant amount is transferred to the doffer. However, in reality, the p and K values for a fixed operating condition will vary because of a randomness of the fiber factors affecting transfer between the rollers, e.g., variation in fiber orientation, length, fineness, friction, and entanglement.

TABLE 4.9
Classification of Irregularities According to Wavelengths

Irregularity	Wavelength
Ultra-short term	Less than the order of a fiber length
Short-term	Grater than fiber length but less than 0.5 m
Medium-term	Greater than 0.5 m up to 100 m
Long-term	Grater than 100 m

Therefore, the p and K values we are considering are the average values. This means that intervals d_1 and d_2 are caused by their corresponding average time delay. We can use the average total time delay to evaluate the evening action of a card or a series of cards. This is called the delay factor, D . In very simple terms, we can say that, under steady-state conditions, if it takes one revolution of a swift for the doffer to remove $Q_1 (= Q_{LC})$, then the number of swift revolutions required to remove a total load, W , of fibers carried by the swift and all the workers and strippers would be W/Q_{LC} , which would be the delay factor for the card.

From Equation 4.8, the load presented for transfer to the doffer per swift revolution

$$= \frac{Q_{LC}}{K}$$

Following the derivation of Equation 4.1, the load carried by each worker and stripper combination per swift revolution

$$= \frac{Q_{LC}}{K} \left\{ \frac{p}{1-p} \right\} \quad (4.24)$$

Hence, if there are n_1 workers with similar surface speeds on a card, then the combined load of all the workers

$$= \frac{Q_{LC}}{K} \left\{ \frac{n_1 p_1}{[1-p_1]} \right\}$$

and the total load W

$$= \frac{Q_{LC}}{K} \left[1 + \left\{ \frac{n_1 P_1}{1-P_1} \right\} \right] \quad (4.25)$$

For a set of, say, three cards, this becomes

$$= \frac{Q_{LC}}{K} \left\{ \frac{n_1 p_1}{[1 - p_1]} + \frac{n_2 p_2}{[1 - p_2]} + \frac{n_3 p_3}{[1 - p_3]} \right\}$$

and

$$W = \frac{Q_{LC}}{K} \left[1 + \left\{ \frac{n_1 P_1}{[1 - P_1]} + \frac{n_2 P_2}{[1 - P_2]} + \frac{n_3 P_3}{[1 - P_3]} \right\} \right] \quad (4.26)$$

So the corresponding delay factors would be

$$D = \frac{1}{K} \left[1 + \left\{ \frac{n_1 p_1}{[1 - p_1]} \right\} \right] \quad (4.27)$$

for one card, and

$$D = \frac{1}{K} \left[1 + \left\{ \frac{n_1 p_1}{[1 - p_1]} + \frac{n_2 p_2}{[1 - p_2]} + \frac{n_3 p_3}{[1 - p_3]} \right\} \right] \quad (4.28)$$

for three cards.

Note that $1/K$ is the delay factor for the swift-doffer-taker-in interaction, and $1/K\{n_1 p_1/[1 - p_1]\}$ and so on are delay factors for worker-stripper combinations.

D can be estimated by measuring the individual parameters in the above equations or, more simply, by stopping the feed to the card and running out the fibers and weighing the collected mass. From this, the fiber mass that was on the doffer at the time the feed was stopped is subtracted to give the total load, W . Thus, D is W divided by the feed rate.

Now that the concept of the delay factor has been established, it is useful see how it can be applied to determine the amount by which a card or a series of cards will smooth out the irregularities in a batt feed.

Step Change in Feed

We will first consider the simplest form of irregularity, a sudden increase or step change in the feed rate. For ease of explanation, let us limit the consideration to the effect of the swift-doffer-taker-in interaction. If it is assumed that the feed rate was uniform prior to the step change, then the output from the doffer per swift revolution would increase according to Equation 4.9, which follows the curve shown in [Figure 4.26](#). Including the effect of worker-stripper combinations would result in the more complex curve shown in [Figure 4.27](#), and this can be suitably approximated by an exponential curve given by (see [Appendix 4A](#) and [Figure 4.26](#)).

$$Q_1 = Q_{LC} [1 - \exp(-t/D)] \quad (4.29)$$

Thus, the output from a step change will increase almost exponentially until again $Q_1 = Q_{LC}$.

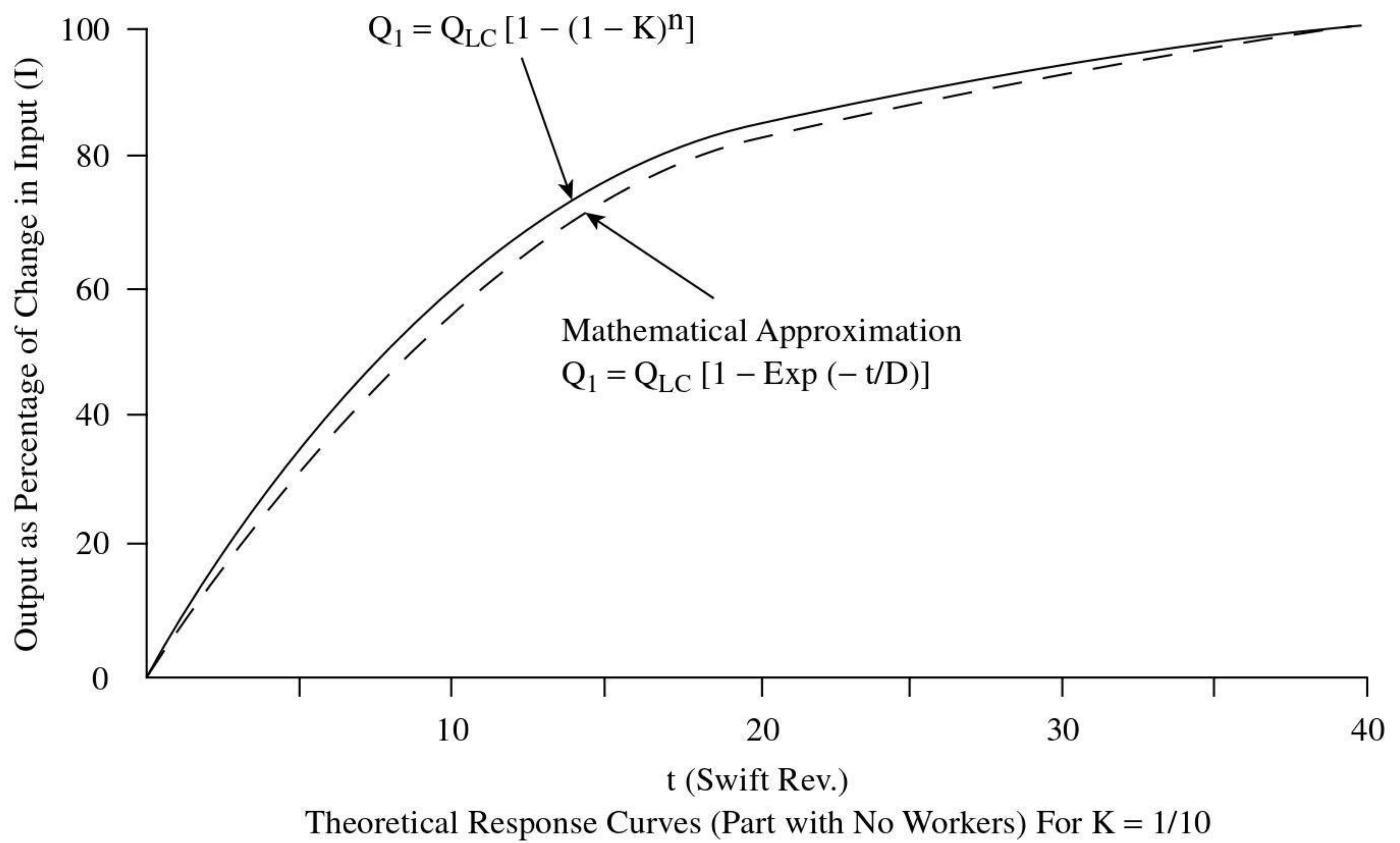


FIGURE 4.26 Cylinder-doffer theoretical response curve for $K = 0.1$. (Courtesy of WIRA.)

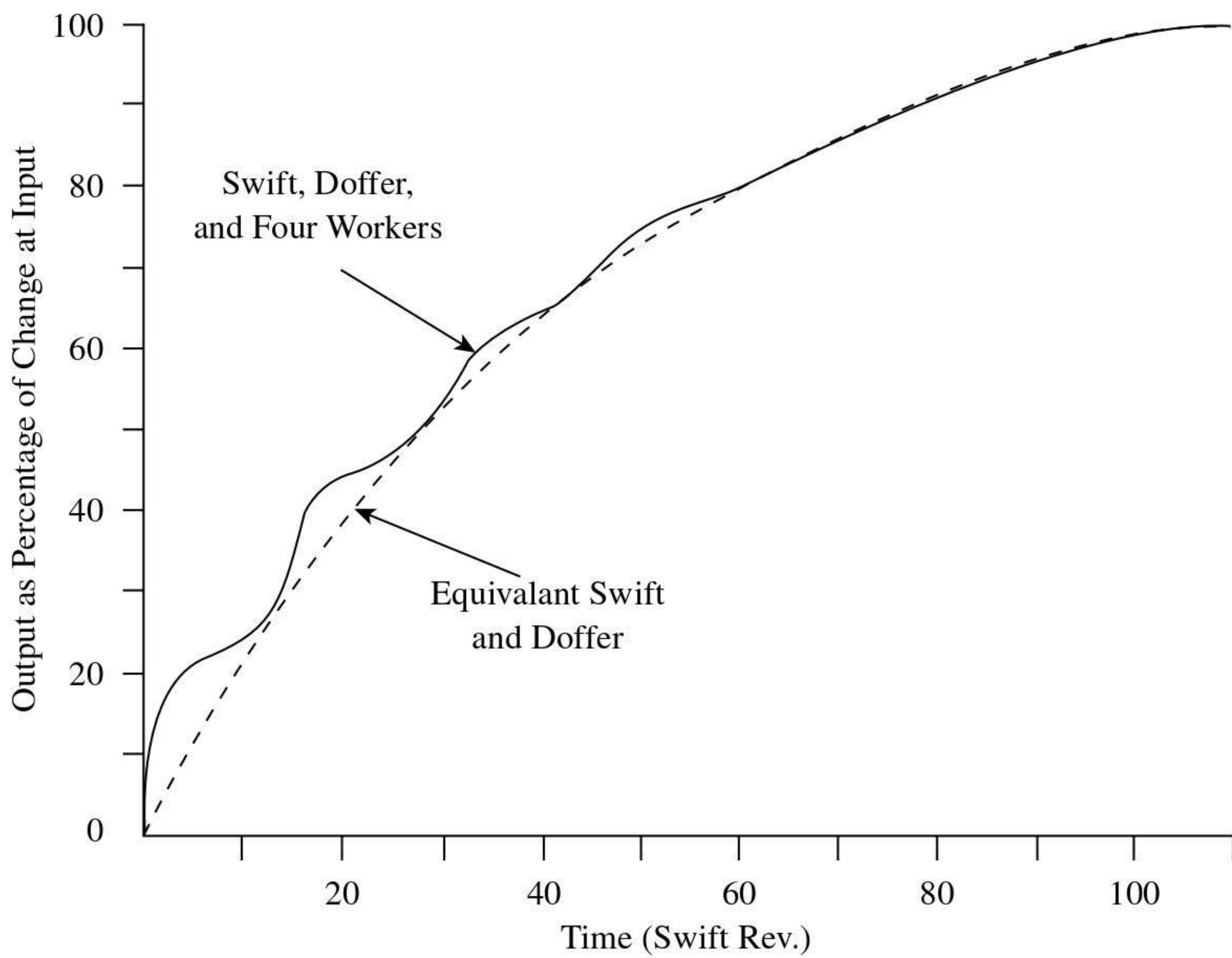


FIGURE 4.27 Cylinder-doffer-worker-stripper combination response curve. (Courtesy of WIRA.)

General or Random Irregularities

In Appendix 4A, the idea of the equivalent transfer coefficient F is explained. If we adopt the idea, then the description given earlier for the blending-leveling effect of the swift-doffer-taker-in interaction illustrates how increasing the delay factor reduces general irregularities.

Periodic Irregularities

Again, using the idea of the equivalent transfer coefficient, we can adopt the input-output performance of a simple resistance-capacitance (RC) filter as an analogy for the input-output response of a roller-top card, where the time constant of the filter is equivalent to the delay factor of the card. Similar to the card's response, a step change in the input voltage of an RC filter results in an exponential change in its output voltage. This equivalence is useful, because there are well known techniques²³ for calculating the response of RC filters to periodically varying voltage inputs. The most elementary form of such an input is a sinewave. The output is a sinewave of the same frequency as the input, but the amplitude is reduced. The ratio of the output and input amplitudes is called the gain, G , at that the particular frequency and is given by the equation

$$G = \frac{\text{Output amplitude}}{\text{Input amplitude}} = \frac{1}{\sqrt{[1 + (2\pi\omega\tau)]^2}} \quad (4.30)$$

where ω = frequency
 τ = time delay

Thus, the card equivalent would be

$$G = \frac{1}{\sqrt{[1 + (2\pi HD)]^2}} \quad (4.31)$$

where H = frequency
 D = delay factor

Figure 4.28 shows a graph of G versus H plotted on logarithmic scales. For a simple prediction of the evening effect of the card, the curve can be approximated by its asymptotes shown by the broken lines. The predicted range of frequencies or wavelengths for which amplitudes will be modified can be obtained as follows. The longest wavelength or minimum frequency, H_b , termed the *break frequency*, is at the point of intersection of the asymptotes. Here, $G = 1$. It is evident that using the asymptotes for predictions will result in a minimum frequency higher than the true value, since, on the actual curve, $G = 0.71$ at H_b . Nevertheless, the error is on the right side of caution, because the actual output irregularity will always be less than the prediction. An important characteristic of the asymptotic shape is the slope PS. It shows that, at $N H_b$, the gain is $1/N$, where N is any number, e.g., 1, 1.5, 2, 2.3, 3, ..., 10, and so on. Thus, if we know the minimum gain, we can determine the

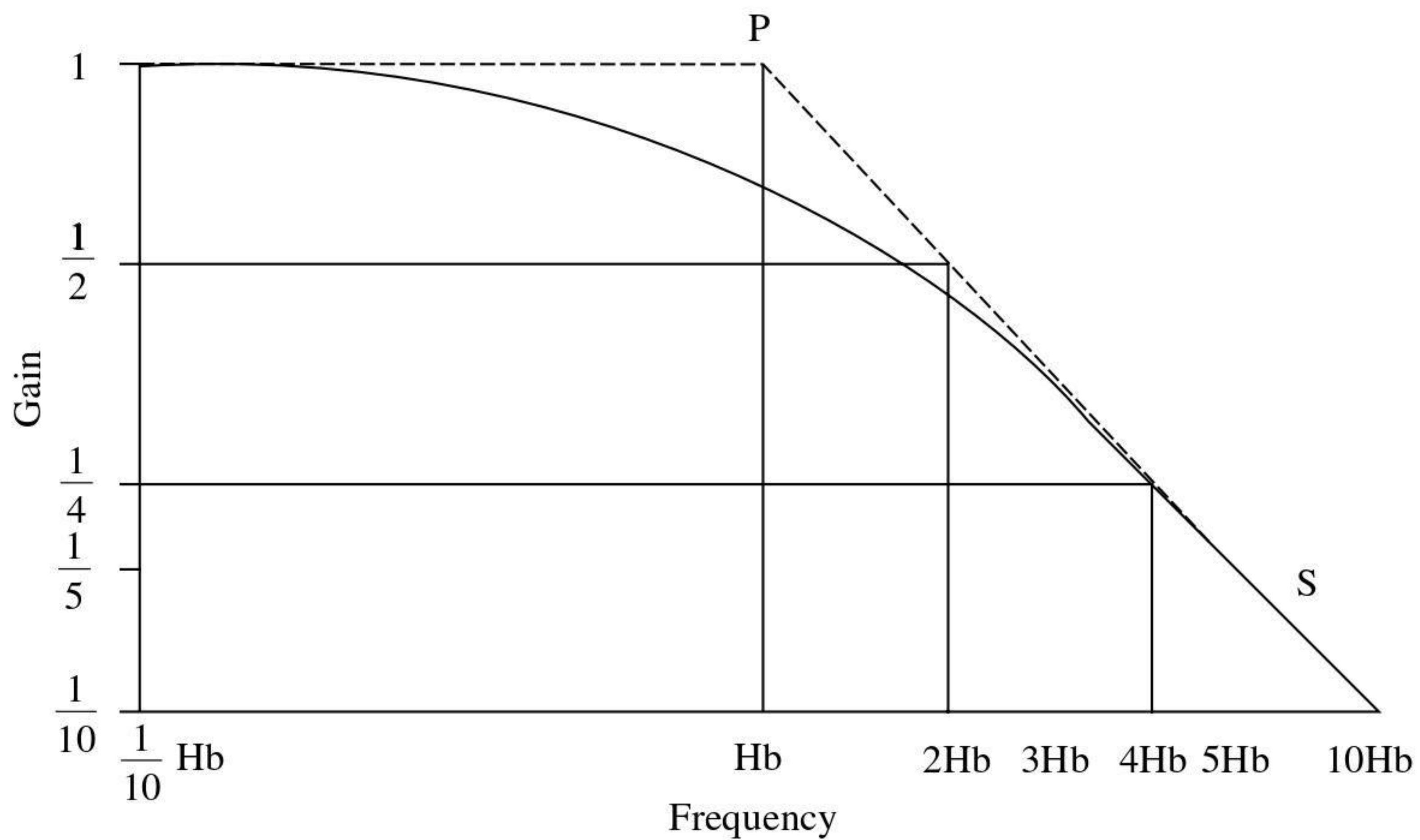


FIGURE 4.28 Filter gain-frequency curve. (Courtesy of WIRA.)

upper frequency limit and complete the asymptotic form. An equation for the minimum gain can be obtained by the following reasoning. If a given mass of fibers Q_{in} were to be transferred to the swift, passed straight through to the doffer, and totally removed by the doffer, then $Q_{in} = Q_{out}$ and $G = 1$. However, when the mass makes contact with n workers, each with a retaining power of p , then only $Q_{in} (1 - p)^n$ passes straight through to the doffer. With a doffer transfer efficiency of K , $Q_{out} = K Q_{in} (1 - p)^n$; hence, the minimum gain, $G_{min} = K(1 - p)^n = 1/N$, and the upper frequency $= H_b/[K(1 - p)^n]$. Knowing the delay factor D , H_b can be calculated and the asymptotic form drawn.

For a series of cards, the overall gain is the product of the gains for each card. For example, say the irregularity entering the card has a frequency of $1.43 H_b$. Then, $G = 0.7$ and, for a series of three cards, $G = 0.7^3 = 0.34$. Similarly, if the minimum gain for a card $= 0.1$, then, for three cards, $G_{min} = 0.001$, and the upper frequency $= 1000 H_b$. Such a figure, however, is of little practical significance, since the card itself would generate irregularities of this frequency.

4.4 FIBER BREAKAGE

4.4.1 MECHANISM OF FIBER BREAKAGE

It is clearly essential that, during carding, any breakage of fibers be kept to a minimum. In discussing how fiber breakage can occur, we must consider the dynamics of the following sequence of events:

1. A saw-tooth or pin of a roller clothing entering the fiber mass
2. Fibers being caught by the tooth or pin
3. Fibers being removed by the tooth or pin

Figure 4.29 illustrates the general situation in which a fiber mass is held as a tooth on a rotating roller enters the mass to remove fibers. In the case of the short-staple card, the fiber mass may be the fringe of the batt held between the feed roller and feed plate or the fiber load caught in a flat. For roller-top cards, it may be the mass at the taker-in or on the stripping roller at the point of contact with the swift, or the mass on the swift at the point of contact with the worker. As the tooth enters the mass, it may hit a fiber at any location along its length. The impulsive force, F_T , will cause the fiber to become hooked by the tooth. Fibers that are hooked may drag others that are not in direct contact with a tooth. Once a fiber is caught by a tooth, the pulling force will give rise to increasing tension and strain in the fiber. Peak tension and strain are reached, at which point

1. If the trailing end remains caught, the peak strain equals the fiber breaking strain, and the fiber breaks.
2. If the end is released before the breaking strain is reached, the fiber is withdrawn.
3. If, while the end remains caught, the tension overcomes the frictional resistance of the hooked length around the tooth, the tooth slips from the fiber, along the hooked length.

A given fiber may have both ends embedded within a mass of fibers or one end within the mass and the other free. Appendix 4B provides a theoretical treatment of both situations, which explains much of the practical observations. Here, we will focus on the practical observations of the effect of how process parameters affect fiber breakage. The parameters of importance are

- State of the fiber mass and fiber characteristics (i.e., degree of entanglement, mass per unit area, regain, bulk, friction, and tensile properties)
- Tooth geometry

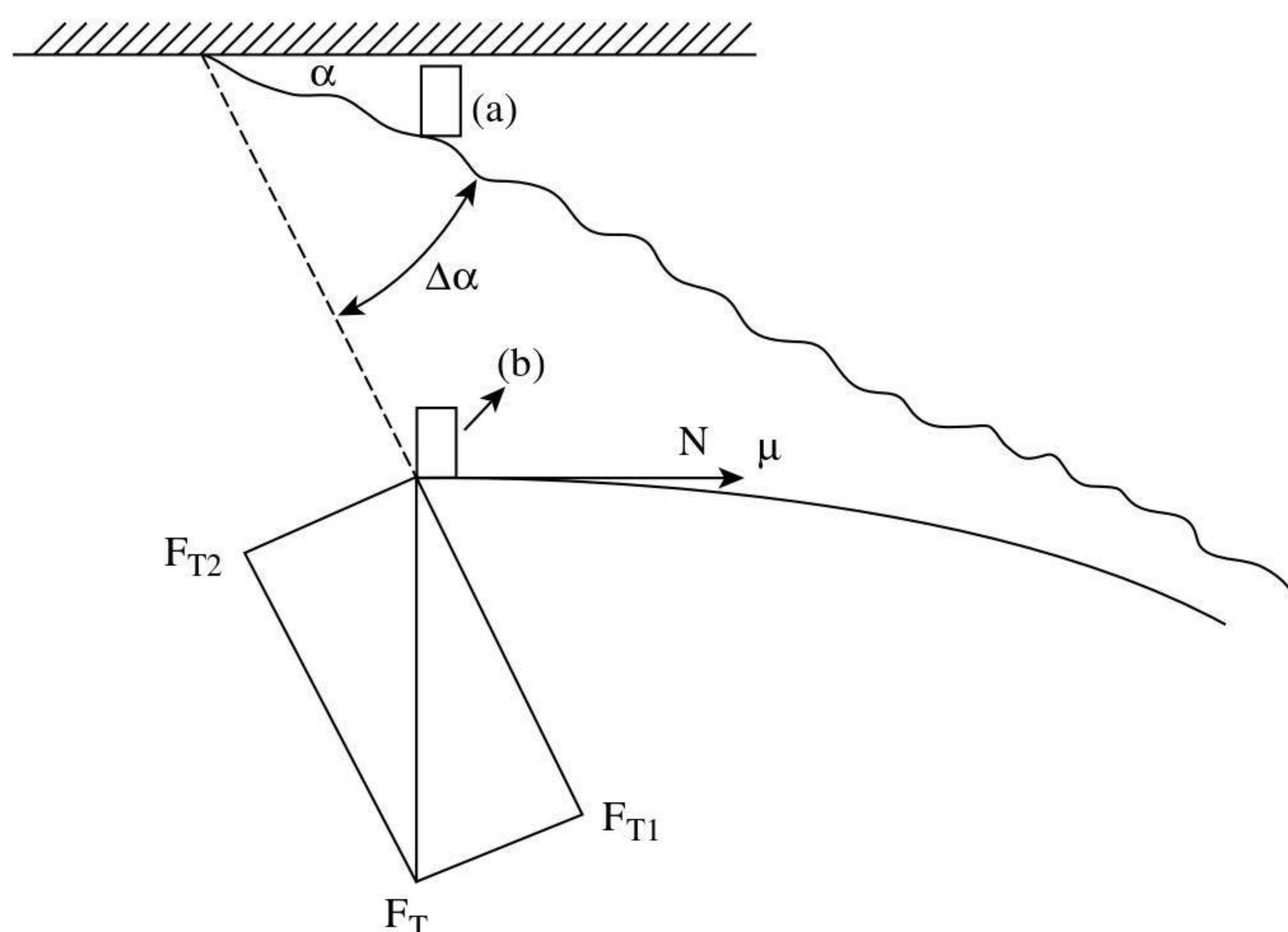


FIGURE 4.29 Forces generated with fiber-pin interaction.

- Roller surface speed
- Production rate
- Card component settings

4.4.2 STATE OF FIBER MASS AND FIBER CHARACTERISTICS

The fact that an impact force and then a withdrawal force is applied to fibers during opening indicates that, to prevent breakage, the breaking strain of fibers under high rates of extension must be greater than the strain induced by these forces. [Figure 4.30](#) illustrates the tension profiles observed for cotton, wool, and polyester when groups of fibers are pulled from different shape tufts; i.e., the tensile property of tufts. On pulling a fiber, any slack or crimp in the freed length is first removed, and fiber tension then occurs. The induced tension increases and peaks at the point where the fiber is fully released from its entanglement with other fibers. The tension decreases as the fiber slips past other fibers, reaching zero as its trailing end leaves the tuft. If the fiber breaking strain was lower than the strain at peak tension, the fiber would have broken, and the fall-off would be more immediate. Work by Li et al.⁴² showed that the withdrawal forces needed to separate an entangled fiber mass were largely dependent on the density of the mass and the contact angle fibers made with the wire clothing.

With respect to [Figure 4.30](#), the elongated tufts had the lower density and fibers more aligned to the direction of the applied pulling force. The fibers would therefore have a lower degree of entanglement. The smaller, rounded tufts were more dense with fibers more entangled. The latter, consequently, required a greater withdrawal force. Because of their surface scales and longer length, the wool fibers had greater entanglement and interfiber frictional contact than the other fibers, resulting in a higher withdrawal force.

Townend and Spiegel studied the effect of alterations in the state of wool on fiber breakage in worsted carding.⁵ They found that the main cause of fiber breakage was the entangled state of the scoured wool fed to the card. Bownass⁴³ found that, if there is a high degree of entanglement, then even removing fibers by hand for staple length measurements can result in breakage, although the utmost care may have been taken. In woolen spinning, stock-dyeing can be result in substantial reduction in fiber length at the card, as a result of fiber entanglement, particularly with the use of high dye-liquor circulation pressures. In general, however, less breakage occurs when wool is carded at regains greater than 20%. The fibers are more extensible at high regains, which lowers the chance of breakage as they are disentangled during carding.

4.4.3 EFFECT RESIDUAL GREASE AND ADDED LUBRICATION

With a highly entangled state of scoured wool, progressive loosening of entanglements is of benefit. This would require a value of fiber-pin friction that enables fibers to be easily caught by the pin or saw-tooth clothing yet allows fibers to slip from the pin if the entangled parts are insufficiently loose for the fiber to be released before its breaking strain is reached. Bownass,⁴³ Henshaw,⁴⁵ and Eley and Harrowfield⁴⁶

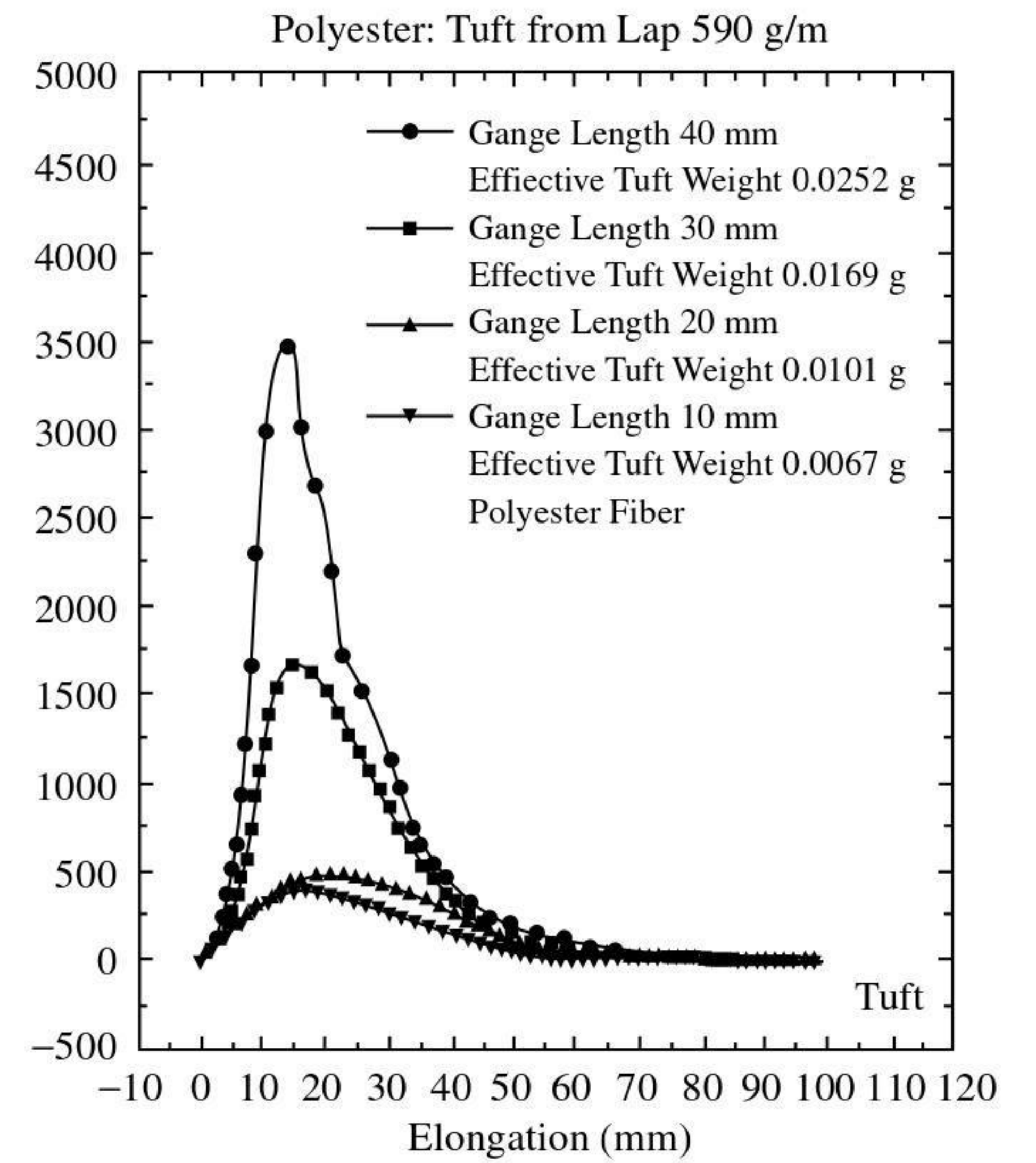
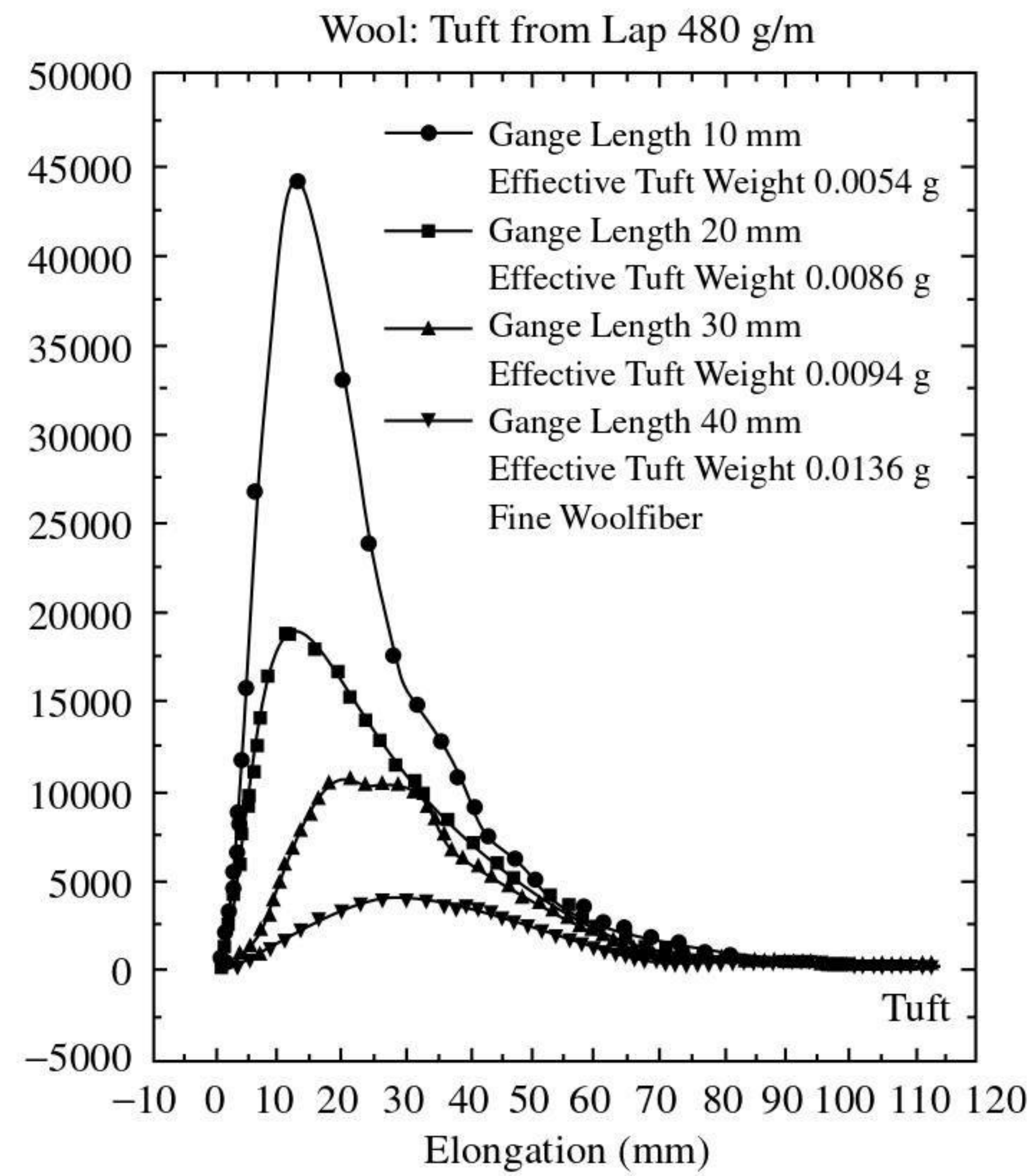
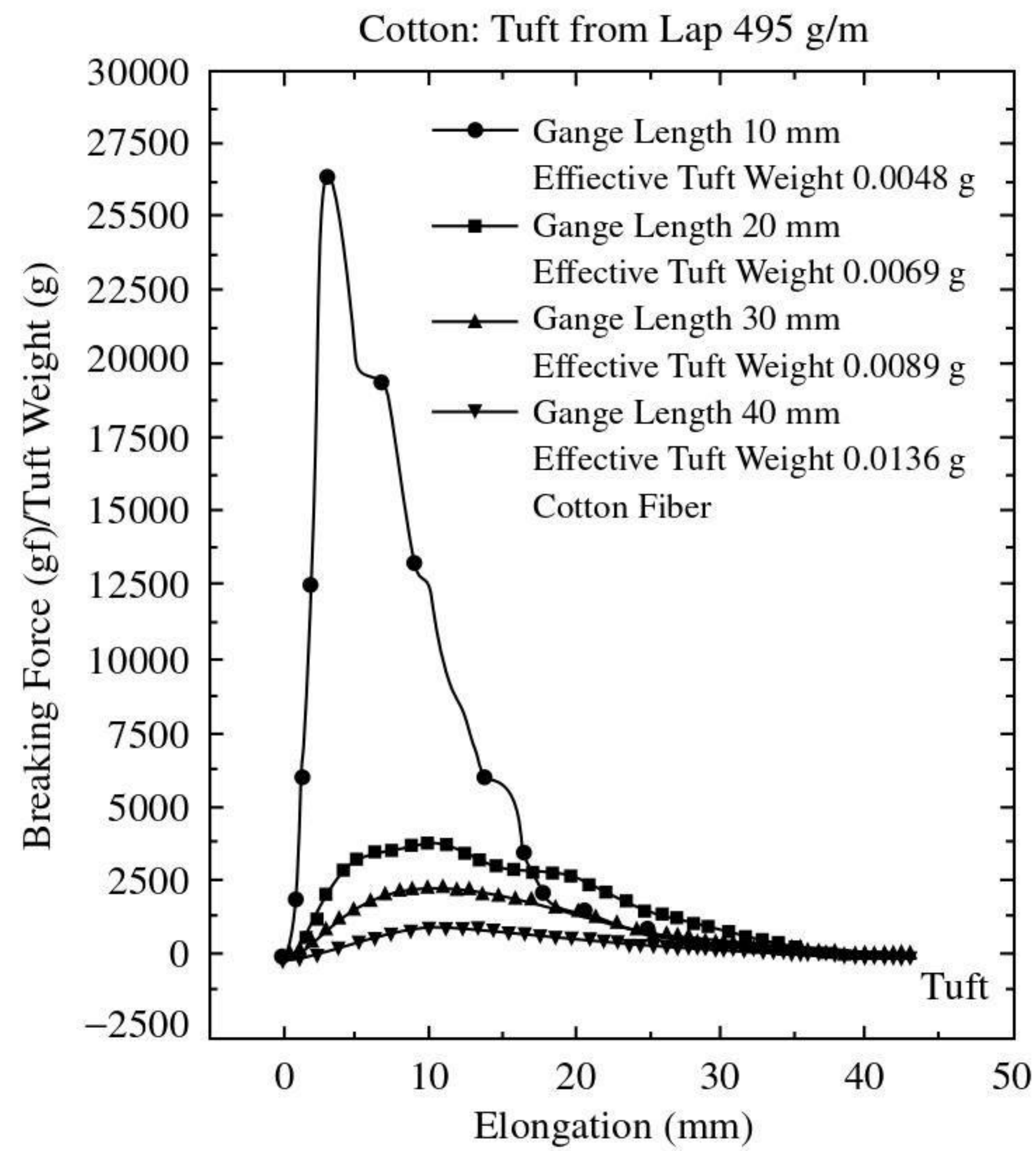


FIGURE 4.30 Fiber pull-out tension profiles.

report the benefit of residual grease content and added lubrication to reduce wool fiber-metal friction in carding. In worsted carding, keeping fiber breakage to a minimum is an essential requirement and, in practice, besides card sliver fiber-length characteristics, the mean fiber length or hauteur of the resulting combed top, the tear, and the percentage noil are often used as indicators of “good” or “bad” carding. Doubts have been expressed⁵ over whether combing is sensitive enough to facilitate a precise measure of fiber breakage in carding, but there is sufficiently close correlation for the stated parameters to be used.

General findings tend to show that, with a residual grease content ranging from 0.3 to 0.9%, and added lubrication of 0.3 to 0.6%, wools of low residual grease content suffer the most breakage. However, higher grease content tends to be associated with poor color and may be unsuitable for dry-combed tops, as backwashing does not readily reduce the grease content. The addition of lubrication very noticeably reduces fiber breakage, especially at low residual grease levels, with the further advantage that added lubrication can usually be removed in backwashing. Increasing card production rate increases fiber breakage and percentage noil, but added lubrication can reduce this effect. There is agreement in the literature that about 0.5% on weight of fiber is about the optimal level.

The viscosity of the lubricant is also of importance. While fiber-fiber friction is independent of lubricant viscosity, fiber-pin friction increases with viscosity. Therefore, the work done in sliding a fiber around pin surfaces also increases. Too high a lubricant viscosity causes surface tension forces to militate against a fiber easily sliding from around a tooth, and this can result in increased fiber breakage. Experimental findings have led to the conclusions that the optimal viscosity for wool is around 20 centipoise.⁴⁴

4.4.4 EFFECT OF MACHINE PARAMETERS

4.4.4.1 Tooth Geometry

With wool fibers, saw-tooth clothing is more damaging than pin clothing, but saw-tooth wire has a low fiber breakage when the card clothing is sharp and smooth.⁵ Gharehaghaji et al.,⁴⁶⁻⁵⁰ studying the damage caused to wool fibers by saw-tooth and pin clothing, found that in addition to actual fiber breakage, micro-damage also occurs, which can subsequently lead to rupture. The damage by saw-tooth clothing was more severe. Appendix 4B.3 gives a brief review of the type micro-damage found.

4.4.4.2 Roller Surface Speed/Setting/Production Rate

Yan and Johnson^{51,52} found that, if the surface speed of the roller is very high, fibers can be damaged and broken by the impulsive force (see Appendix 4B). Generally, fiber breakage is dependent on the interaction of roller speed and production rate.

The Taker-in Zone

The equation for the degree of opening indicates that high taker-in speeds give better fiber opening, and the trend (described earlier) of a decreased number of tuftlets and

increased amount of individual fibers with increased taker-in speed agrees with the equation. There is, however, the practical limitation of fiber damage, which restricts the maximum taker-in speed that can be used.

Fibers hooked by the taker-in teeth while their trailing lengths are either held in the nip of the feed system or entangled in the batt mass will be stretched at a rate equal to the surface speed of the taker-in. The fibers will break if their trailing ends are not released or if their hooked lengths do not slip from the taker-in teeth before they reach their breaking extensions (see [Appendix 4B](#)). Since fiber entanglement is likely to be greater in tufts fed to the taker-in than in tuftlets fed to the cylinder, it may be reasoned that significant fiber breakage can occur at the taker-in zone. It is also reasonable to assume that, with a given feed roller speed, the higher the taker-in speed, the greater the chance of fiber breakage because of the increased rate of extension. Honold et al.⁵³, Krylov,¹³ and Artzt et al.⁵⁴ found that, when processing cotton fibers, increasing the taker-in speed up to 1,380 rpm did not significantly increase fiber shortening. This may be attributed to hooked lengths slipping from the taker-in teeth. However, the level of breakage is also dependent on production rate and the setting of batt fringe to the taker-in.

The effect of speed depended on production rate. Figure 4.31 shows that, with high production rates achieved by increased sliver counts and constant output speed, fiber breakage increases with taker-in speed. It was also found that, because of the shorter distance to contact with the taker-in clothing, fibers on the upper surface of the batt fringe were more easily broken as compared with those at the bottom surface. Townend and Spiegel⁵ and Townend⁵⁵ report that, in worsted carding with a single-pair roller feed to the taker-in, the greatest amount of fiber breakage occurred at the taker-in due largely to the entangled state of scoured wool. Increases in the production rate and taker-in speed lead to significant increases in fiber breakage.

This interaction of taker-in speed and production rate on fiber breakage is a further illustration of the effect of fiber entanglement. The increased production rate

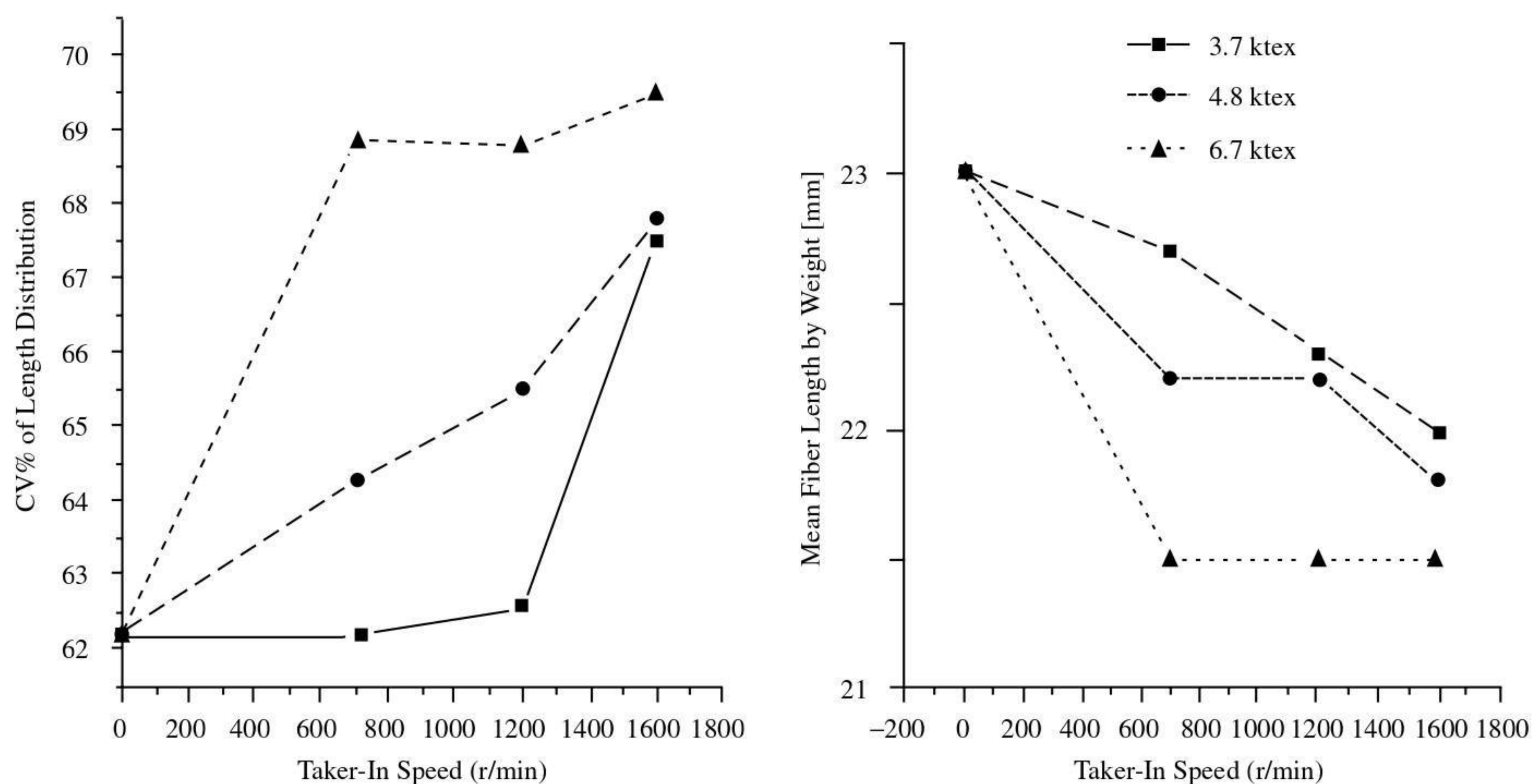


FIGURE 4.31 Effect of taker-in speed and sliver count on fiber length.

was achieved by increased mass per unit area of the batt feed. This results in greater withdrawal forces and fiber extensions and hence a greater chance of fiber breakage. Eley and Harrowfield⁴⁵ found that, for fixed batt density, fiber breakage was independent of production speed. Thus, if increased production speed is required, it is likely to be less damaging to fibers if the material is processed, within practical limits, at a lower batt mass and higher feed rates than the converse. Haigh and Harrowfield⁶⁰ found that, with the triple-merelle feed to the worsted card, changes in taker-in speed and setting had only a negligible effect on hauteur and percentage noil. The triple-merelle feed presents a more opened, less entangled fiber mass to the taker-in. Eley and Harrowfield's work supports the view that, with triple feed rollers, fiber breakage in worsted carding is more likely to occur at the swift-worker interaction. Their findings suggest that the forepart (i.e., taker-in and breast section) and morels have a much smaller effect on fiber breakage than the swift-doffer section.

Effect of Cylinder-Flats and Swift-Worker Interaction

Van Alphen⁵⁶ reports that, in revolving flat cards, increased cylinder speed caused more fiber breakage than increased taker-in speed and that this is reflected in yarn strength. Rotor yarn tenacity was reduced by up to 5% with increasing cylinder speeds between 480 and 600 rpm, whereas ring spun yarns showed a 5% reduction for speeds between 260 and 380 rpm and 10% at 600 rpm. The higher sensitivity of ring spun yarns to fiber breakage is attributable to the negative effect of short fibers during roller drafting. Krylov¹³ found no evidence of fiber shortening at speeds up to 380 rpm, which suggests the influence of other factors such as flat-setting. Force elongation profiles from experiments simulating the shearing action between flats and cylinder clothing have been reported by several authors.^{57-59,63} It was found that the tension induced on fibers increased with speed but that the rate of increase was much greater for close flat settings. The closer the setting, the higher the pressure on the fiber mass between the cylinder and flats, and the more compact the mass will be, including the entangled areas. A greater withdrawal force is then needed, and therefore there is a greater the chance of fiber breakage.

Similar to the cylinder-flat combination, fiber breakage increases with closeness of swift-worker settings,⁵ depending on how well opened is the fiber mass fed to the swift. Closer settings, however, improve the individualization of fibers, and this leads to less breakage in combing and a reduction in the percentage noil. Usually, the worker setting decreases as we move toward the doffer; therefore, the setting of the final worker is the most critical. For a given final worker setting, Haigh and Harrowfield⁶⁰ found that, in worsted carding, increasing the number of workers on the swift-doffer section reduced the percentage noil and increased fiber length. This indicates that a progressive increase in carding action is beneficial. Townend's work in woolen carding showed similar findings in that more gentle carding was obtained as the number of working points increased. Unlike the cylinder-flat combination, the effect of swift-worker speed ratio is complex. We saw earlier that the retaining power, p , of a worker increases with worker speed and more work will be done on the fiber mass. Despite the increased work, fiber breakage and noil were observed to decrease with worker speed up to an optimal speed ratio of between 40 and 80.

REFERENCES

1. Artz, P. and Schreiber, O., Fiber strain in high efficiency cards due to the licker-in at production rates above 30 kg/hr, *Melliand Textilberichte*, Eng. ed., 2, 107–115, 1973.
2. Dehghani, A., Lawrence, C. A., Mahmoudi, M., Greenwood, B., and Iype, C., Fibre dynamics in a revolving-flats card: An assessment of changes in the state of fibre mass during the early stages of the carding process, *J. Text. Inst.*, 91, 359, 2000.
3. Niitsu, Y., Nazaki, C., Mineo, Y., Ando, K., Hasegawa, S., and Kimura, H., Cleaning action in the licker-in part of a cotton card, part 1: Opening action in the licker-in part., *J. Text. Mach. Soc. Japan*, 10, 218–228, 1964.
4. Fujino, K. and Itani, W., Effects of carding on fibre orientation, *J. Text. Mach. Soc. Japan*, 8(1), 1–8, 1962.
5. Townend, P. P. and Spiegel, E., Fibre breakage in worsted carding, *J. Text. Inst.*, 37, T58.–76, 1946.
6. Bogdan, J. F., The control of carding waste, *Text. Res. J.*, 25, 377, 1955.
7. Hodgson, R., Cotton carding: A preliminary study, *Shirley Inst. Memoirs*, Series A, III(7), 1934.
8. Varga, V., Varga, M. J., and Cripps, H., *A theory of carding*, Crosrol UK Ltd., 1995, 1–20.
9. Oxley, A. E., The mechanism of the carding engine and the results obtained with simplified cards in various mills, *Shirley Inst. Memoirs*, August, 24–27, 1989.
10. Sengupta A. K., Vijayaraghavan N., and Singh A., Studies on carding force between cylinder and flat in a card: part 1: Effect of machine variables on carding force, *Indian J. Text. Inst.*, 8, 59–63, September 1983.
11. Artzt, P., Textling, E. B., and Maidel, H., Influence of various card clothing parameters on the results obtained in high-speed carding of cotton, *Melliand Textilberichte*, Eng. ed., 789–796/707–713, October 1985.
12. Martindale, J. G., The distribution and movement of wool on woollen cards, *J. Text. Inst.* (transactions), T213–T227, 1945.
13. Krylov, V. V., Some theoretical and experimental data concerning the design of high-speed cotton cards, *Technol. of Text. Ind., USSR*, 2, 47–53, 1962.
14. Kaufman, D., Studies on the revolving-flat card, *Textil Praxis*, 16(3), 1073–1096, 1193–1199, 1961; 17(4), 13–19, 111–117, 1962; 17(4), 1962, 326–336; 17(5), 1962, 437–443; 17(6), 1962, 539–546; 17(7), 1962, 646–656; 17(8), 1962, 760–769; 17(10), 1962, 982–989; 18(11), 1962, 1094–1100; 17(12), 1962, 1207–1212.
15. Townend, P. P., Some factors governing the transfer of material to a worker from a swift, *J. Text. Inst.* (transactions), T385–T393, December 1948.
16. Kamogawa, H., Kanda, E., and Imai, H., A study on card by means of high speed motion pictures, *J. Text. Mach. Soc. Japan, Eng. ed.*, 8(4), 19–27, 1962.
17. Lauber, M. and Wulforth, B., Non-contact gauging of the fibre flow during carding and drafting of cotton, *Melliand Textilberichte*, 5, E77–E78/294–298, 1995.
18. Viellier, P. and Drean, J. Y., Carding action in a modern short-staple card, *Text. Praxis International*, Eng. ed., I–IV, 1063–1067, October 1989.
19. Sengupta, A. K., and Chattopadhyay, R., Change in configuration of fibres during transfer from cylinder to doffer in a card, *Text. Res. J.*, 52, 178, 1982.
20. Morton, W. E. and Summers, R. J., Fibre arrangement in card slivers, *J. Text. Inst.*, 40, 106, 1949.
21. Simpson, J., Relation between minority hooks and neps in card web, *Text. Res. J.*, 42(10), 590–591, 1972.

22. Ghosh, G. C. and Bhaduri, S. N., Transfer of fibres from cylinder to doffer during cotton staple-fibre carding, *Text. Res. J.*, 39(4), 390–392, 1969.
23. *Woollen Carding*, WIRA/British Textile Technology Group, Leeds, U.K., 1968.
24. Dehghani, A. A., Lawrence, C. A., and Mahmoudi, M., Fibre transfer in short-staple carding (in press).
25. Ghosh, G. C. and Bhaduri, S. N., Studies on hook formation and cylinder loading on the cotton card, *Text. Res. J.*, May, 535–543, 1966.
26. Simpson, J. and Fiori, A. L., Effect of mixing cottons differing in micronaire reading and carding variables on cotton sliver quality, yarn properties, and end breakage, *Text. Res. J.*, 44(5), 327–331, 1974.
27. Simpson, J. and Fiori A. L., Some relationships of cotton micronaire reading and carding parameters to card loading, sliver quality, and processing performance, *Text. Res. J.*, August, 691–696, 1971.
28. Simpson, J., DeLuca, L. B., and Fiori A. L., Effect of carding rate and cylinder speed on fibre hooks and spinning performance for irrigated acala cotton, *Text. Res. J.*, 37, 504–509, 1967.
29. Simpson, J., Fiori, A. L., Castillion, A. V., and Little, H. W., Effects of blends of medium-staple low and high micronaire reading cottons, sliver weight, and carding rate on card loading, sliver quality, and processing performance, *Text. Res. J.*, November, 661–666, 1972.
30. Simpson, J., and Patureau, M. A., A method and instrument for measuring fibre hooks and parallelisation, *Text. Res. J.*, 40, 956–957, 1970.
31. De Barr, A. E. and Watson, K. J., Some experiments with radioactive tracer fibres in a flat card, *J. Text. Inst.*, 49, 588–607, 1958.
32. Baturin, Y. A., The effect of the number of passes in carding on web quality, *Technol. of Text. Ind., USSR*, 5, 50–55, 1964.
33. De Swaan, A., The function of the doffer in carding, *J. Text. Inst.*, 42, 209–212, 1951.
34. Emmanuel, M. V. and Katser, B. M., Fibre shedding from the card cylinder, *Technol. of Text. Ind., USSR*, 2, 44–48, 1964.
35. Baturin, Y. A., The load of the carding surfaces and the proportion of fibre transferred between the surfaces, *Technol. of Text. Ind., USSR*, 4, 37–43, 1964.
36. Karasev, G. I., On the efficient utilization of the cylinder clothing of the card, *Technol. of Text. Ind., USSR*, 3, 159–162, 1964.
37. Singh, A. and Swani, N. M., A quantitative analysis of the carding action by the flats and doffer in a revolving-flat card, *J. Text. Inst.*, 64, 115–123, 1973.
38. Singh, A. and Swani, N. M., The carding action in a revolving-flat card—reply, *J. Text. Inst.*, 64, 329, 1973.
39. Borzunov, I. G., Analysis of the accumulating action of the card, *Technol. of Text. Ind., USSR*, 2, 39–43, 1968.
40. Buturovich, I. K. H., Analysis of the equalising action of the flat card from the frequency characteristics, *Technol. of Text. Ind., USSR*, 1, 38–43, 1968.
41. Cherkassy, A., Analysis of the smoothing effect of the card cylinder using simulation, *Text. Res. J.*, 65(12), 723–730, 1995.
42. Li, B., Johnson, N. A. G., and Wang, X., The measurement of fibre-withdrawal forces in simulated high-speed carding, *J. Text. Inst.*, 2(87), 311–320, 1996.
43. Bownass, R., Fibre breakage in early worsted processing, *Proc. Int. Wool Text. Res. Conf.*, Australia, E, 203–215, 1955.
44. Henshaw, D. E., The role of a lubricant and its viscosity in worsted carding, *J. Text. Inst.* (transactions), December, T537–553, 1961.

45. Eley, J. R. and Harrowfield, B. V., Reduced fibre breakage in continental worsted carding as a result of wool lubrication, *J. Text. Inst.*, 4, 274–281, 1986.
46. Gharehaghaji, A. A. and Johnson, N. A. G., Wool-fibre micro-damage caused by opening process; part I: Sliver opening, *J. Text. Inst.*, 3(84), 336–347, 1993.
47. Gharehaghaji, A. A. and Johnson, N. A. G., Wool-fibre micro-damage caused by opening process, part II: A study of the contact between opening elements and wool fibre in controlled extension, *J. Text. Inst.*, 3(86), 402–414, 1995.
48. Gharehaghaji, A. A. and Johnson, N. A. G., Wool-fibre micro-damage caused by opening process, part III: *In-situ* studies on the tensile failure of damaged-induced fibres, *J. Text. Inst.*, 1(90), 1–22, 1999.
49. Gharehaghaji, A. A. and Johnson, N. A. G., Wool-fibre micro-damage caused by opening process, part IV: *In-situ* SEM studies on the compressive micro-damage and failure of wool fibres looped around opening elements, *J. Text. Inst.*, 1(90), 23–34, 1999.
50. Gharehaghaji, A. A. and Johnson, N. A. G., Wool-fibre micro-damage caused by opening process, part V: The effect of compressive damage on fibre strength, *J. Text. Inst.*, 1(90), 34–46, 1999.
51. Yan, Y. and Johnson, N. A. G., The behaviour of fibres struck by high-speed pins, part I: Theory, *J. Text. Inst.*, 1(83), 1–14, 1992.
52. Yan, Y. and Johnson, N. A. G., The behaviour of fibres struck by high-speed pins, part II: Experiment, *J. Text. Inst.*, 1(83), 15–23, 1992.
53. Honold, E. and Brown, R. S., *Text. Bull.*, 12, 93, 25, 1967.
54. Arzt, P., and Schreiber, O., Fibre strain in high efficiency cards, due to the licker-in at production rates above 30 kg/h, *Melliand Textilberichte*, Eng. ed., February, 94–101, 1973.
55. Townend, P. P., Emulsion oiling of merino wool, *J. Text. Inst.* (transactions), March, T31– T36, 1940.
56. Van Alphen, W. F., The card as a dedusting machine, *Melliand Textilberichte*, Eng. ed., 12, 1523, 1980.
57. Grosberg, P., Strength of twistless sliver, *J. Text. Inst.*, 54, T223 –T233, 1963.
58. Taylor, D. S., Measurement of fibre friction and its application to drafting force and fibre control calculations, *J. Text. Inst.*, 46, P59–P81, 1955.
59. Wood, E. J., Stanley-Boden, P., and Carnaby, G. A., Fibre breakage during carding, part II: Evaluation, *Text. Res. J.*, 54, 419–424, 1984.
60. Haigh, M. G. and Harrowfield, B. V., The effect of settings and speeds throughout the worsted card on combing performance, *J. Text. Inst.*, 81(3), 227–240, 1980.
61. Simpson, J., Observations for improving cotton carding, *Text. Res. J.*, January, 103–104, 1968.
62. Brown, R. S., Rhodes, P. L., and Miller, A. L., The effect of production rate on card loading, *Text. Bull.*, 92(11), 30–32, 1966.
63. Kato, M., Sakaoku, K., and Yoshida, K., Measuring the degree of opening of a tuft, *J. Text. Mach. Soc. Japan*, December, 35–38, 1960.

APPENDIX 4A

Consider the simple case of only the swift-doffer–licker-in interaction. Then, the rate of increase of the output, Q_1 , at time, t revolutions, after the input change will be proportional to the difference between the input, Q_{LC} , and output, the constant of proportionality being K . Thus,

$$\frac{dQ_1}{dt} = K[Q_{LC} - Q_1]$$

The solution is $Q_1 = Q_{LC} \{1 - \exp(-Kt)\}$.

To obtain an approximation for the effect of having workers present, we can assume that F is the swift-doffer transfer coefficient of a card or series of cards without workers, which results in the equivalent delay factor when workers are present. That is, for example, for three cards,

$$Q_1 = Q_{LC} \{1 - \exp(-Ft)\}$$

$$\frac{1}{F} = D = \frac{1}{K} \left[1 + \left\{ \frac{n_1 p_1}{[1 - p_1]} + \frac{n_2 p_2}{[1 - p_2]} + \frac{n_3 p_3}{[1 - p_3]} \right\} \right]$$

F is termed the equivalent transfer coefficient.

APPENDIX 4B

The Opening of a Fibrous Mass

4B.1 REMOVAL OF FIBERS WHEN BOTH ENDS ARE EMBEDDED IN THE FIBER MASS

The impulsive force, F_N , of the tooth acts on the fiber mass in the direction tangentially to the arc I and can be resolved into the components F_P and F_T . The former is a result of the penetration of the tooth into the fiber mass, and the latter is the force that pulls fibers from the mass (see Figure 4B.1). As the tooth begins to remove fibers, there is a resisting force, F_R , from the cohesiveness of the fiber mass. This is attributable to fiber entanglement, interfiber friction, and the elastic compressive and tensile properties of the fiber mass. As illustrated in the diagram, a component of F_R causes fibers to slide along the tooth and become held by it. This occurs provided that

$$F_R \sin \beta > \mu F_R \cos \beta$$

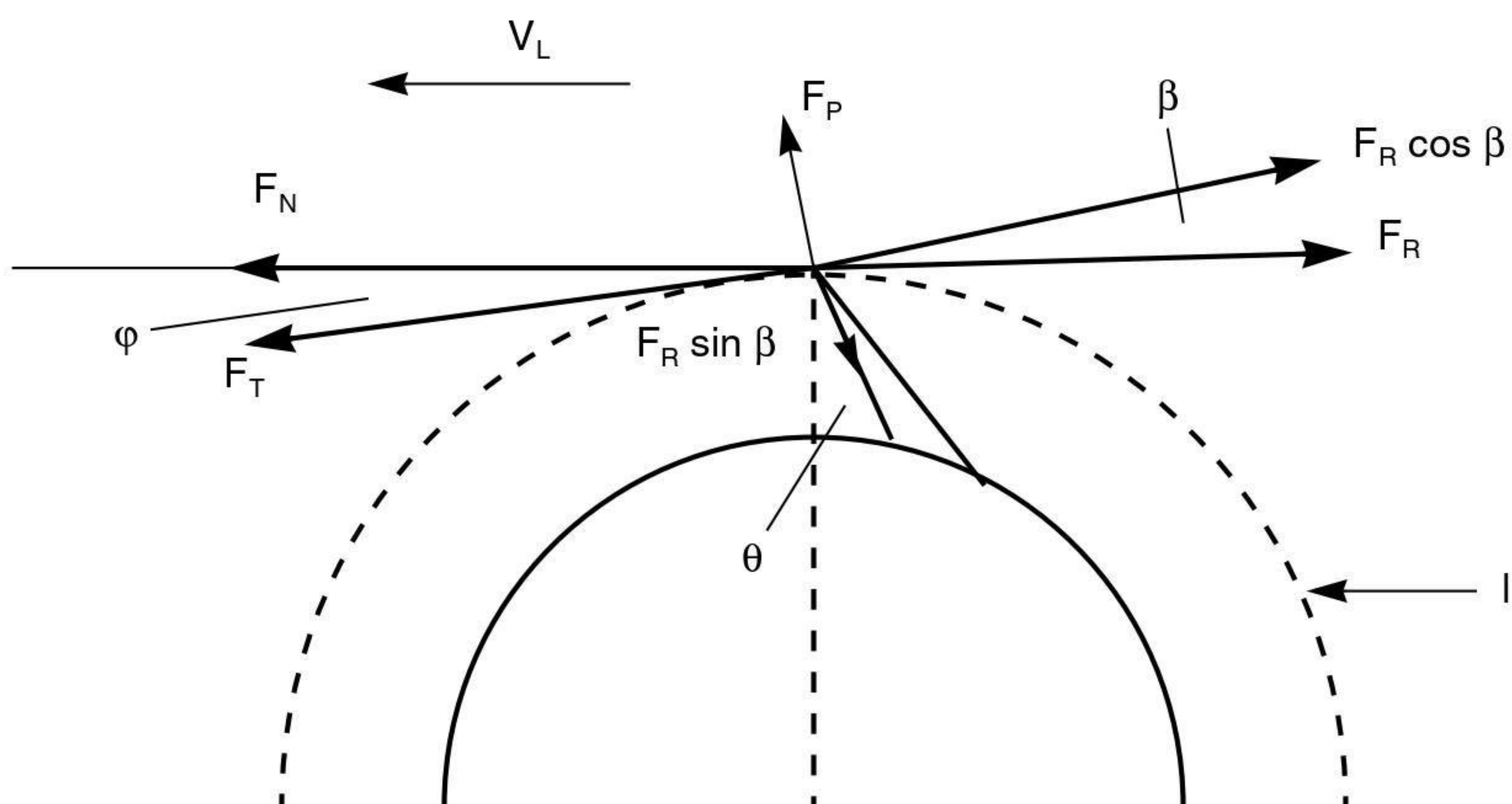


FIGURE 4B.1 Forces present during fiber removal from tufts.

Hence,

$$\tan\beta > \tan\phi$$

where μ = coefficient of fiber friction against a tooth

ϕ = friction angle

To initially hold fibers within the fiber mass, the working angle of the tooth theoretically must be

$$\theta = \beta + \phi > \phi + \phi$$

Once the tooth catches fibers, they are accelerated from the surface speed, V_F , of the machine component holding the fiber mass to the surface speed of the roller from which the tooth projects, V_L . It is during this acceleration that fibers can be broken, depending on the distance from the holding point to the contact point with the tooth, their orientation relative to direction of V_L , and also depending on the magnitude of F_R and V_L .

Fibers in tufts or tuftlets have various configurations and are likely to be inclined at an angle to the direction at which the fiber mass moves through the card, i.e., the machine direction. [Figure 4.29](#) shows what may occur when a tooth makes contact with a fiber inclined laterally at an angle, α . When the tooth moves from position (a) to (b) in the figure, the contact point is accelerated to reach the surface speed of the taker-in. The tooth will deflect the fiber length between the contact and nip points, L_s , to cause an angular change of, say, $\Delta\alpha$ per unit time. In deflecting the fiber, components F_{T1} and F_{T2} of force F_N have to overcome the components of the resisting force F_R (not shown) caused by contact with other fibers. F_{T1} is responsible for the fiber wrapping around the tooth. A normal force, $N = f(F_R)$, will develop at the front of the tooth. The friction force, μN , will resist the fiber slipping from the grip of the tooth. If the fiber is still nipped, the tooth will stretch the length L_s at a rate equal to $V_L \operatorname{cosec}(\alpha + \Delta\alpha)$. The increasing tension in the fiber length increases the component force F_{T2} . If F_{T1} exceeds μN , the fiber will slip from around the tooth and remain in the fringe to be processed by another tooth until ultimately removed. It should be noted that, if a fiber undergoes numerous stretch-and-slip cycles that induce permanent fiber strain, the fiber may break before being removed from the fringe.

If F_{T1} is less than μN , and the contact is made near the holding point, then the increase in α per unit time will be high, and L_s will undergo large extension per unit time and reach its breaking extension before slipping from the tooth.

4B.2 BEHAVIOR OF A SINGLE FIBER STRUCK BY HIGH-SPEED PINS

[Figure 4B.2](#) shows a fiber with its trailing end held and its leading end free, being struck at angle α by a pin (or sawtooth) projecting from a rotating roller and traveling at a speed of V_L .

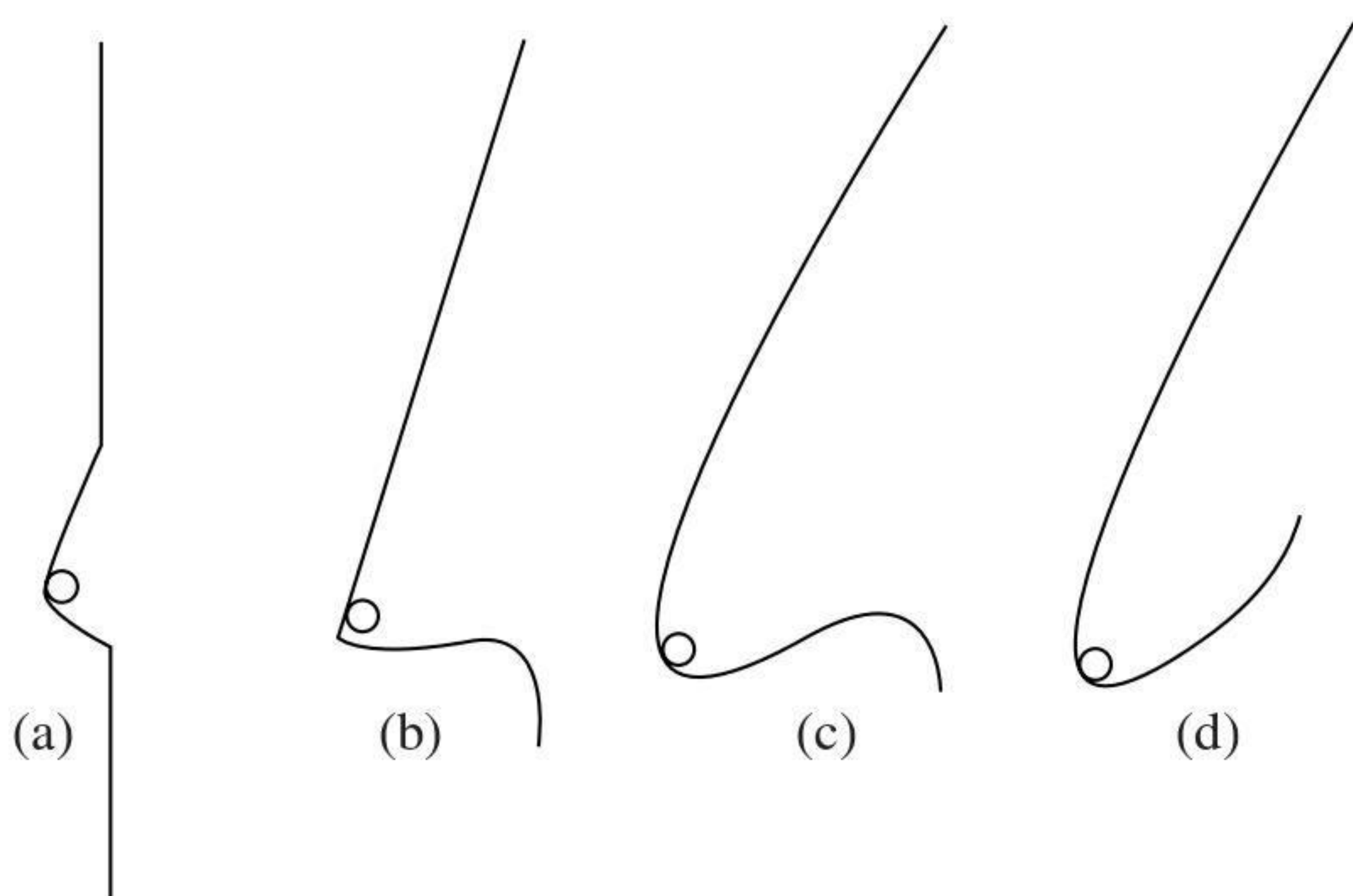
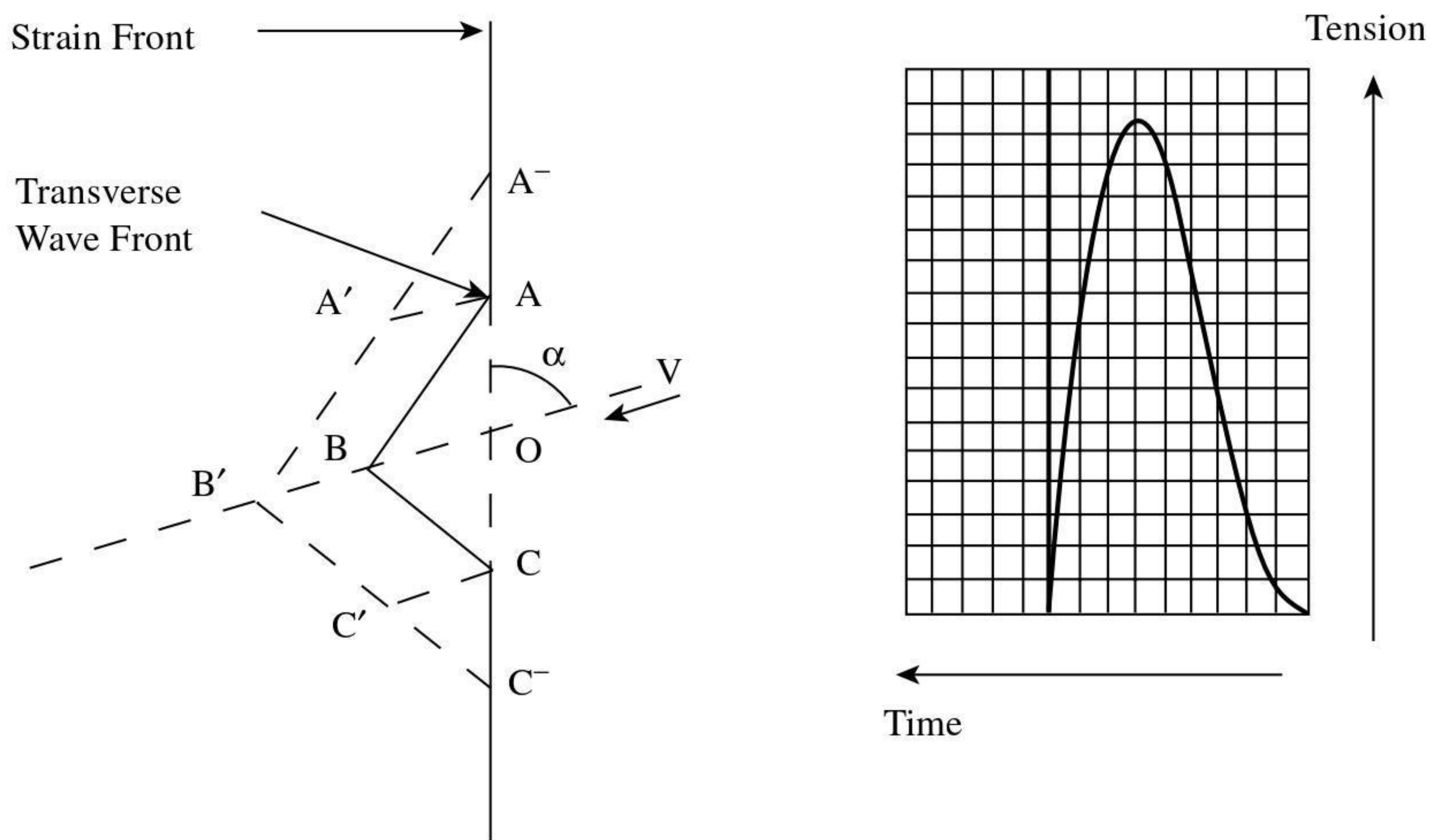
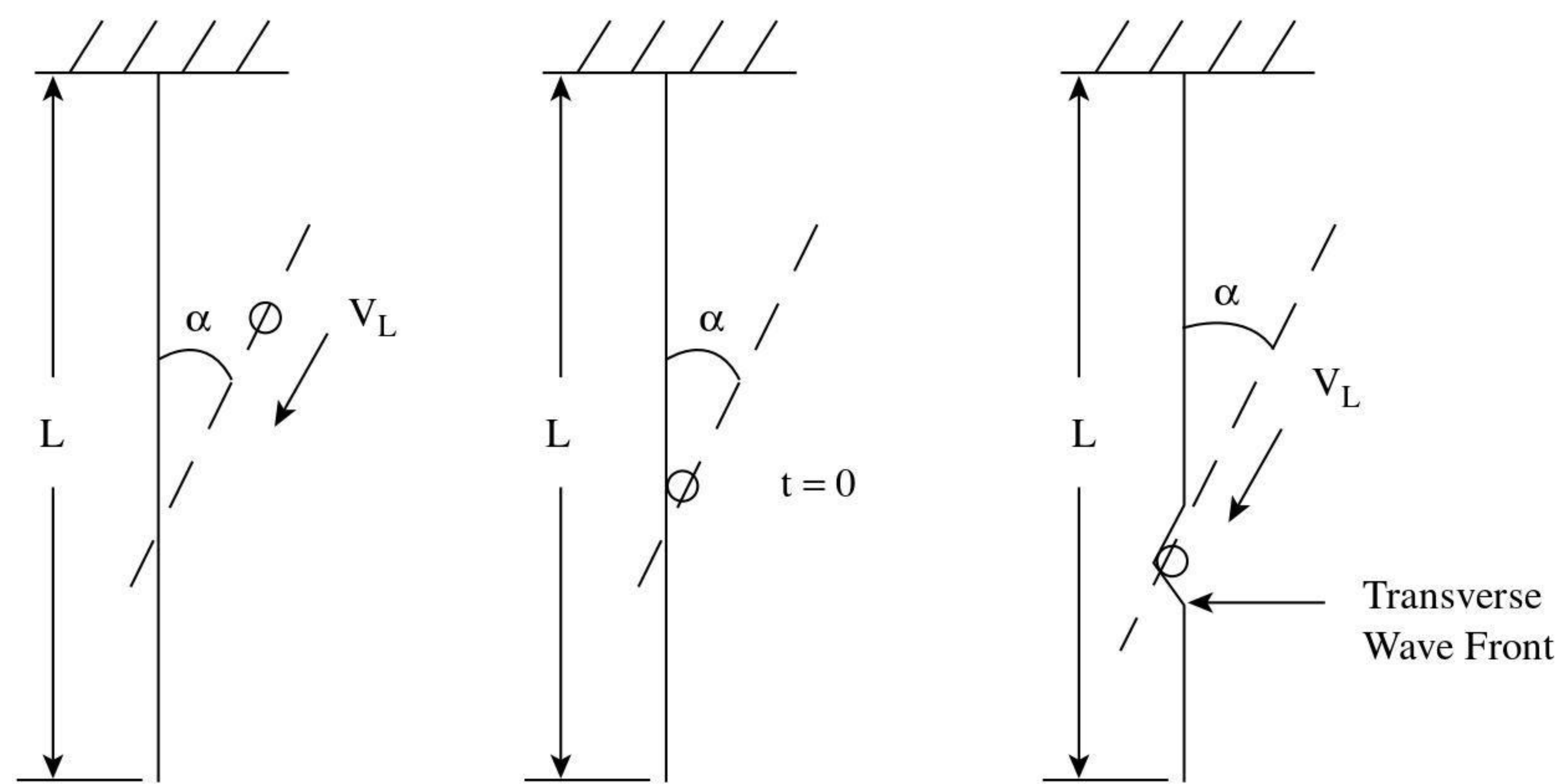


FIGURE 4B.2 Force elongation profiles.

From experimental observations,¹ it can be assumed that, at very short time intervals after impact, the fiber-pin interaction causes the fiber to adopt the configurations (a) through (d) shown. Figure 4B.2 also shows a tension curve for (a), which illustrates the suddenly induced tension in the trailing length with pin impact. Since strain is a function of tension, $\epsilon = f(\sigma A)$, a similar shape strain curves would therefore apply for (b) to (d) as the fiber continues to be strained.

- On impact, the fiber is deformed into a V shape with the apex at the impact point and with both sides of the V shape straight. Air resistance has no significant effect.²⁻⁵ The radius of curvature, R , subsequently formed by A, B, C will depend on the fiber stiffness according to

$$R = EI/M$$

where E = Young's modulus

I = moment of inertia

EI = flexural rigidity

M = bending moment

- At the deformation, the fiber is strained

$$\epsilon_o = \frac{ABC}{AC} - 1$$

- This axial strain, resulting from the impact, propagates along the fiber toward both ends with a velocity⁶

$$v_1 = \sqrt{[E/\rho]}$$

where E = Young's modulus of the fiber for high strain rates

ρ = fiber density

- After a time, the pin travels from B to B' , and the distance traveled by the strain front is $v_1 \Delta t$. A moves to A' , and C moves to C' . The fiber stretches to accommodate the increased distance traveled by the pin. Therefore, more of the fiber length outside the impact zone becomes strained so that, behind the strain front, all parts of the fiber stretch at the speed v_o , and the level of strain between the pin and the strain front is ϵ . Thus, $\epsilon = v_o \Delta t / v_1 \Delta t = v_o / v_1$.
- Since $v_o = f(V_L)$, there must be a limiting pin speed at which $\epsilon = \epsilon_b$ the fiber breaking strain. At this pin speed, the fiber breaks immediately at the point of impact.

- In addition to the strain wave, the motion of the pin produces a transverse wave that spreads to both ends of the fiber. The general equation for the speed of transverse propagation is

$$v_t = \sqrt{(T/\mu)} = \sqrt{(\sigma/\rho)} = \sqrt{E\varepsilon_o}$$

where T = tension = σA
 μ = fiber linear density
 A = fiber cross-sectional area
 ρ = μ/A

- The ratio $v_t/v_1 = 1/\sqrt{\varepsilon_o}$, so the strain front reaches the fiber ends well before the transverse wavefront, and this causes the length between the transverse wavefront and free fiber end to move up past the pin before the transverse wave reaches the fiber end. Therefore, the fiber becomes hooked around the pin.

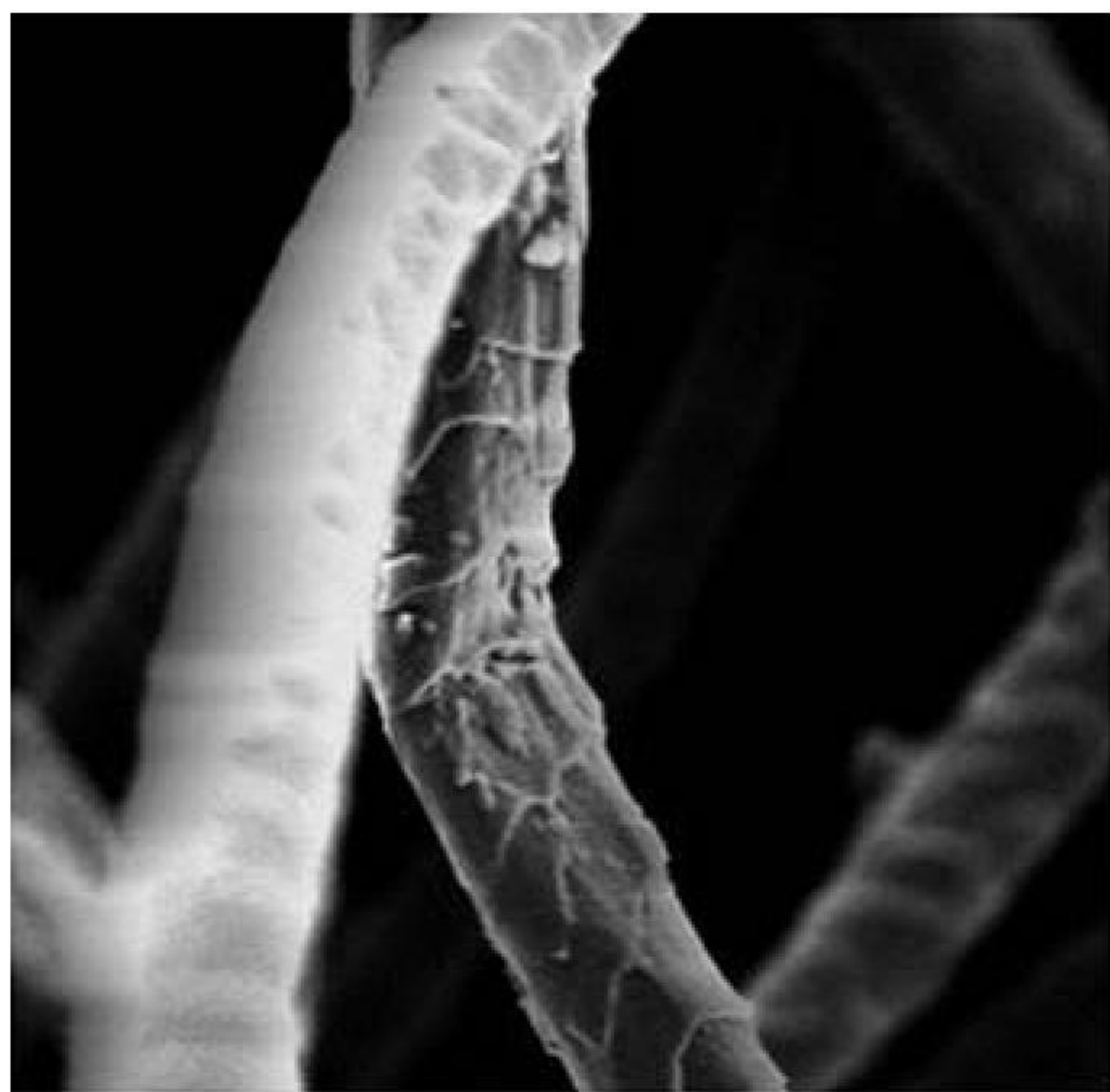
4B.3 MICRO-DAMAGE OF FIBERS CAUSED BY THE OPENING PROCESS

During the separation of a fiber mass into smaller groups or individual fibers, the forces resulting from contact between the metal clothing and the fibers can cause localized complex stress patterns inside fibers that result in microdamage. The damage is more severe with saw-tooth than pin-type clothing.

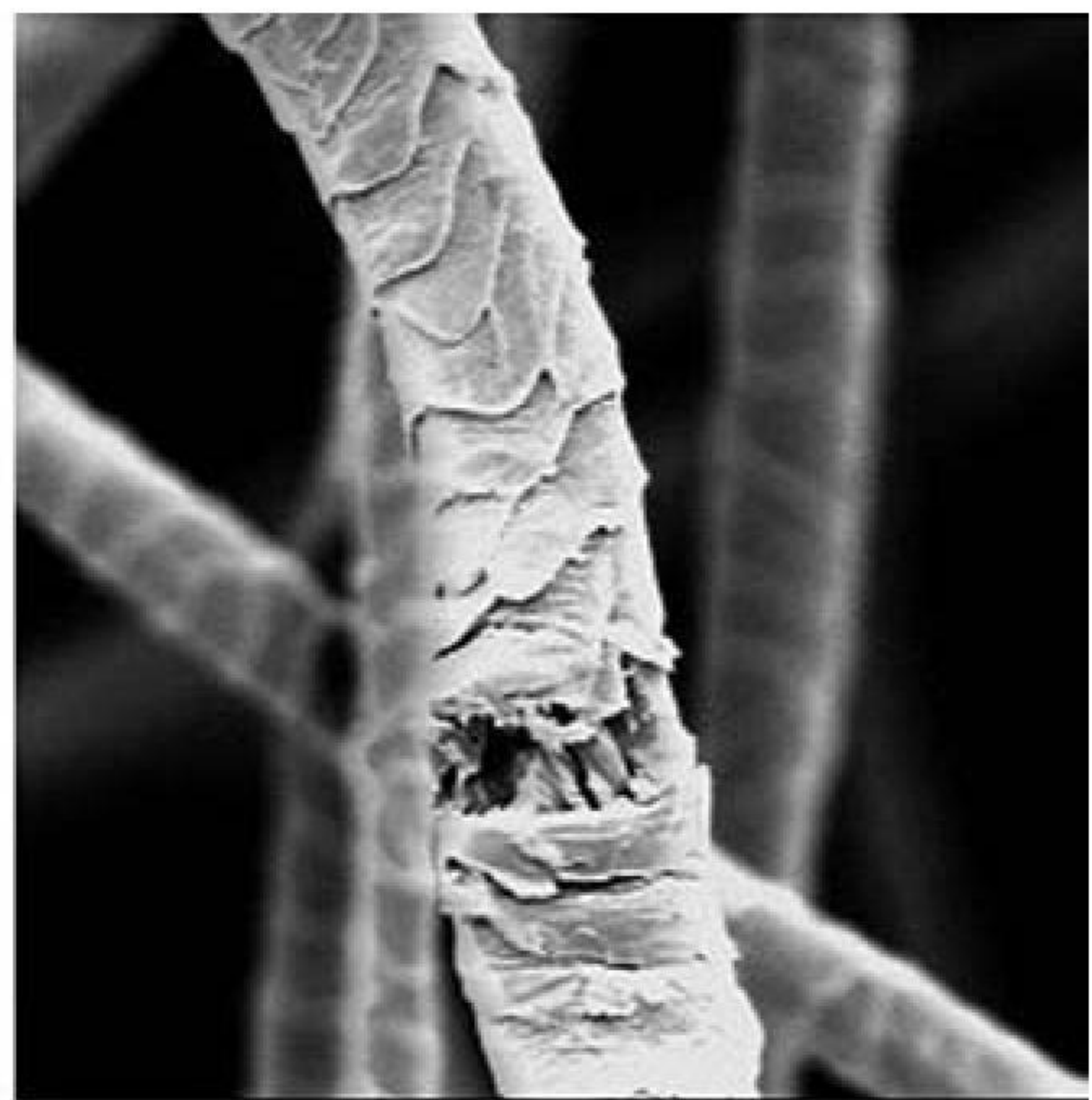
For example, the types of damage observed with wool fibers included⁸⁻¹¹

1. *Transverse and longitudinal cracks.* These are attributed to the presence of micro-defects reducing the local elastic properties of the fiber.
2. *Rupture and partial rupture of scales,* resulting from the sliding action of pins or sawteeth along the lengths of fibers. Repeated sliding action causes surface abrasion, and this would take place where a fiber mass is held and the clothing of the opening device repeatedly combs through fringe at a high speed to remove individual or groups of fibers. Fibers that are removed after repeated combing show surface abrasion.
3. *Puncture holes, giving a honeycomb appearance.* These are caused by the points of the clothing and, therefore, are more frequently found with pin rather than saw-tooth clothing.
4. *Small flattened areas.* These are due to compressive stresses over the contact area. This suggests a similar action to Hertzian contact stress theory.¹²

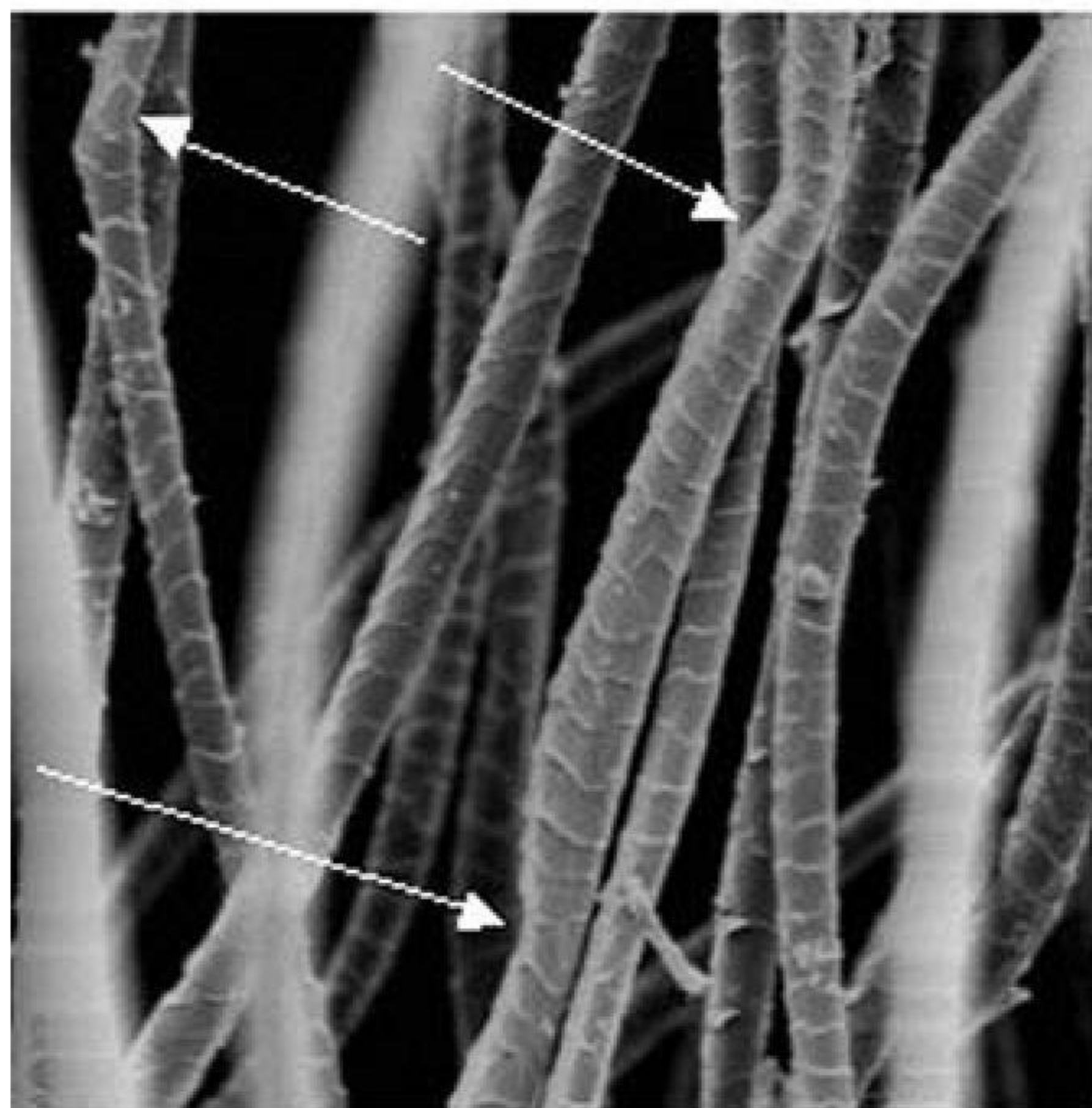
Figure 4B.3 gives examples of some micro-damage seen in wool fibers. Wool fibers are especially prone to damage because of their unique composite structure.⁸ Such micro-damage can lower the breaking load of fibers and lead to premature breakage in subsequent process stages.



Torn Areas



Puncture Holes



Flattened Areas

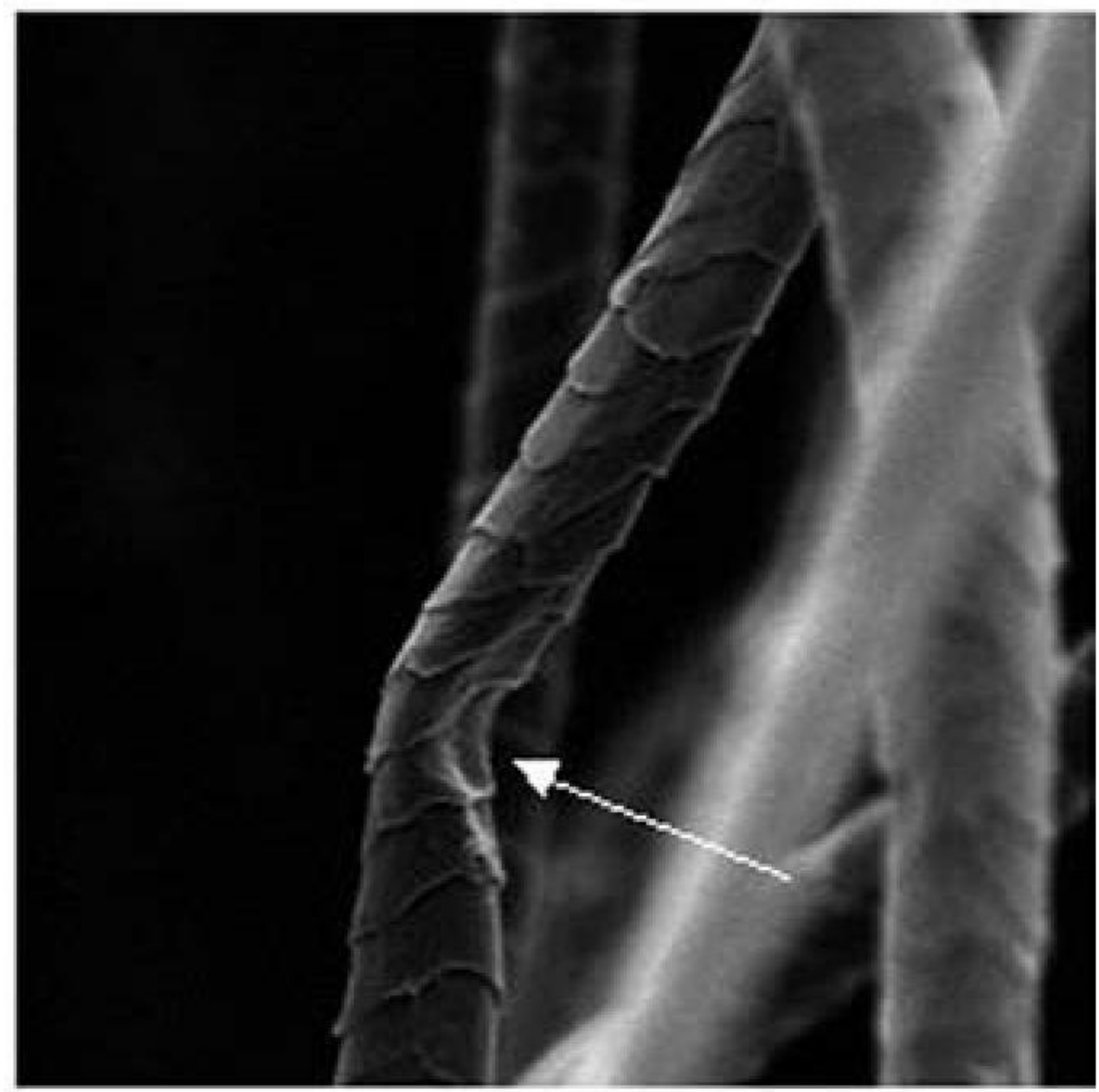


FIGURE 4B.3 Examples of wood fiber damage during carding.

REFERENCES

1. Yan, Y. and Johnson, N. A. G., The behaviour of fibers struck by high-speed pins, part II: Experiment, *J. Text. Inst.*, 83(1), 15, 1992.
2. Yan, Y. and Johnson, N. A. G., The behaviour of fibers struck by high-speed pins, part I: Theory, *J. Text. Inst.*, 83(1), 1, 1992.
3. Li, B., Johnson, N. A. G., and Wang, X., The measurement of fibre-withdrawal forces in simulated high-speed carding, *J. Text. Inst.*, 87(2), 1996.
4. Petterson, D. R., Stewart, G. M., Odell, F. A. and Maheux, R. C., Dynamic distribution of strain in textile materials under high speed impact, part I: Experimental methods and preliminary results on single yarns, *Text. Res. J.*, 30, 411, 1960.
5. Jameson, J. W., Stewart, G.M., Petterson, D.R., and Odell, F. A., Dynamic distribution of strain in textile materials under high speed impact, part III: Strain-time position history in yarns, *Text. Res. J.*, 32, 858, 1962.

6. Smith, J. C., Fenstermaker, C.A., and Shouse, P. J., Stress-strain relationship in yarns subjected to rapid impact loading, part XI: Strain distribution resulting from rifle bullet impact, *Text. Res. J.*, 35, 743, 1965.
7. Lyons, W. J., *Impact phenomena in textiles*, MIT Press, Cambridge, MA, 1962.
8. Gharhaghaji, A. A. and N. A. G. Johnson, Wool-fiber micro-damage caused by opening processes, part I: Sliver opening, *J. Text. Inst.*, 84(3), 33, 1993.
9. Gharhaghaji, A. A. and Johnson, N. A. G., Wool-fiber micro-damaged caused by opening processes, part II: A study of the contact between elements and wool fiber in controlled extension, *J. Text. Inst.*, 86(3), 403, 1995.
10. Gharhaghaji, A. A. and Johnson, N. A. G., Wool-fiber micro-damage caused by opening processes, part III: *In-situ* studies on the tensile failure of damaged-induced fibers, *J. Text. Inst.*, part 1, 90(1), 1, 1999.
11. Gharhaghaji, A. A. and Johnson, N. A. G., Wool-fiber micro-damaged caused by opening processes, part IV: *In-situ* studies on the compressive micro-damage and failure of wool fibers loped around opening elements, *J. Text. Inst.*, part 1, 90(1), 22, 1999.
12. Timoshenko, S. P., *Theory of elasticity*, 3rd ed., McGraw-Hill, New York, 1970.